EPRI

Further Development and Evaluation of Models-3/CMAQ-APT

Technical Report

Further Development and Evaluation of Models-3/CMAQ-APT

1005161

Final Report, November 2001

EPRI Project Manager
N. Kumar

EPRI • 3412 Hillview Avenue, Palo Alto, California 94304 • PO Box 10412, Palo Alto, California 94303 • USA
800.313.3774 • 650.855.2121 • askepri@epri.com • www.epri.com

DISCLAIMER OF WARRANTIES AND LIMITATION OF LIABILITIES

ORGANIZATION(S) THAT PREPARED THIS DOCUMENT

Atmospheric & Environmental Research, Inc.
Titan Corporation

ORDERING INFORMATION

Requests for copies of this report should be directed to EPRI Customer Fulfillment, 1355 Willow Way, Suite 278, Concord, CA 94520, (800) 313-3774, press 2.

CITATIONS

This report was prepared by

Atmospheric & Environmental Research, Inc.
2682 Bishop Drive, Suite 120
San Ramon, CA 94583

Principal Investigators
P. Karamchandani
C. Seigneur
K. Vijayaraghavan
S. Wu

Titan Corporation
P.O. Box 2229
Princeton, NJ 08543-2229

Principal Investigators
L. Santos
I. Sykes

This report describes research sponsored by EPRI.

The report is a corporate document that should be cited in the literature in the following manner:

Further Development and Evaluation of Models-3/CMAQ-APT, EPRI, Palo Alto, CA: 2001. 1005161.

REPORT SUMMARY

Models-3/CMAQ-APT, a state-of-the science plume-in-grid model, has been applied to thirty power plant plumes in the northeastern United States. This report describes results of that project along with recent improvements to the model.

Background

Experimental and theoretical studies have shown that rates of ozone and acid formation in a plume rich in nitrogen oxides (NO_x) differ significantly from those in the ambient background atmosphere. The reason for this difference between plume and background chemistry is that high NO concentrations in the plume lead to a depletion of oxidant levels until sufficient plume dilution has taken place. Three-dimensional (3-D) modeling of air quality is typically based on a gridded representation of the atmosphere where atmospheric variables such as chemical concentrations are assumed to be uniform within each grid cell. Such a grid-based approach, however, may lead to significant errors for sources that have a spatial dimension much smaller than that of the grid system. EPRI has sponsored development of a new state-of-the-science plume-in-grid (PiG) air quality model that addresses these issues and more realistically represents behavior of reactive plumes in the atmosphere. This PiG model consists of the reactive plume model SCICHEM imbedded into a three-dimensional grid-based model, the Models-3 Community Multiscale Air Quality modeling system (Models-3/CMAQ). It is referred to as Models-3/CMAQ with Advanced Plume Treatment (APT), or Models-3/CMAQ-APT

Objective

To describe several recent improvements made to the Models-3/CMAQ-APT and its application to a new domain for the explicit treatment of thirty power plant plumes.

Approach

The project team applied Models-3/CMAQ-APT to the NARSTO-Northeast area in the United States with two nested domains of 12-km and 4-km horizontal resolution for a five-day episode during July 1995. The thirty largest NO_x point sources in the 12 km resolution domain were explicitly simulated with PiG treatment. Six of these sources were in the 4-km resolution domain. The team also conducted a "background" simulation for the 12-km resolution domain in which emissions from the 30 point sources were neglected. Differences in the results between the background simulation and the base and APT simulations provided a measure of the contribution of these point sources to O_3 and HNO_3 concentrations with and without PiG treatment.

Results

This report provides an overview of Models-3/CMAQ-APT and describes improvements made since its last review. The document also presents results of the base and Models-3/CMAQ-APT

Results

This report provides an overview of Models-3/CMAQ-APT and describes improvements made since its last review. The document also presents results of the base and Models-3/CMAQ-APT plume-in-grid simulations for the NARSTO-Northeast domain. It also discusses results of the Models-3/CMAQ-PinG simulation for the same domain. Conclusions are provided.

EPRI Perspective

Project results suggest that it is preferable to treat major NO_x point sources with Models-3/CMAQ-APT since both O_3 and HNO_3 production downwind of these sources are generally overpredicted if a PiG treatment is not used. Differences between the Models-3/CMAQ-APT and Models-3/CMAQ-PinG simulations are likely due to earlier plume-to-grid transfers in Models-3/CMAQ-PinG than in Models-3/CMAQ-APT. These results suggest that the time for plume-to-grid transfer is very influential and should be selected carefully to ensure an accurate simulation.

Keywords

Plume-in-grid
Ozone
Power plants
Models-3
Advanced plume treatment
Northeastern U.S.

ACKNOWLEDGMENTS

We would like to thank the Coordinating Research Council (CRC) for allowing us to use the CRC Project A-23 meteorological and emission input files for the NARSTO-Northeast 12 km and 4 km resolution domains. We would also like to thank the Division of Air Resources at the New York State Department of Environmental Conservation (NYSDEC) for providing surface ozone concentrations from the Aerometric Information Retrieval System (AIRS) database for evaluating the models used in this work.

CONTENTS

LIST OF FIGURES

LIST OF TABLES

1
INTRODUCTION

Both experimental studies (e.g., Richards et al., 1981; Gillani et al., 1998) and theoretical studies (e.g., Karamchandani et al., 1998) have shown that the rates of ozone and acid formation in a plume rich in nitrogen oxides (NO_x) differ significantly from those in the ambient background atmosphere. The reason for this difference between plume chemistry and background chemistry is that the high NO concentrations in the plume lead to a depletion of oxidant levels until sufficient plume dilution has taken place. Three-dimensional (3-D) modeling of air quality is typically based on a gridded representation of the atmosphere where atmospheric variables such as chemical concentrations are assumed to be uniform within each grid cell. Such a grid-based approach necessarily averages emissions within the volume of the grid cell where they are released. This averaging process may be appropriate for sources that are more or less uniformly distributed at the spatial resolution of the grid system. However, it may lead to significant errors for sources that have a spatial dimension much smaller than that of the grid system. For example, stack emissions lead to plumes that initially have a dimension of tens of meters, whereas the grid cell horizontal size is typically several kilometers in urban applications up to about 100 km in regional applications. This artificial dilution of stack emissions leads to (1) lower concentrations of plume material, (2) unrealistic concentrations upwind of the stack, (3) incorrect chemical reaction rates due to the misrepresentation of the plume chemical concentrations and turbulent diffusion, and (4) incorrect representation of the transport of the emitted chemicals. The errors associated with the grid-averaging of stack emissions can be eliminated by using a subgrid-scale representation of stack plumes that is imbedded in the 3-D grid system of the air quality model.

The first subgrid-scale treatment of plumes in 3-D air quality models was developed by Seigneur et al. (1983). Other treatments of subgrid-scale effects have been developed over the years (e.g., Gillani, 1986; Sillman et al., 1990; Morris et al., 1991; Kumar and Russell, 1996; Myers et al., 1996; Gillani and Godowitch, 1999). All these models treat the plume at a subgrid-scale, thereby eliminating some of the errors associated with the 3-D grid representation. However, they fail to represent the complex dispersion processes associated with the plume mixing into the background air because the plume dimensions are represented by simple geometric functions (columns, grids, ellipses, or Gaussian distributions). Physical phenomena such as the effect of wind shear on plume dispersion, the effect of plume overlaps (e.g., under conditions of reversal flow or merging of adjacent plumes), and the effect of atmospheric turbulence on chemical kinetics are not (or poorly) represented by such models.

Over the past few years, EPRI has sponsored the development of a new state-of-the-science plume-in-grid air quality model that can address the physical phenomena enunciated above explicitly, thereby providing a more realistic representation of the behavior of reactive plumes in the atmosphere. The development of the plume-in-grid model was described in a previous report by Karamchandani et al. (2000a). This plume-in-grid model consists of the reactive plume

model SCICHEM imbedded into a three-dimensional grid-based model, the Models-3 Community Multiscale Air Quality modeling system (Models-3/CMAQ). It is referred to as Models-3/CMAQ with Advanced Plume Treatment (APT). Models-3/CMAQ-APT was applied to explicitly simulate the plumes of two power plants for a five-day simulation in the Nashville/western Tennessee area (Karamchandani et al., 2000a).

In this report, we describe some recent improvements made to the formulation of Models-3/CMAQ-APT and its application to a new domain for the explicit treatment of thirty power plant plumes. We also applied the original plume-in-grid (PinG) formulation of Models-3/CMAQ (hereafter referred to as Models-3/CMAQ-PinG) to the same simulation.

The report is organized as follows. Section 2 provides an overview of Models-3/CMAQ-APT and describes the improvements made since the last report of Karamchandani et al. (2000a). Section 3 presents the results of the base and Models-3/CMAQ-APT plume-in-grid simulations for the NARSTO-Northeast domain. Section 4 presents the results of the Models-3/CMAQ-PinG simulation for the same domain. Conclusions are provided in Section 5.

2
DESCRIPTION OF MODELS-3/CMAQ-APT

2.1 Models-3/CMAQ

Models-3/CMAQ was developed by the U.S. Environmental Protection Agency (EPA) to address multiscale multi-pollutant air pollution problems (Byun and Ching, 1999). Models-3 is the computational framework and CMAQ is the air quality model. Models-3/CMAQ treats the emissions, transport, dispersion, chemical transformations, gas-particle conversion and removal processes that govern the behavior of chemical pollutants in the atmosphere. Emissions include those from area sources (e.g., industrial, residential, agricultural, mobile and biogenic emissions) and point sources (e.g., power plants and smelters). The plume rise of point source emissions is treated in a pre-processor to CMAQ. Transport processes include advection, large-scale convection and, in the presence of cumulus clouds, subgrid-scale convection. Dispersion includes both horizontal and vertical dispersion. Chemical transformations include reactions in the gas phase and reactions in the aqueous phase (i.e., in cloud droplets). The formation of secondary aerosols is treated and includes the gas-particle partitioning of volatile chemical species. Dry deposition is simulated for gases and particles. Wet deposition is treated for precipitating clouds that are resolved by the grid system as well as for clouds that are treated at the subgrid-scale. For the current plume-in-grid applications, Models-3/CMAQ was used in its gas-phase formulation, i.e., aerosols and clouds were not treated.

Models-3/CMAQ offers several options for some science modules. These options are summarized in Table 2-1. Note that one of the options for the numerical solution of the gas-phase chemical kinetics, the Young & Boris solver, was added under this project. The selection of the Young & Boris solver and its implementation into Models-3/CMAQ are discussed in Section 2.4.2.

The version of Models-3/CMAQ released by EPA in August 2000 (Version 4.0) was used here.

Table 2-1
Options available in CMAQ (options in bold are those used in this work).

Science Module	Options
Advection	**Bott** Piecewise parabolic method (PPM)
Gas-phase chemistry	**CBM-IV** RADM2
Numerical solver for chemical kinetics	SMVGEAR **QSSA**[(a)] **Young & Boris**[(b)]
Plume-in-grid	PING_SMVGEAR **PING_QSSA**[(a)] **PING_APT**[(b)]

(a) used for the Models-3/CMAQ-PinG application

(b) used for the Models-3/CMAQ-APT application and developed during this work

2.2 SCICHEM

The reactive plume model used for the plume-in-grid treatment is the Second-order Closure Integrated puff model (SCIPUFF) with CHEMistry (SCICHEM). Plume transport and dispersion are simulated with SCIPUFF, a model that uses a second-order closure approach to solve the turbulent diffusion equations (Sykes et al., 1988, 1993; Sykes and Henn, 1995). The plume is represented by a myriad of three-dimensional puffs that are advected and dispersed according to the local micrometeorological characteristics. Each puff has a Gaussian representation of the concentrations of emitted inert species. The overall plume, however, can have any spatial distribution of these concentrations, since it consists of a multitude of puffs that are independently affected by the transport and dispersion characteristics of the atmosphere. SCIPUFF can simulate the effect of wind shear since individual puffs will evolve according to their respective locations in an inhomogeneous velocity field. As puffs grow larger, they may encompass a volume that cannot be considered homogenous in terms of the meteorological variables. A puff splitting algorithm accounts for such conditions by dividing puffs that have become too large into a number of smaller puffs. Conversely, puffs may overlap significantly, thereby leading to an excessive computational burden. A puff merging algorithm allows individual puffs that are affected by the same (or very similar) micro-scale meteorology to combine into a single puff. Also, the effects of buoyancy on plume

rise and initial dispersion are simulated by solving the conservation equations for mass, heat, and momentum.

The chemical reactions within the puffs are simulated using a general framework that allows any chemical kinetic mechanism to be treated. The user enters the chemical reactions and their associated rate parameters, and SCICHEM sets the corresponding system of ordinary differential equations (ODE) to be solved. Chemical species concentrations in the puffs are treated as perturbations from the background concentrations. The formulation of nonlinear chemical kinetics within the puff framework is described by Karamchandani et al. (2000b).

The effect of turbulence on chemical kinetics can be simulated explicitly (the user selects the reactions for which the turbulent kinetic term is simulated). This effect is more pronounced near the stack (Karamchandani et al., 2000b) and requires additional computational time for its simulation. In the Models-3/CMAQ-APT applications described here, we did not implement this option.

The puff chemistry can be simulated using a staged chemical kinetic mechanism where the number of reactions treated increases as the puff mixes with background air. This multistage approach offers reasonable accuracy (within 10%) with increased computational speed (Karamchandani et al., 1998). The full chemical kinetic mechanism is that used by the 3-D gridded air quality model and can also be used by SCICHEM instead of the staged mechanism. For the Models-3/CMAQ-APT applications presented here, the Carbon-Bond Mechanism (CBM-IV) was used.

The SCICHEM model formulation and its evaluation with plume data from the 1995 Southern Oxidants Study (SOS) Nashville/Middle Tennessee Ozone Study have been presented by Karamchandani et al. (2000b).

2.3 Imbedding of SCICHEM into Models-3/CMAQ

Models-3/CMAQ is highly modular. This modularity is achieved by virtually eliminating data flow dependencies among the various process modules. Each process module reads and manipulates the direct access data files independently of the other modules. The only data shared by the various modules are the three-dimensional gridded species concentrations. The data files are manipulated using the Input/Output Applications Program Interface (I/O API) (MCNC Web Page, http://envpro.ncsc.org/products/ioapi; Coats et al., 1993). The I/O API is built on top of UCAR's NetCDF (Rew and Davis, 1990) which provides self-describing files accessible from both FORTRAN and C, is compatible with a variety of platforms, and makes data portable across heterogeneous computing environments.

The interface between SCICHEM and the host model exploits these structural aspects of Models-3. Figure 2-1 illustrates the interface between the host model and SCICHEM.

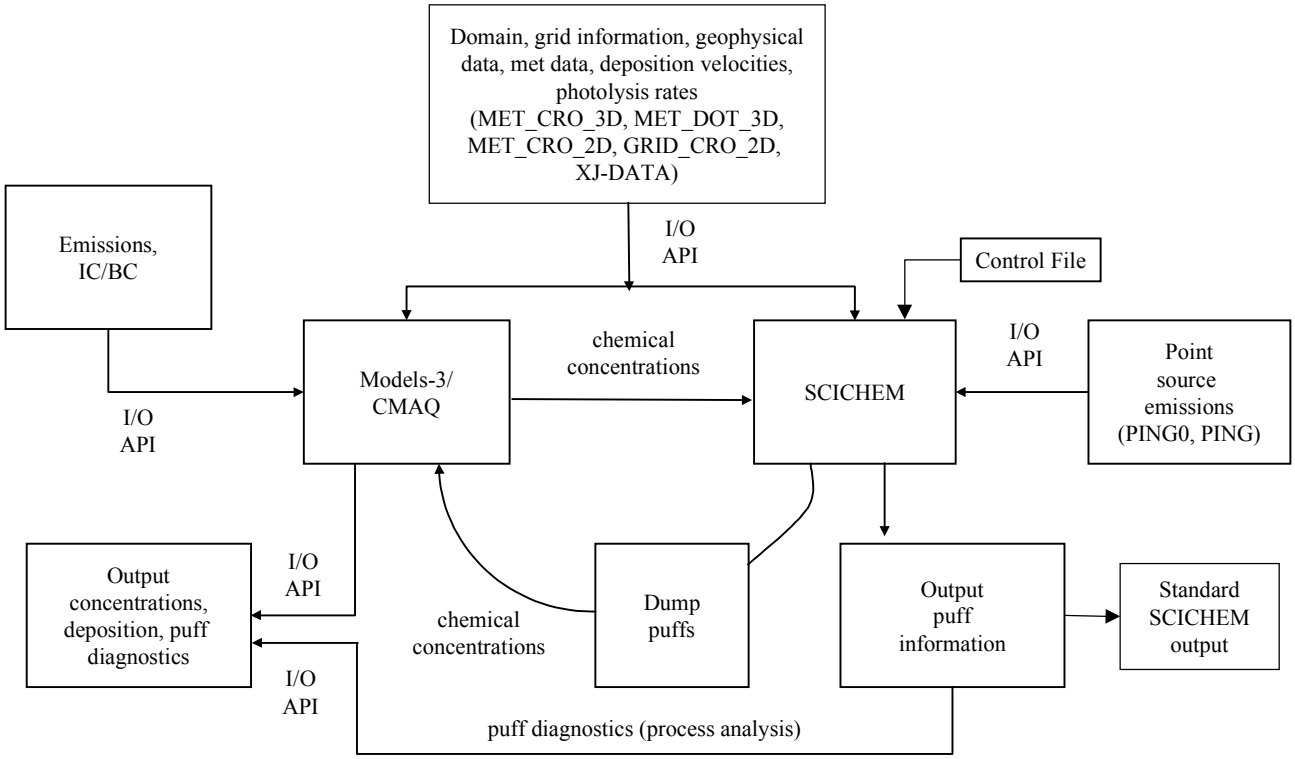

Figure 2-1
Interface between Models-3/CMAQ and SCICHEM.

Like the other process modules in Models-3/CMAQ, all relevant information related to the emissions and the dynamical state of the atmosphere required by SCICHEM are accessed directly from the input files via the I/O API; only the three-dimensional concentration fields are directly shared between the host model and SCICHEM. On input to SCICHEM, these host model concentrations serve as the background (ambient) concentrations for SCICHEM calculations. On output from SCICHEM, these concentrations are updated whenever plume-to-grid transfer occurs and are returned to the host model.

SCICHEM is invoked in Models-3/CMAQ-APT by a single subroutine call similar to that of any other physical or chemical process of the host model. The SCICHEM code is compiled as a library that is linked to the host model when the executable is being built.

2.4 Improvements to Models-3/CMAQ-APT

2.4.1 Background

The first version of Models-3/CMAQ-APT was developed in 1999. In this version, SCICHEM was incorporated into the 1998 release of Models-3/CMAQ. The model was applied to explicitly simulate the plumes of two power plants for a five-day simulation in the Nashville/western Tennessee area. The development of the model and results from its application have been described by Karamchandani et al. (2000a). For convenience, we will refer to this version of Models-3/CMAQ-APT as Version 1.0.

This section describes the various improvements to Models-3/CMAQ-APT since the development of Version 1.0. These improvements include modifications to both SCICHEM and Models-3/CMAQ-APT to improve the computational efficiency of the model as well as refinements to the criteria used to determine when the contents of a puff could be transferred to the host model grid. In addition, code was added to both SCICHEM and Models-3/CMAQ-APT to convert the SCICHEM diagnostic output to a form that could be readily viewed using PAVE.

2.4.2 Speeding up Models-3/CMAQ-APT

The CPU requirements of Version 1.0 were excessive. For example, for the Nashville application described in Karamchandani et al. (2000a), where two power plant plumes were explicitly simulated by SCICHEM within Models-3/CMAQ-APT, the CPU time required for a 5-day simulation increased by 40%. This added overhead would make it impractical to use Models-3/CMAQ-APT to explicitly simulate many point sources. Thus, it was necessary to improve the computational efficiency of the model.

The following options were investigated to improve the computational efficiency of Models-3/CMAQ-APT:

1. Streamlining SCICHEM

2. Alternative plume rise algorithm in SCICHEM

3. New chemistry solver in SCICHEM and Models-3/CMAQ-APT

The first option, performed by Titan/ARAP, involved standard streamlining techniques to modify SCICHEM, such as the removal of “dead” or unused code, as well as the removal of redundant or unnecessary calculations. These modifications resulted in a slight improvement in the computational efficiency of the model. The other two options explored for computational efficiency are described in more detail below.

Alternative Plume Rise Algorithm

Titan/ARAP (with some assistance from AER) was also primarily responsible for implementing this option. The original SCICHEM formulation for plume rise uses a dynamic model for the buoyancy and momentum rise calculations that results in a large number of puffs that must be carried in the simulation (EPRI, 2000). This considerably increases the computational time requirements of SCICHEM. To reduce the number of puffs, an alternative plume rise algorithm was implemented in SCICHEM. With this option, the puffs are assumed to be "passive" and the dynamic buoyancy and momentum rise calculations are not performed.

Titan/ARAP implemented an alternative plume rise algorithm in SCICHEM that is based on that used in the Sparse Matrix Operator Kernel Emissions (SMOKE) modeling system. This algorithm is also used in the Models-3/CMAQ Emission-Chemistry Interface Processor (ECIP) as well as in the processor developed by MCNC for EPRI for converting UAM files to Models-3/CMAQ format. Thus, the implementation of this algorithm within SCICHEM has the added benefit of ensuring that elevated point source emissions are consistently treated within both Models-3/CMAQ and Models-3/CMAQ-APT as far as their final release heights are concerned. This is particularly important when comparing results from a simulation in which some point sources are treated using the plume-in-grid approach with results from a simulation in which all point sources are treated within the host grid model.

After the alternative plume rise algorithm was implemented in SCICHEM, AER tested the scheme for the Nashville domain. As part of the testing, the plume rises calculated in SCICHEM for the Cumberland and Paradise plants were checked with those calculated from the MCNC emissions preprocessor. We found several differences between the plume rises calculated by the two approaches. Some of these differences were associated with errors in the SCICHEM implementation and these errors were corrected jointly by Titan/ARAP and AER. However, the testing of the plume rise calculations also identified an error in the original SMOKE implementation. AER notified MCNC, the developer of SMOKE, by e-mail about the error in SMOKE. MCNC (Houyoux, 2000) confirmed the error and informed AER that the error would be corrected in the next release of SMOKE. The error was corrected in AER's version of the MCNC emissions preprocessor.

The testing of the alternative plume rise algorithm within Models-3/CMAQ-APT for the Nashville domain showed a marked improvement in the computational efficiency of the model. For a 19-hour simulation, there was a factor of 4 decrease in the additional SCICHEM overhead in Models-3/CMAQ-APT.

Chemistry Solver

Because the plume-in-grid treatment of a large number of point sources increases the computational requirements of a simulation, it is essential to optimize all computational aspects of a plume-in-grid model. The numerical solution of the chemical kinetic

equations typically dominates the computational time of an air quality simulation. Therefore, we reviewed several numerical solvers suitable for the stiff ordinary differential equations (ODE) of gas-phase chemical kinetics. The solvers that were available in SCICHEM included LSODE, an accurate but slow numerical solver, and Young & Boris, a faster but slightly less accurate solver. The aqueous-phase chemistry version of SCICHEM uses the VODE solver, a faster version of LSODE. The solvers that were available in Models-3/CMAQ included SMVGEAR, an accurate but slow solver on scalar machines, and QSSA, a faster but less accurate solver.

To improve the computational efficiency of SCICHEM, we first used the VODE solver (already implemented in SCICHEM to solve the aqueous-phase chemistry equations) for the gas-phase chemistry solution. We found that this solver did not provide the desired speed-up, and, in fact, was slower than the Young and Boris solver that was already in SCICHEM. The version of the Young and Boris solver implemented in SCICHEM is an optimized version and is similar to that used in other air quality models such as ADOM, PLMSTAR, and EPRI's reactive plume model, ROME.

We also reviewed recent comparisons of stiff ODE solvers (Dabdub and Seinfeld, 1995; Verwer et al., 1996; Sandu et al., 1997; Mathur et al., 1998). Based on these previous analyses, it appeared that the most promising solvers in terms of numerical efficiency and ease of implementation were Young & Boris and RODAS3. We implemented the sparse matrix version of the RODAS3 solver into SCICHEM. We conducted tests comparing LSODE (benchmark), Young & Boris, and RODAS3. The results from these tests are described below.

A simple reactive plume test case was run for 6.5 hours during daytime using fixed winds for both a small and a large NO_x source. Longer simulations, of 30 hours duration, were also conducted. The relative (1.E-3) and absolute tolerances (species-dependent) were the same for all solvers. The tests were conducted for two cases: integration of all species (including radicals); and steady-state approximations for 12 radical species (NO3, N2O5, C2O3, XO2, XO2N, CRO, O, OH, O1D, HO2, ROR, and TO2). Note that, for these tests, the concentrations were advanced using the total (plume "perturbation" + background) concentrations, which is different from the stepping of the plume perturbation concentrations normally done in SCICHEM. The reason for doing this was that it was easier to implement RODAS3 for total concentrations than for the plume perturbations. Since our primary objective was to determine the computational efficiency and accuracy of the solvers, stepping the total concentrations instead of the plume perturbations was not regarded as a limitation for these tests.

The relative performance of the solvers can be summarized as follows. From the computational efficiency perspective, the RODAS3 solver was slightly slower or comparable to the Young & Boris solver for all the tests. Both solvers were about 4 to 5 times faster than LSODE for the tests in which all species were integrated. When steady-state approximations were used for the radicals, the RODAS3 and Young & Boris solvers were about 2 times faster than LSODE.

From the accuracy perspective, Young & Boris and RODAS3 were of comparable accuracy when steady-state approximations were made for the fast-reacting radical species. Both solvers compared very well with the benchmark solver (LSODE). Figure 2-2 illustrates the results for selected species from the tests using steady-state approximations for radicals. When no steady-state approximations were made, RODAS3 was more accurate than Young & Boris, particularly for radical species concentrations, as shown in Figure 2-3. However, because the implementation of RODAS3 into SCICHEM would have required significant effort, and because RODAS3 did not show any computational speed gains compared to Young & Boris, we could not justify using RODAS3 for SCICHEM. Also, Dabdub and Seinfeld (1995) and Mathur et al. (1998) have concluded that Young & Boris was a faster solver than QSSA, one of the solvers currently used in CMAQ. Therefore, we chose to incorporate Young & Boris into Models-3/CMAQ and use it as the numerical solver for Models-3/CMAQ-APT. Note that this approach also has the advantage of ensuring consistency between the solvers used in the host model and the embedded plume model. For a 19-hour Models-3/CMAQ simulation for the Nashville domain, the Young & Boris solver was about 1.7 times faster than QSAA. For the five-day NARSTO 12 km resolution simulation described later in this report, the Young & Boris solver was about 1.65 times faster than QSSA.

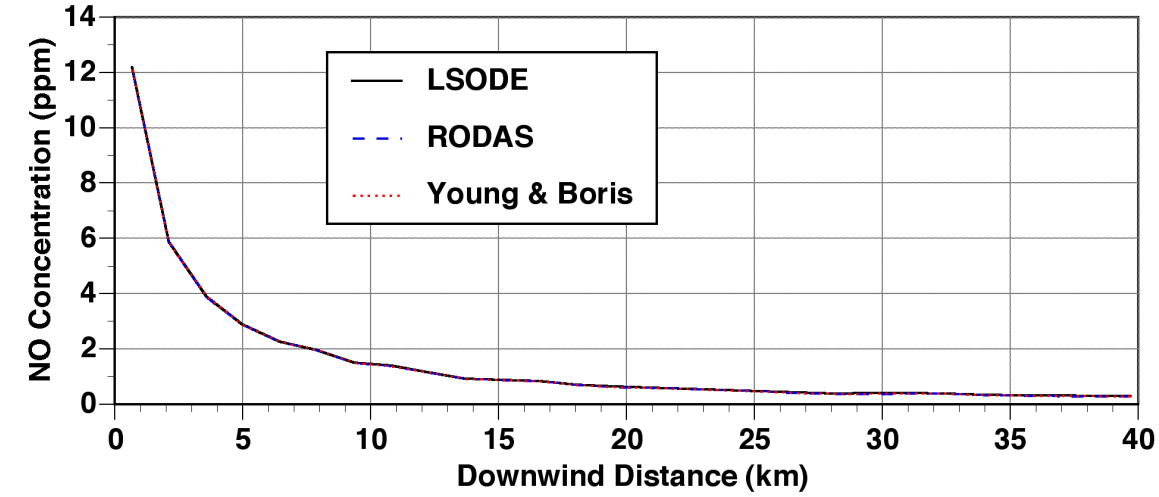

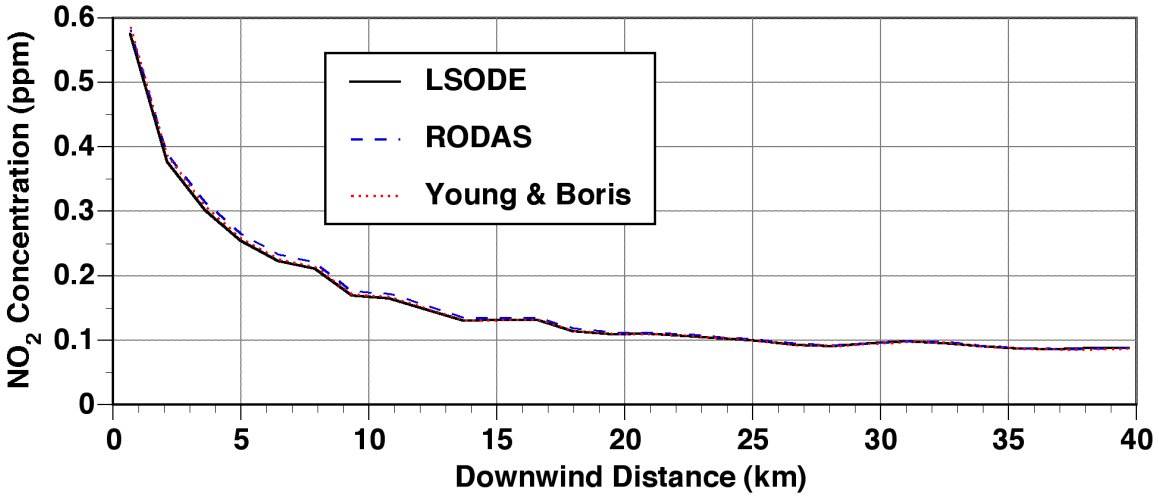

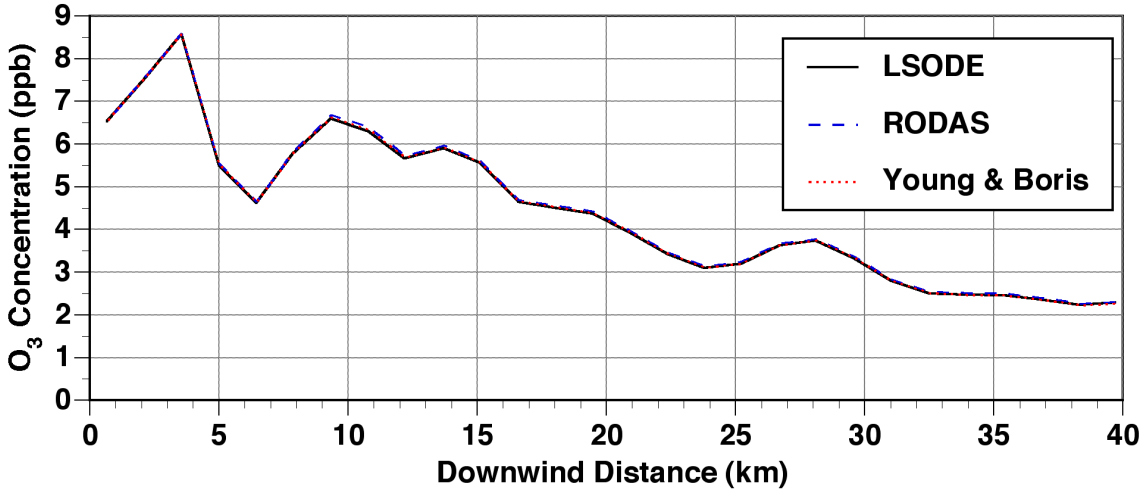

Figure 2-2 (a)
Chemistry solvers test results with radicals treated as steady-state species: NO, NO_2, and O_3 concentrations.

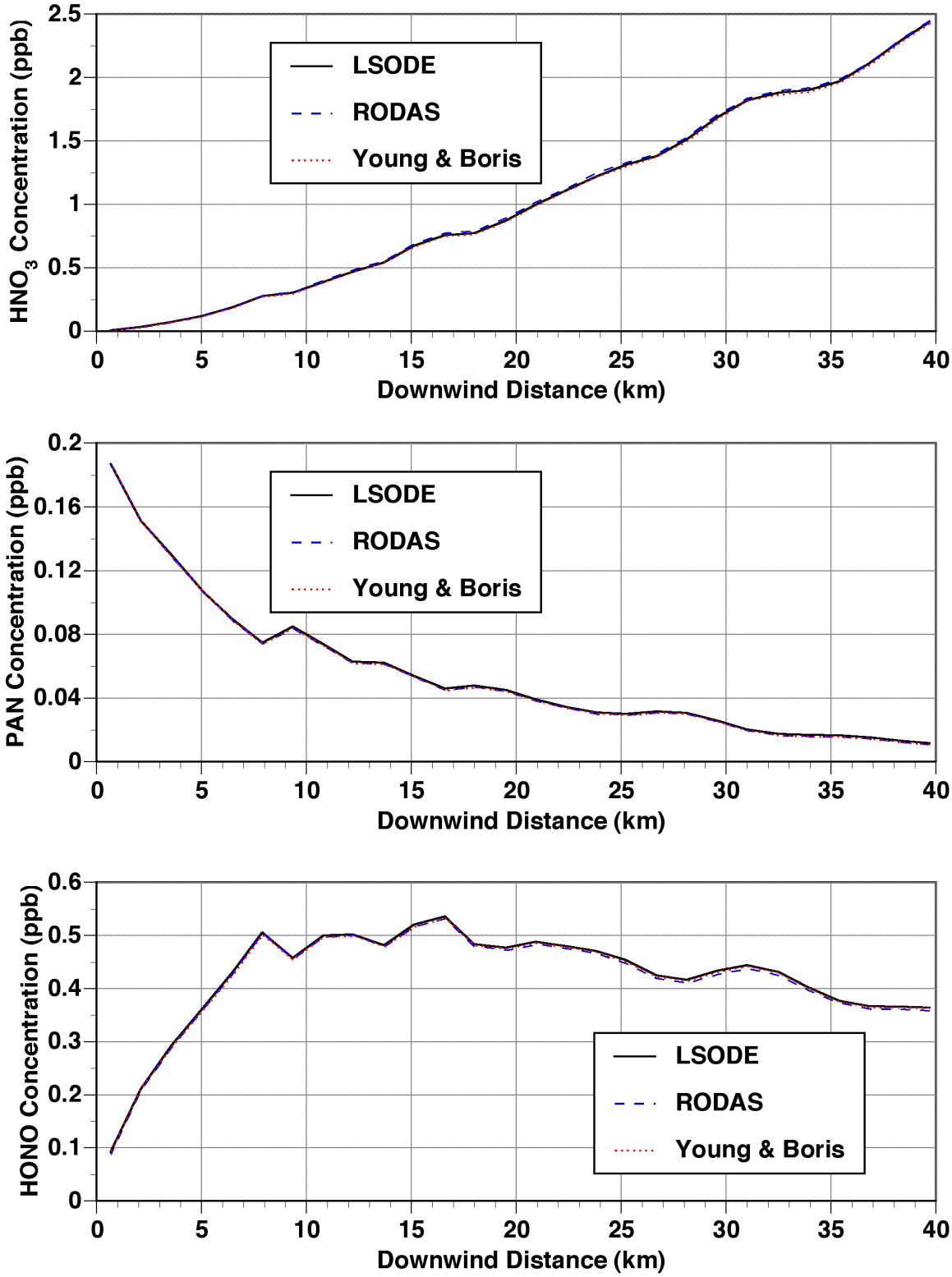

Figure 2-2 (b)
Chemistry solvers test results with radicals treated as steady-state species: HNO_3, PAN, and HONO concentrations.

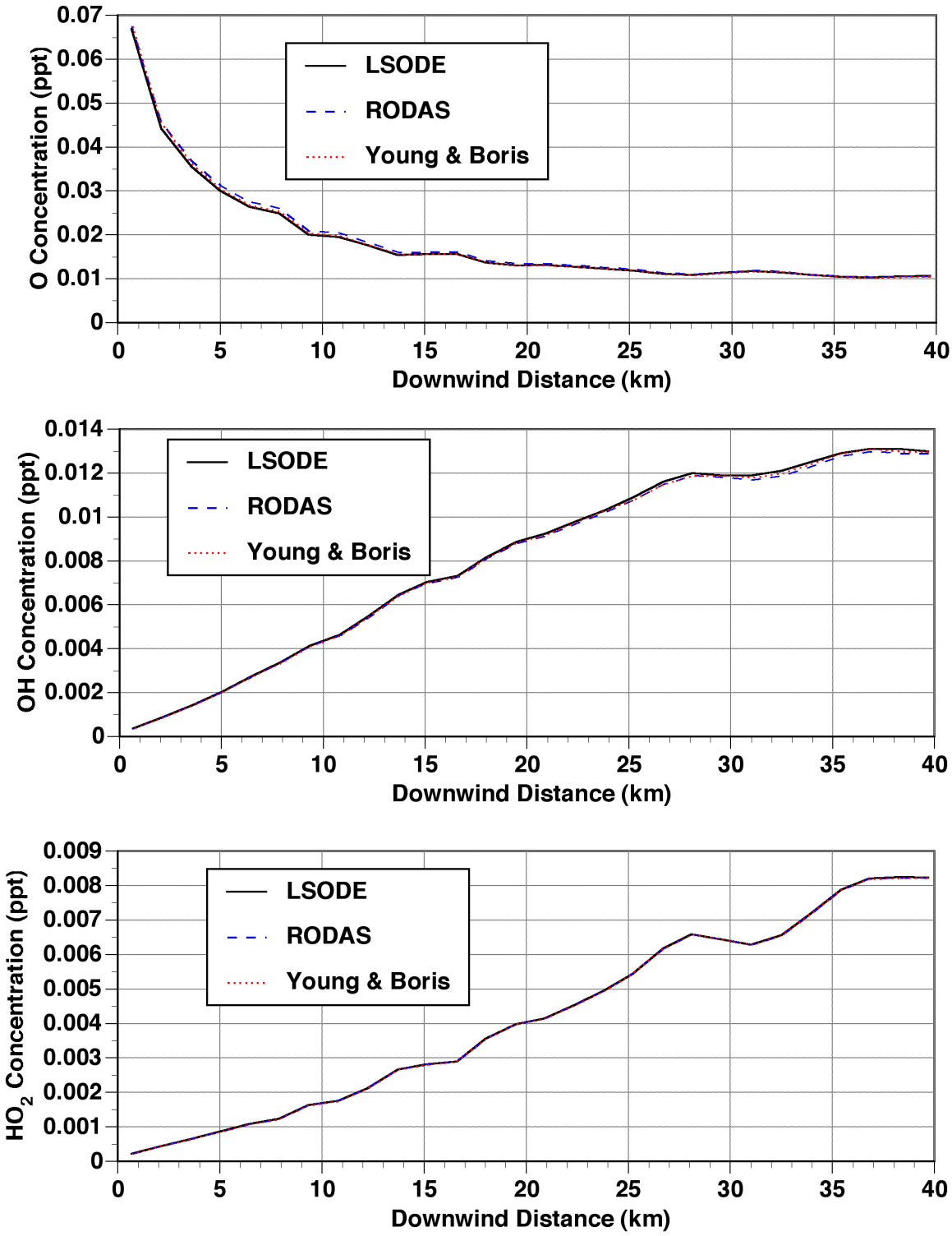

Figure 2-2 (c)
Chemistry solvers test results with radicals treated as steady-state species: O, OH, and HO_2 concentrations.

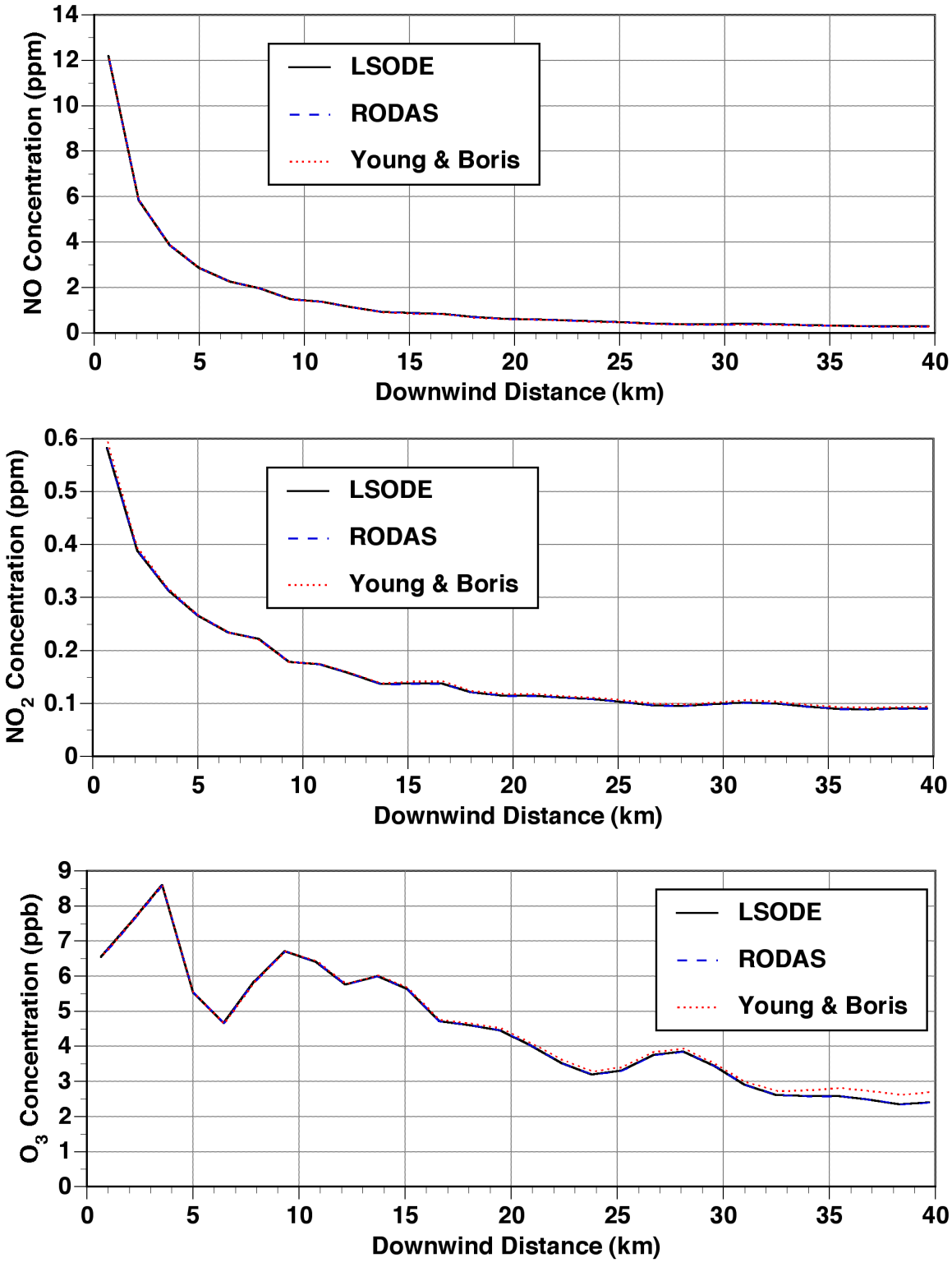

Figure 2-3 (a)
Chemistry solvers test results with all species (including radicals) integrated: NO, NO_2, and O_3 concentrations.

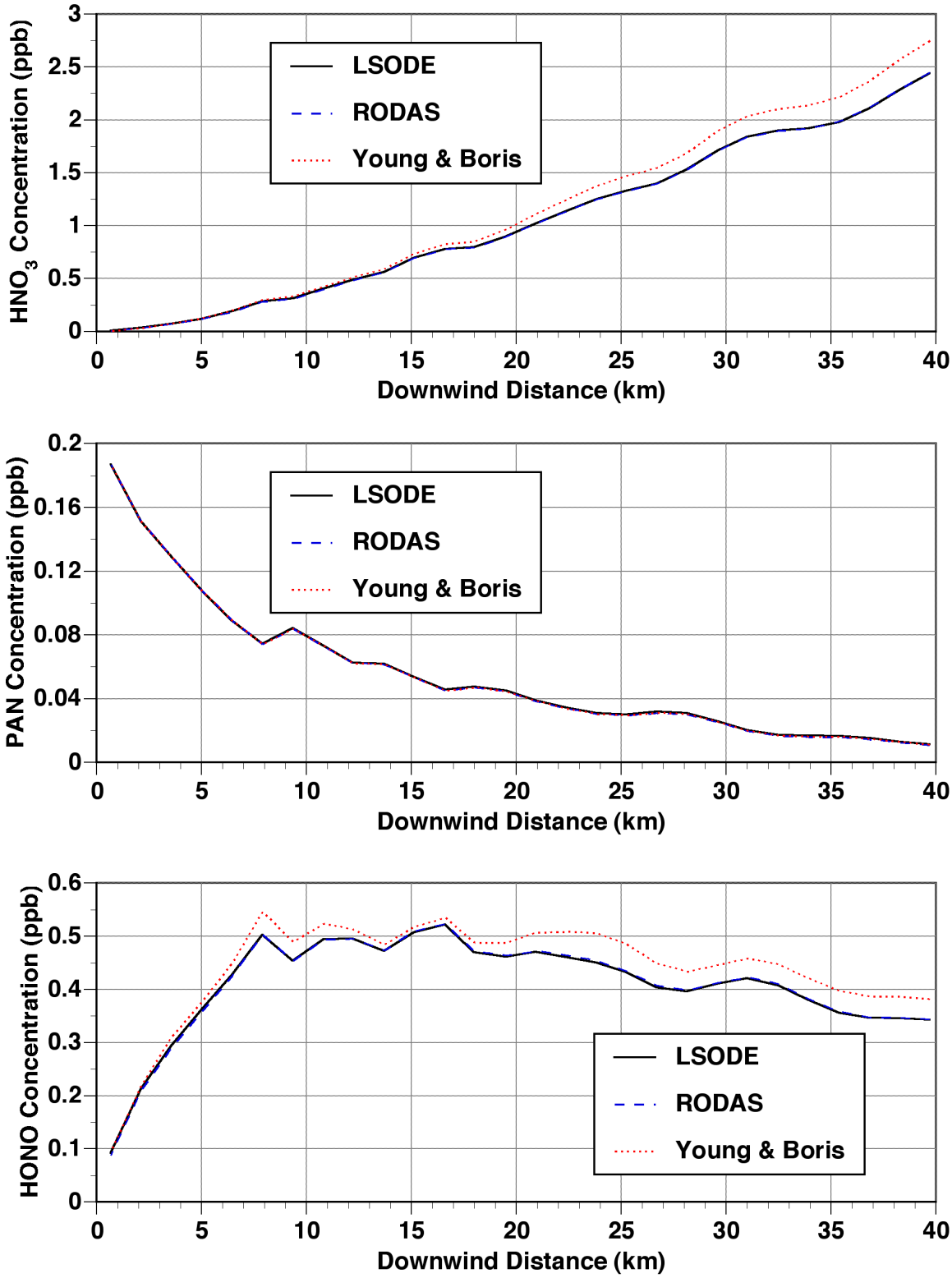

Figure 2-3 (b)
Chemistry solvers test results with all species (including radicals) integrated: HNO_3, PAN, and HONO concentrations.

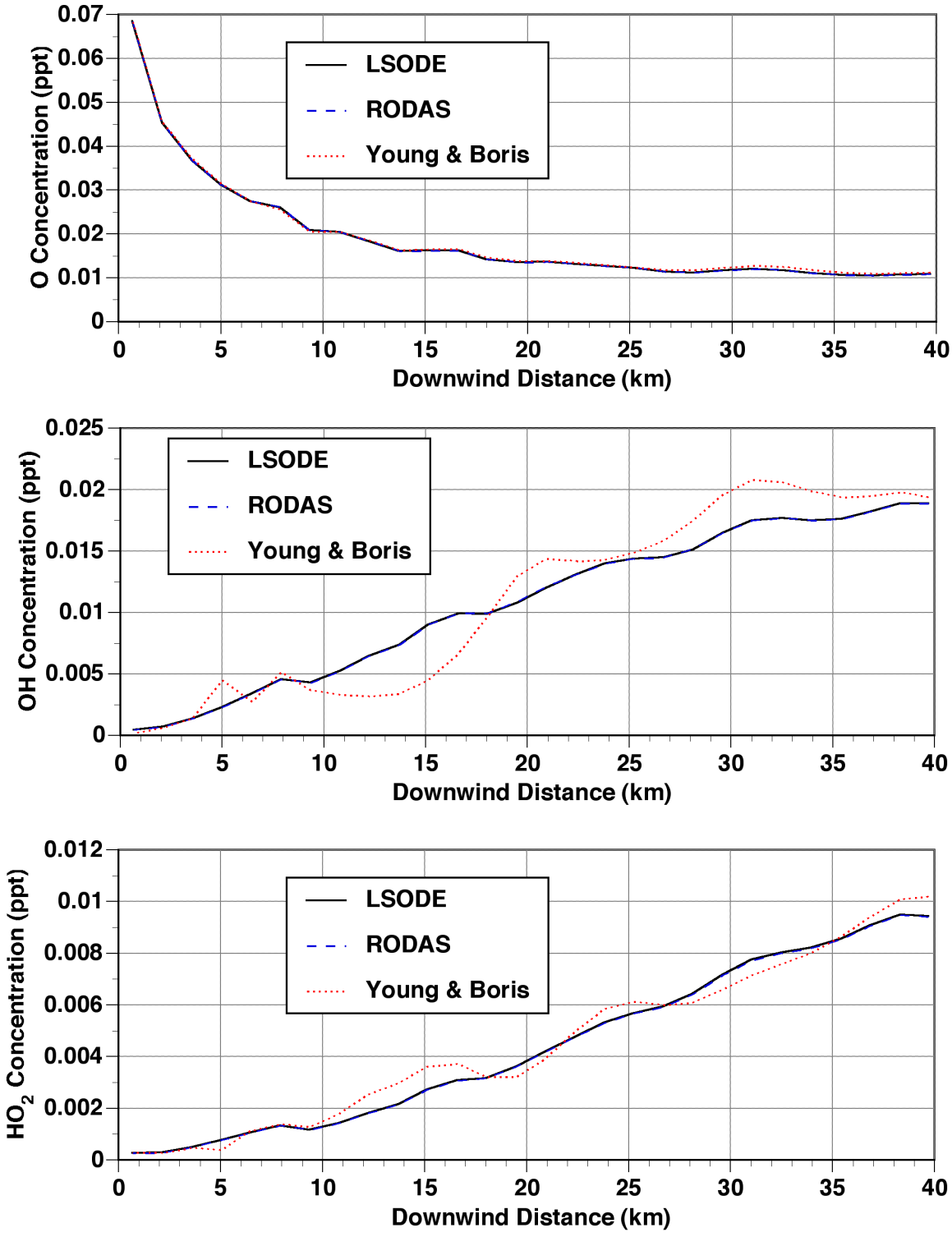

Figure 2-3 (c)
Chemistry solvers test results with all species (including radicals) integrated: O, OH, and HO_2 concentrations.

2.4.3 Refinement of Puff Dumping Criteria

The criterion for releasing puff material to the host model grid in Models-3/CMAQ-APT Version 1.0 was based on the size of the puff relative to the size of the grid cell. In the application of Version 1.0 to the Nashville domain with a horizontal grid resolution of 4 km, Karamchandani et al. (2000a) found that a large number of the puffs were dumped very quickly, within a distance of about 20 km, i.e., about 4 to 5 grid cells, from the source. These results suggest that using a purely physical criterion may result in premature transfer of the plume material to the grid. As pointed out by Gillani and Pleim (1996), the chemical maturation of emissions from a large power plant is likely to take much longer than the time it takes for the plume to grow to the grid size for simulations with fine grids such as that used in the Nashville application. For coarser grid resolutions (of the order of 20 to 30 km), the two conditions (plume growth and chemical maturity of the plume) are likely to be satisfied more or less simultaneously (Gillani and Pleim, 1996).

In the latest version of Models-3/CMAQ-APT, we have added puff-to-grid transfer criteria that take the chemical maturity of the puff into account. We explored a number of options to develop the chemical criteria before selecting the most promising and useful approach. The various options that we investigated are described briefly below.

As a first step, we used the three-stage evolution of plume chemistry described by Karamchandani et al. (1998) to determine the chemical maturity of a puff. The chemistry of a plume from a large NO_x source is significantly different from the chemistry in the background during the early stages of plume dispersion, when NO_x concentrations in the plume are high. This chemistry can be described in terms of a few reactions among a small number of species. As the plume disperses and becomes more dilute, the chemistry in the plume involves additional species and reactions. In the third stage of plume evolution, the plume chemistry requires a full representation of NO_x and VOC chemical reactions. Using this description, we assumed that a puff was chemically mature when it reached the third chemical stage, as defined by Karamchandani et al. (1998). When this criterion was used for a 19-hour Models-3/CMAQ-APT simulation for the Nashville domain, we found that the results were almost identical to those from the simulation that only used the physical criterion. This indicated that, at least for this simulation, most puffs that reached a size commensurate with the grid cell dimensions also reached the third chemical stage.

Next, we assumed that the puff reached chemical maturity if it was in the third chemical stage and the total NO_x concentrations in the puff were within a user-specified percentage of the host model concentrations. Using this criterion with a relatively lax tolerance of 10% resulted in a long simulation and a large number of puffs (nearly 50 times the number of puffs generated when only the physical criterion was used) for the 19-hour Nashville test case. Since this penalty on performance was unacceptable, we discarded this approach and selected the following approach, based on Gillani and Godowitch (1999).

Gillani and Godowitch (1999) use the plume concentration ratio of O_3/O_x, where $O_x = O_3 + NO_2$, as a surrogate for the chemical age of the plume in the EPA plume-in-grid version of Models-3/CMAQ. We used this concept to develop the chemical criteria for puff-to-grid transfer in Models-3/CMAQ-APT. First, a check is made to determine if the puff is in the third chemical stage. If it is, then the following additional criteria are considered. If the puff concentration of O_3 is within a certain percentage (user-specified) of the puff concentration of O_x, then the plume-to-grid transfer occurs. For the simulations presented here, the ratio O_3/O_x was chosen to be 0.99. Furthermore, an additional criterion is also used to prevent plumes with very low concentrations from aging indefinitely. If the plume NO_x concentration is very low (less than 0.1 ppb in this application) or the concentration of O_x is low (less than 1 ppb in this application), the plume-to-grid transfer occurs regardless of the value of the O_3/O_x ratio. For the 19-hour Nashville test case, the CPU requirements increased by about 10% and about 10 times more puffs were generated as compared to the case when only the physical criterion was used. The current version of Models-3/CMAQ-APT uses these criteria for determining the chemical maturity of the puff.

Figures 2-4 and 2-5 illustrate the effect of changing the dumping criteria on the transfer of puff material to the host model grid for the 19-hour Nashville simulation. Both figures show the fraction of total cumulative tracer (SCICHEM carries an inert tracer species in addition to the chemical species corresponding to the host model species) mass dumped as a function of the distance from the source for the Cumberland plume after 19 hours of simulation. Figure 2-4 corresponds to the case when the physical criterion is used for puff dumping, while Figure 2-5 corresponds to the chemical criteria described above. As can be seen from the figures, when the chemical criteria are used, the puffs travel for much longer distances before being dumped as compared to the case when the physical criterion is used. For the physical criterion case, the mode of the distribution occurs at approximately 10 km from the source, while for the chemical criteria case, the mode occurs at approximately 30 km from the source. The 50^{th} percentile value is about 24 km when the physical criterion is used, and about 40 km when the chemical criteria are used. The 99^{th} percentile values are about 60 km and 150 km, respectively, for the physical criterion and the chemical criteria. The area over which puffs are transferred to the host model for the chemical criteria case is about 3 times larger than that for the physical criterion case.

2.4.4 Models-3/CMAQ-APT Diagnostic Outputs

Models-3/CMAQ provides an option to conduct a process analysis of the simulation results. This process analysis includes information on both Integrated Process Rates (IPRs) and Integrated Reaction Rates (IRRs). The IPRs are obtained during a CMAQ simulation by computing the change in each species concentration due to the various processes (e.g., advection, chemistry, etc.) while the IRR analysis involves information on the contributions of individual chemical reactions.

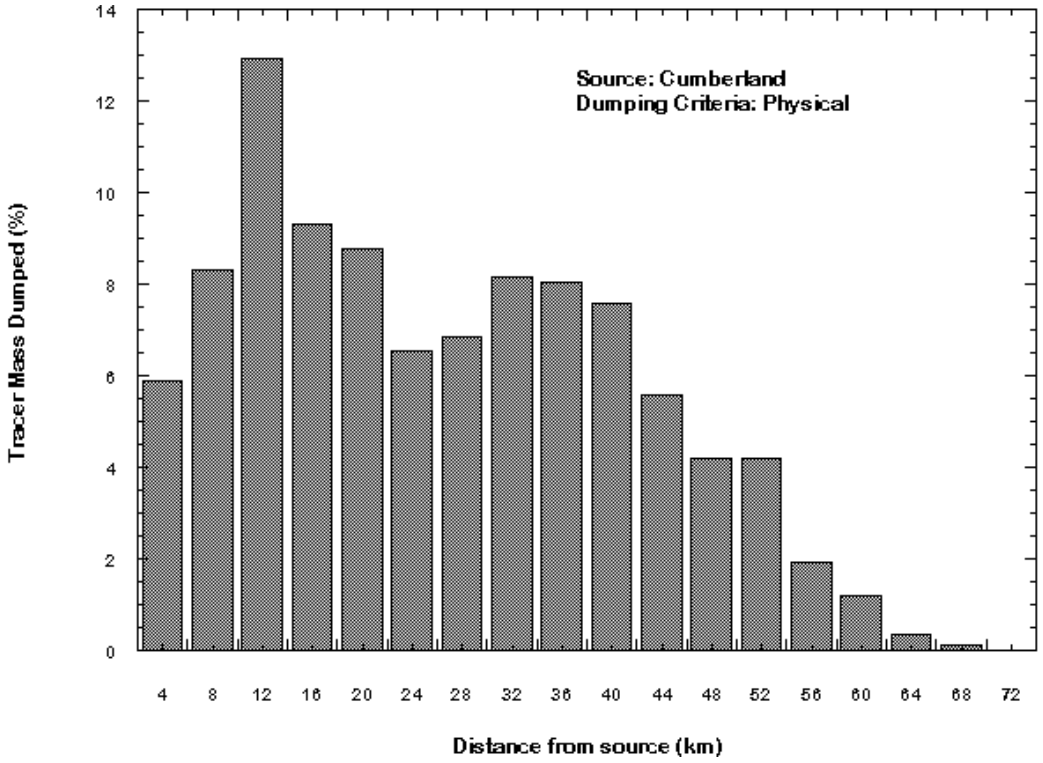

Figure 2-4
Normalized cumulative (over 19 hours) tracer mass dumped when physical criterion is used for puff-to-grid transfer.

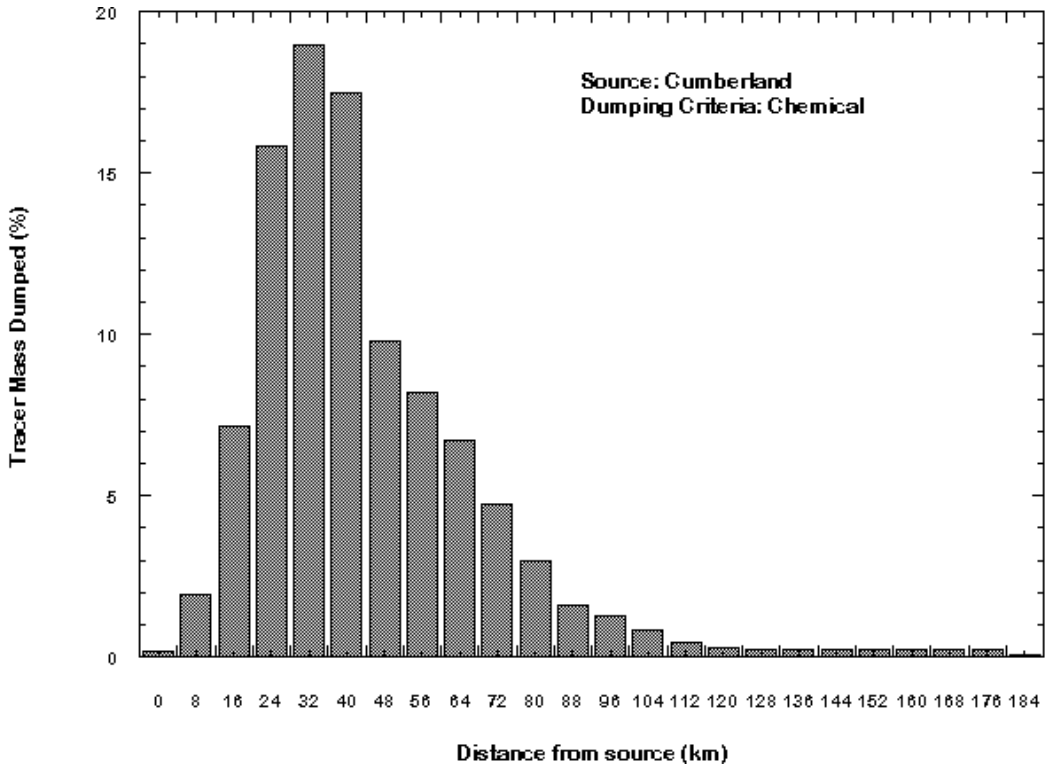

Figure 2-5
Normalized cumulative (over 19 hours) tracer mass dumped when chemical criteria are used for puff-to-grid transfer.

We have incorporated an IPR process analysis capability in Models-3/CMAQ-APT. This analysis provides information (on a total puff basis) for the following processes in the plume simulation: emissions, chemistry, dry deposition, material crossing the domain boundaries, and material transferred to the host grid.

The CMAQ-APT IPR analysis information is written to 7 NetCDF files containing the puff diagnostics. These files are all time-dependent one-dimensional files containing IPRs on a total puff basis for each chemical species for different processes at every output time step. Because the files are in the NetCDF format, the information contained in these files can be visualized using PAVE. The temporal variation in the process rates can be viewed separately for each process, or the information for different processes can be combined for mass budget purposes. Detailed descriptions of these process analysis files and their contents are provided in the accompanying Models-3/CMAQ-APT User's Guide. Figures 2-6 through 2-9, which are time series plots obtained using PAVE, illustrate the information provided by the CMAQ-APT process analysis files. Figure 2-6 shows the total mass (expressed as ppm-m^3) of NO emitted from all the point sources treated with SCICHEM as a function of time for the 19-hour Nashville simulation referred to previously. Figure 2-7, which depicts the change in plume NO mass at every time step due to chemical conversion, shows that the plume chemistry results in a net consumption of plume NO for the time period shown here. Figure 2-8 shows the mass of plume NO that is dry deposited at every time step, while Figure 2-9 shows the amount of plume NO mass transferred to the host model grid at every time step.

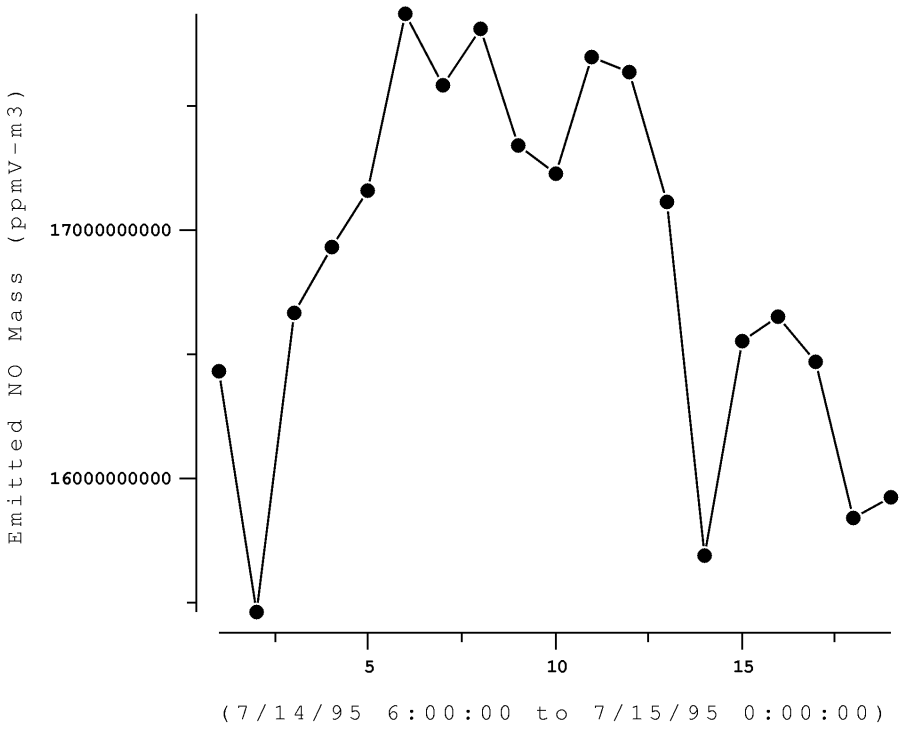

Figure 2-6
Hourly NO mass emitted from point sources (Cumberland and Paradise) treated with SCICHEM for 19-hour Models-3/CMAQ-APT Nashville simulation.

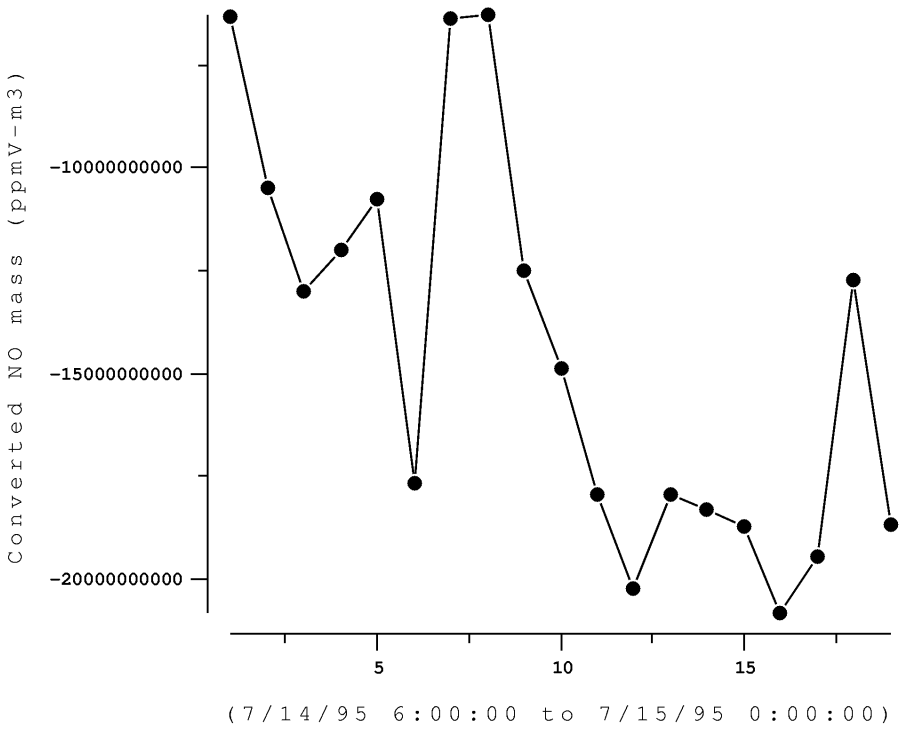

Figure 2-7
Hourly change in plume NO mass as a result of chemical conversion for 19-hour Nashville Models-3/CMAQ-APT simulation.

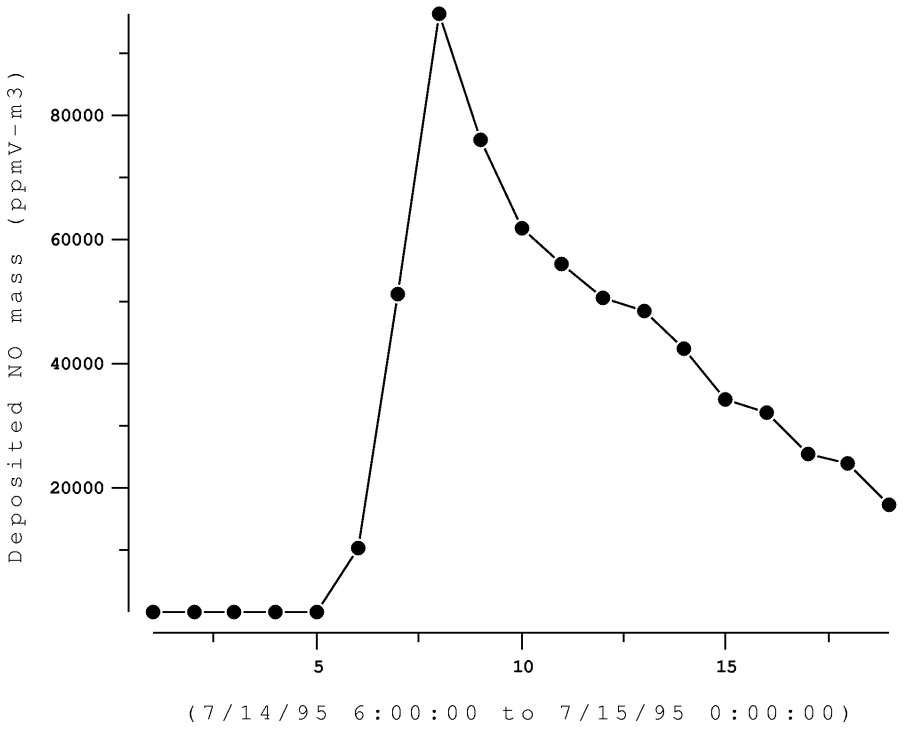

Figure 2-8
Hourly plume NO mass dry deposited for 19-hour Nashville Models-3/CMAQ-APT simulation.

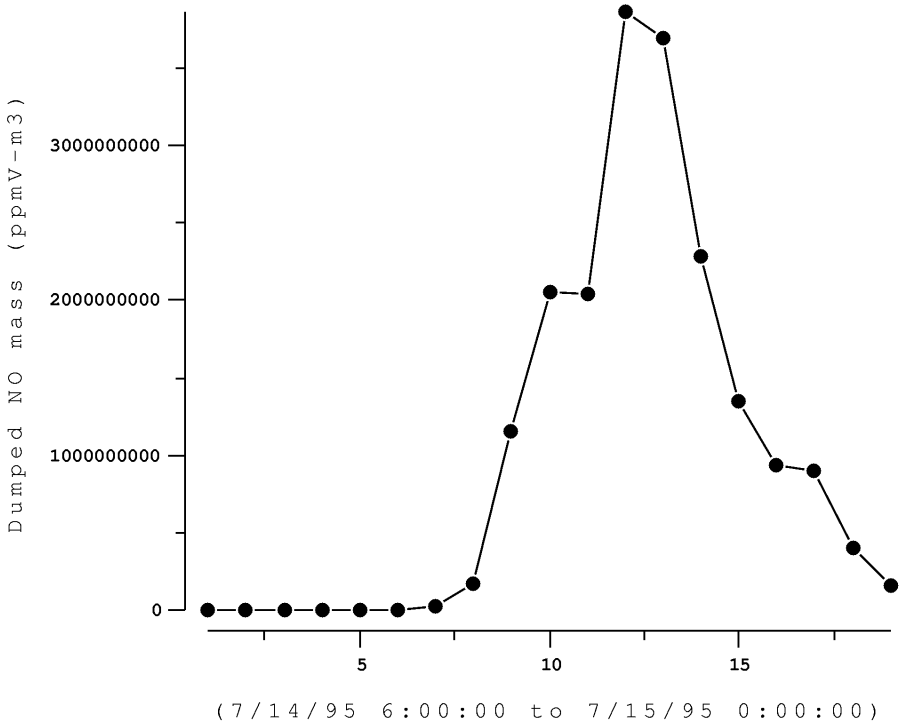

Figure 2-9
Hourly plume NO mass transferred to host model grid for 19-hour Nashville Models-3/CMAQ-APT simulation.

3
MODELS-3/CMAQ APPLICATION TO THE NARSTO-NORTHEAST DOMAIN

3.1 Models-3/CMAQ Base Simulation

3.1.1 Overview of the Base Simulation

The Models-3/CMAQ simulation was conducted over a domain covering the Northeastern U.S. with two nested grids. The outer grid uses a 12 km horizontal resolution and the inner grid uses a 4 km horizontal resolution. The vertical grid structure consists of 13 layers from the surface to the tropopause with finer resolution near the surface (e.g., the surface layer is 18 m deep). Figure 3-1 depicts the two nested domains and Table 3-1 lists the heights of the grid layers in sigma coordinates.

The input files for emissions, meteorology, and initial and boundary conditions were previously developed under a project sponsored by the Coordinating Research Council (CRC) and were provided to us by Environ International Corporation. The meteorological fields are from a prognostic simulation conducted with the non-hydrostatic meteorological model, MM5, using four-dimensional data assimilation (FDDA) (Seaman and Michelson, 2000).

The ozone episode covers a five-day period from 11 to 15 July 1995. This period was simulated for the 12 km resolution domain. The first two days (11 and 12 July) were used to spin-up the model. The 4 km resolution domain simulations were conducted for the last four days of this period (12 to 15 July). The model simulation results are presented for the last three days of the period (13, 14 and 15 July) for both domains.

Model simulation results are presented as spatial tile plots at selected times for the surface O_3 and HNO_3 concentrations and as time series at selected locations for the surface O_3 concentrations. The spatial plots are presented at the times of the maximum observed O_3 concentration in the modeling domain. These times were 3 p.m. Eastern Daylight-saving Time (EDT) for all 3 days (13, 14 and 15 July) for the 12 km resolution simulation. They were 4 p.m., 3 p.m. and 3 p.m. EDT on 13, 14 and 15 July, respectively, for the 4 km resolution simulation. The time series are presented at the locations of the maximum observed O_3 concentration in the modeling domain. For the 12 km resolution domain, these locations are Holland, MI; Madison, CT; and Fort Meade, MD on 13, 14 and 15 July, respectively. For the 4 km resolution domain, these locations are Danbury, CT; Madison, CT; and Fort Meade, MD. The surface O_3 observations were obtained from the U.S. EPA Aerometric Information Retrieval System (AIRS) data base, provided to us by the Division of Air Resources at New York State Department of Environmental Conservation (NYSDEC).

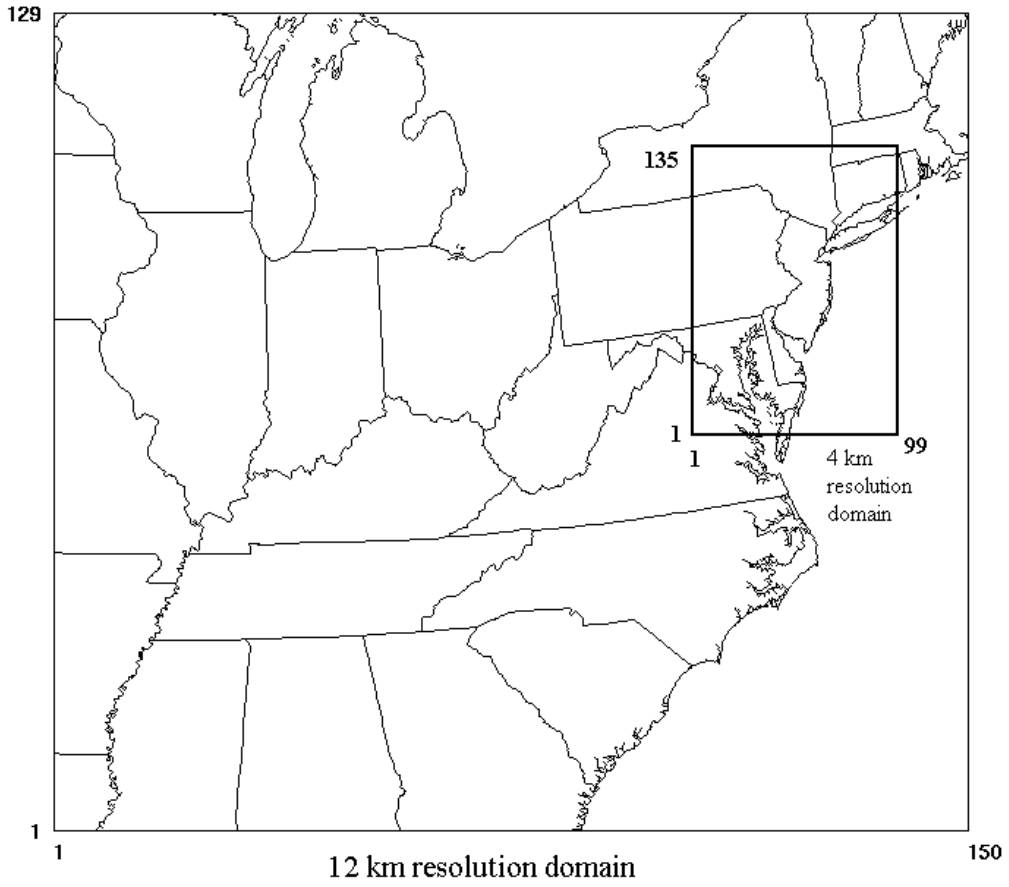

Figure 3-1
Modeling domain for the NARSTO-Northeast simulation.

Table 3-1
Models-3/CMAQ grid layers for the NARSTO-Northeast simulation.

Layer Number	σ-p	Approximate layer top (m agl)
13	0.00	15374
12	0.198	9534
11	0.372	6485
10	0.556	4095
9	0.694	2631
8	0.814	1515
7	0.866	1068
6	0.902	770
5	0.934	513
4	0.966	261
3	0.987	101
2	0.993	51
1	0.998	18

3.1.2 O_3 Concentrations

The spatial patterns of surface O_3 concentrations in the 12 km resolution domain are presented in Figures 3-2 to 3-4 for July 13 to 15, respectively. On July 13, the maximum O_3 concentrations are predicted to occur in the Midwest, primarily in central Illinois and over Lake Michigan with 1-hour average concentrations in the range of 120 to 170 ppb. On July 14, the maximum O_3 concentrations occur in two principal areas: an area that extends from southern Ohio into western Pennsylvania and an area that extends along the Atlantic coast from Washington, D.C. to Boston, Massachusetts. These two areas show O_3 concentrations in the range of 130 to 170 ppb. On July 15, the maximum O_3 concentrations occur primarily along the Atlantic coast in the northeastern urban corridor from Washington D.C. to New York City in the range of 140 to 227 ppb. An area around the Ohio River Valley shows O_3 concentrations in the range of 140 to 200 ppb, and the Chicago area shows O_3 concentrations in the range of 140 to 170 ppb.

For comparison with Figures 3-2 to 3-4, Figures 3-5 to 3-7 show the observed surface O_3 concentrations for the three days. On July 13, Figures 3-2 and 3-5 show that the observed and predicted spatial patterns are qualitatively consistent for the most part, with some differences in a few regions. The spatial patterns are generally comparable in the southern and eastern portions of the modeling domain. For example, in southeastern Pennsylvania, we see that both the observed and simulated O_3 concentrations range from about 80 to 120 ppb. Similarly, in

southern North Carolina, there is an observation in the range of 100 to 120 ppb, which compares with the simulated values at about the same location. In eastern Arkansas, near the boundary with Tennessee, we note an observed value in the range of 120 to 145 ppb, while the simulated values range from 100 to 145 ppb in the region. The spatial patterns of observed and simulated O_3 concentrations are also qualitatively similar in New York State, showing generally clean conditions, with concentrations ranging from 40 to 100 ppb. However, there are some high O_3 concentrations observed in south-central Connecticut (125 ppb) and western Connecticut (140 ppb), along the border with New York State, that are not reproduced by the model. The simulated values in the region range from about 80 to 120 ppb.

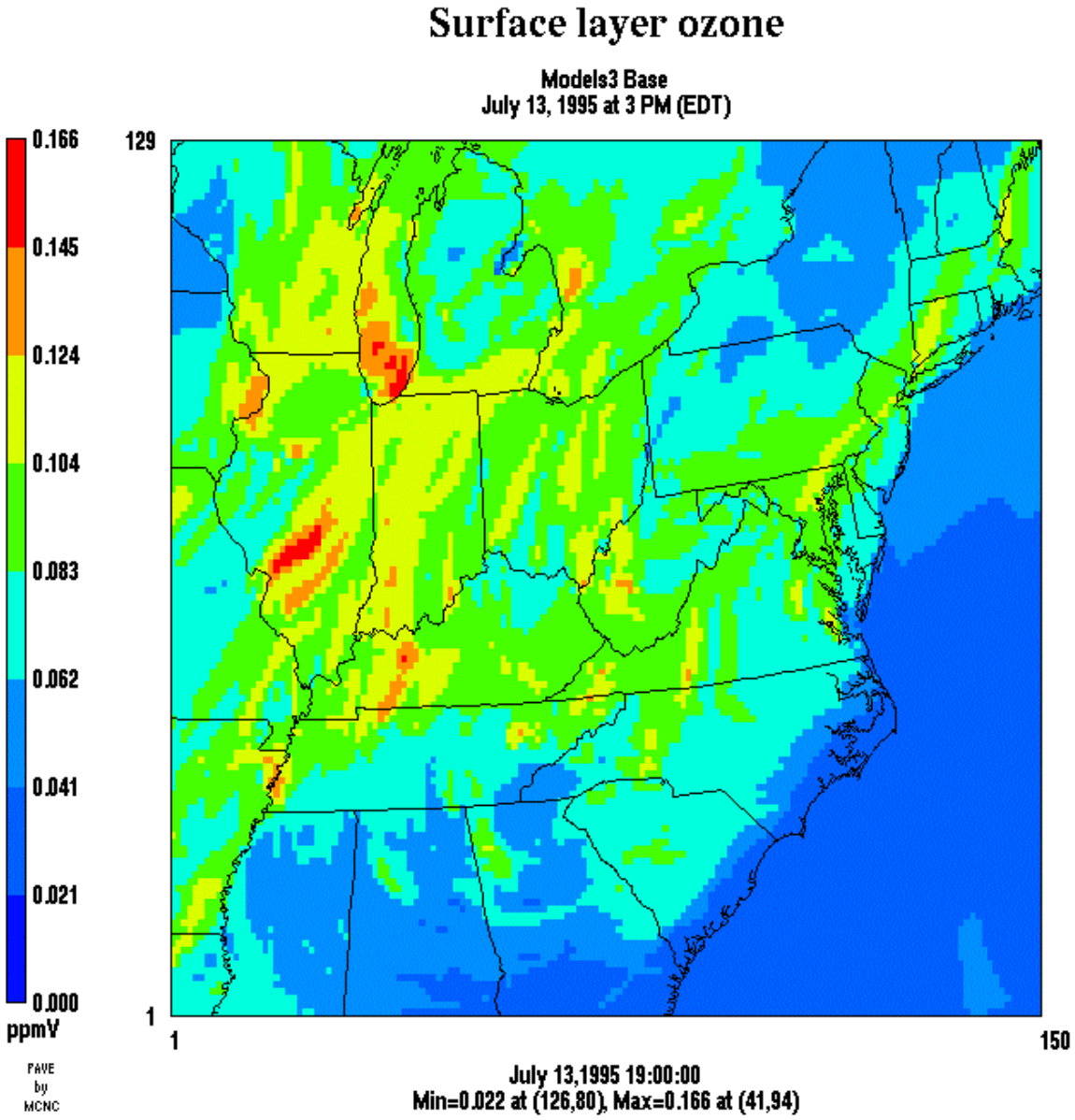

Figure 3-2
Surface O_3 concentrations, Models-3/CMAQ simulation, 12 km resolution domain, 3 p.m. EDT, 13 July 1995.

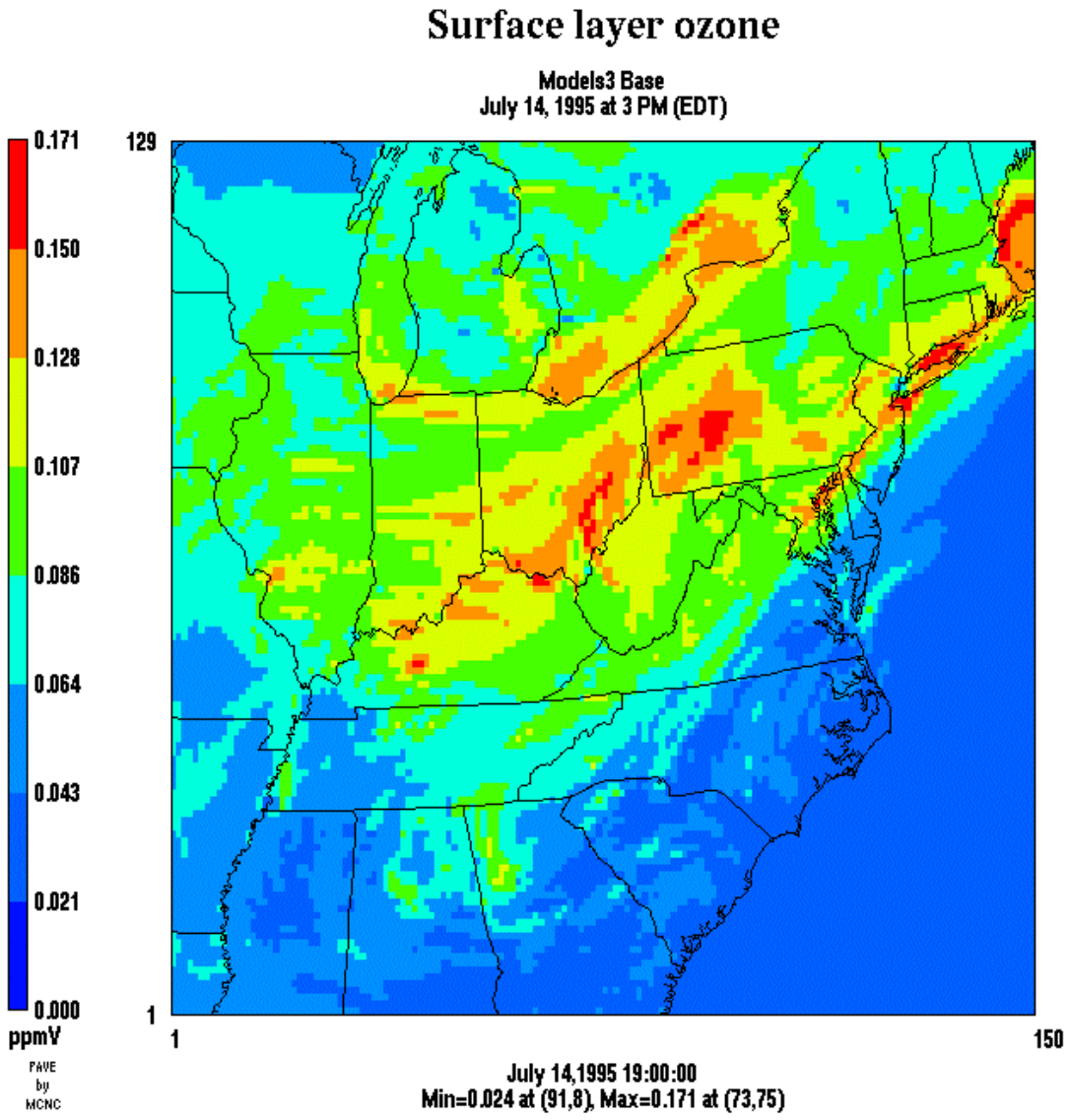

Figure 3-3
Surface O_3 concentrations, Models-3/CMAQ simulation, 12 km resolution domain, 3 p.m. EDT, 14 July 1995.

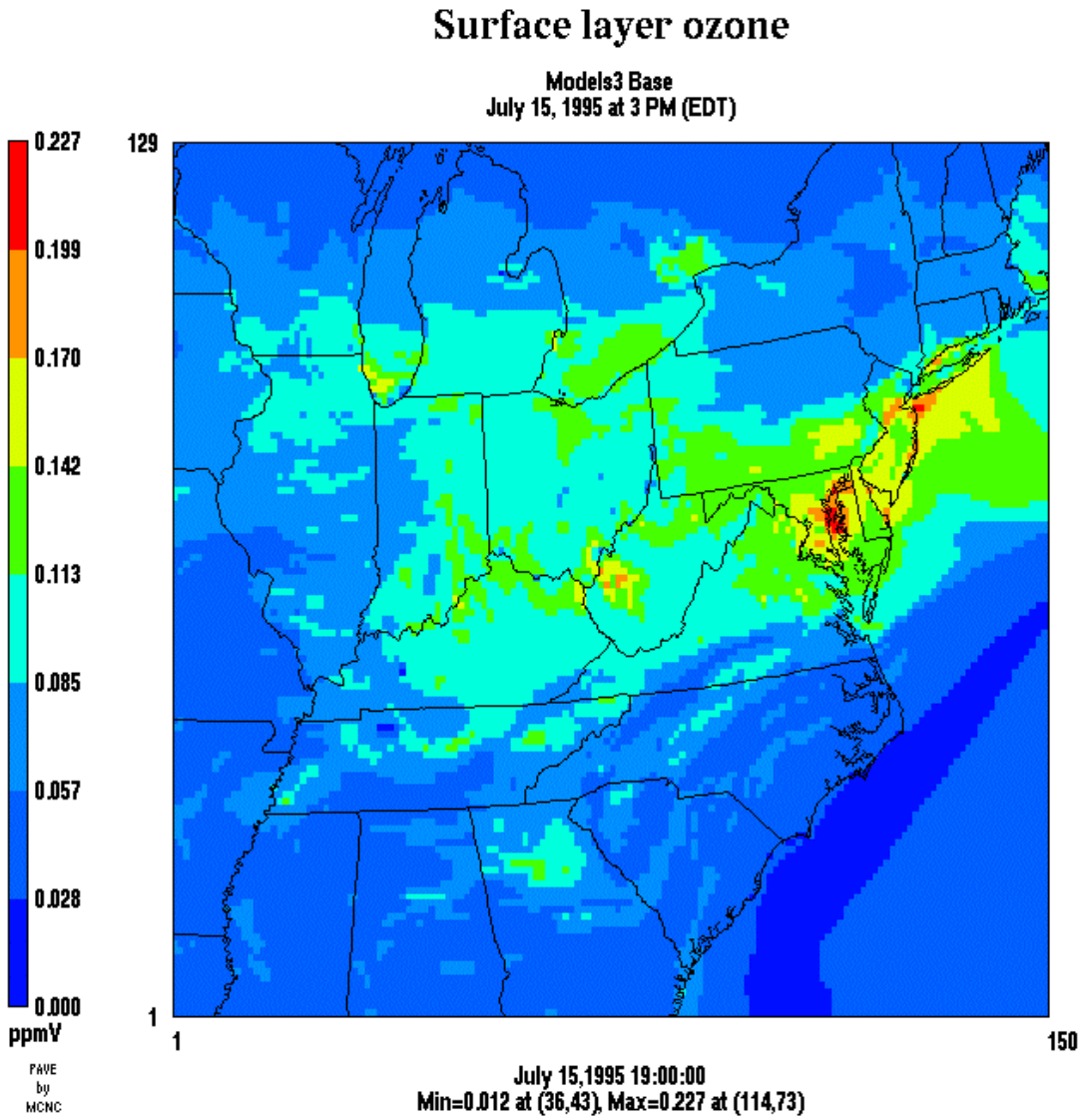

Figure 3-4
Surface O_3 concentrations, Models-3/CMAQ simulation, 12 km resolution domain, 3 p.m. EDT, 15 July 1995.

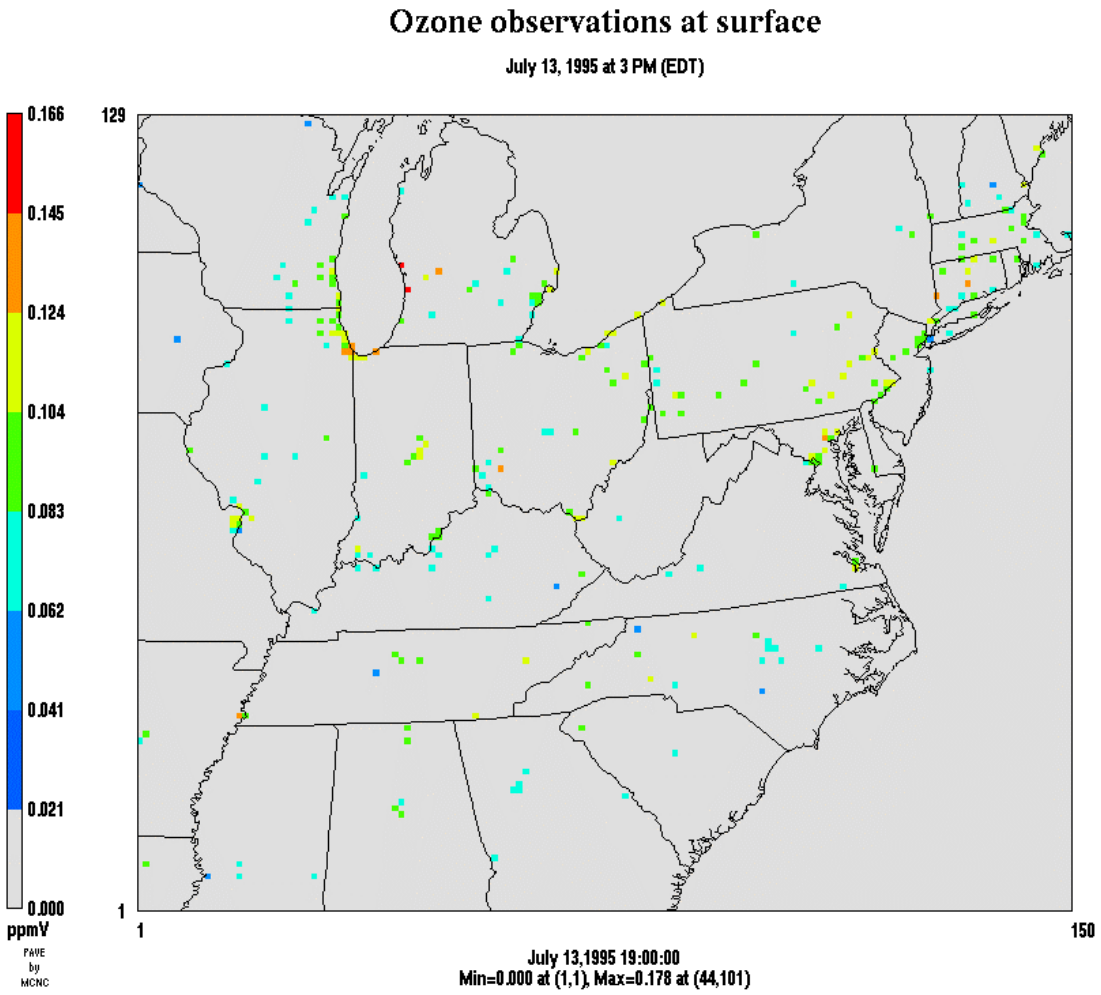

Figure 3-5
Observed surface O_3 concentrations at 3 p.m. EDT on 13 July 1995.

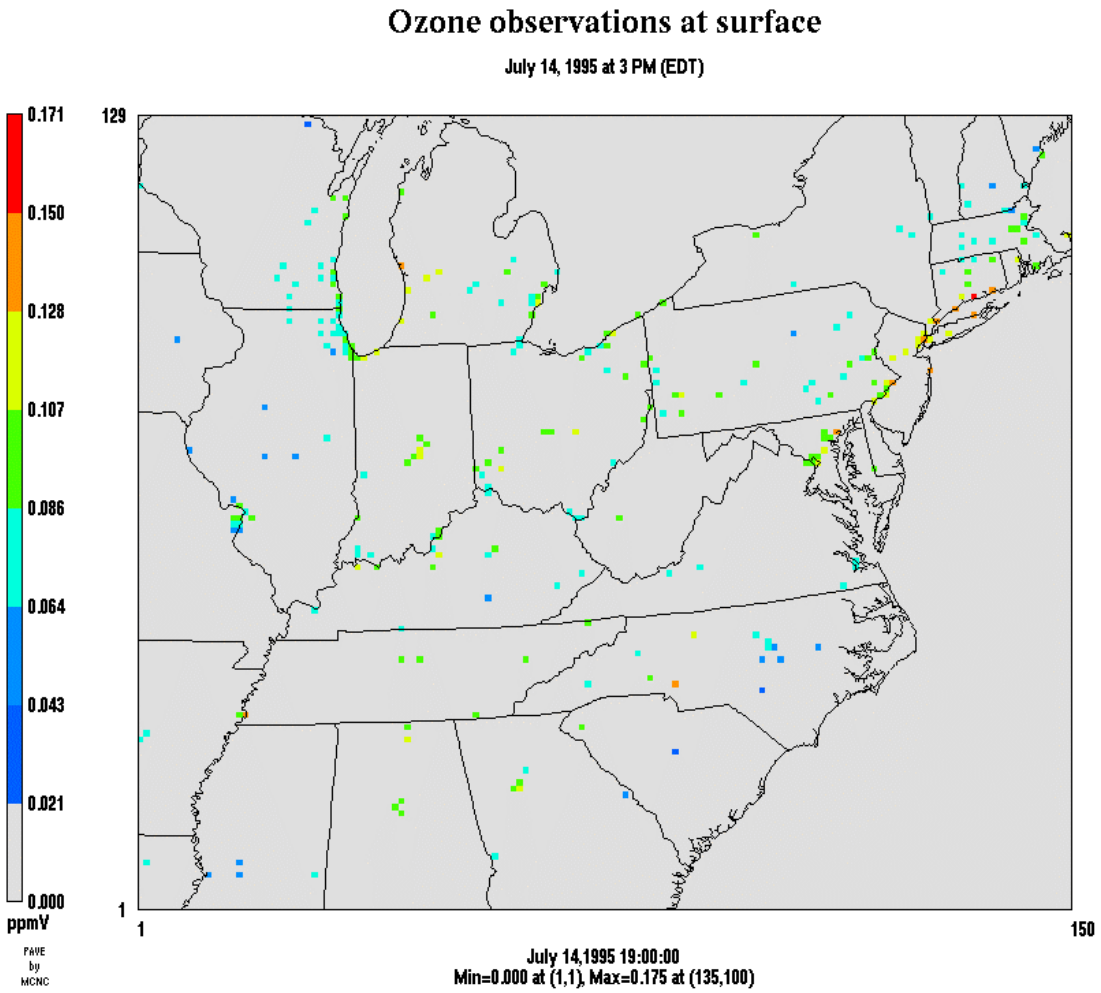

Figure 3-6
Observed surface O_3 concentrations at 3 p.m. EDT on 14 July 1995.

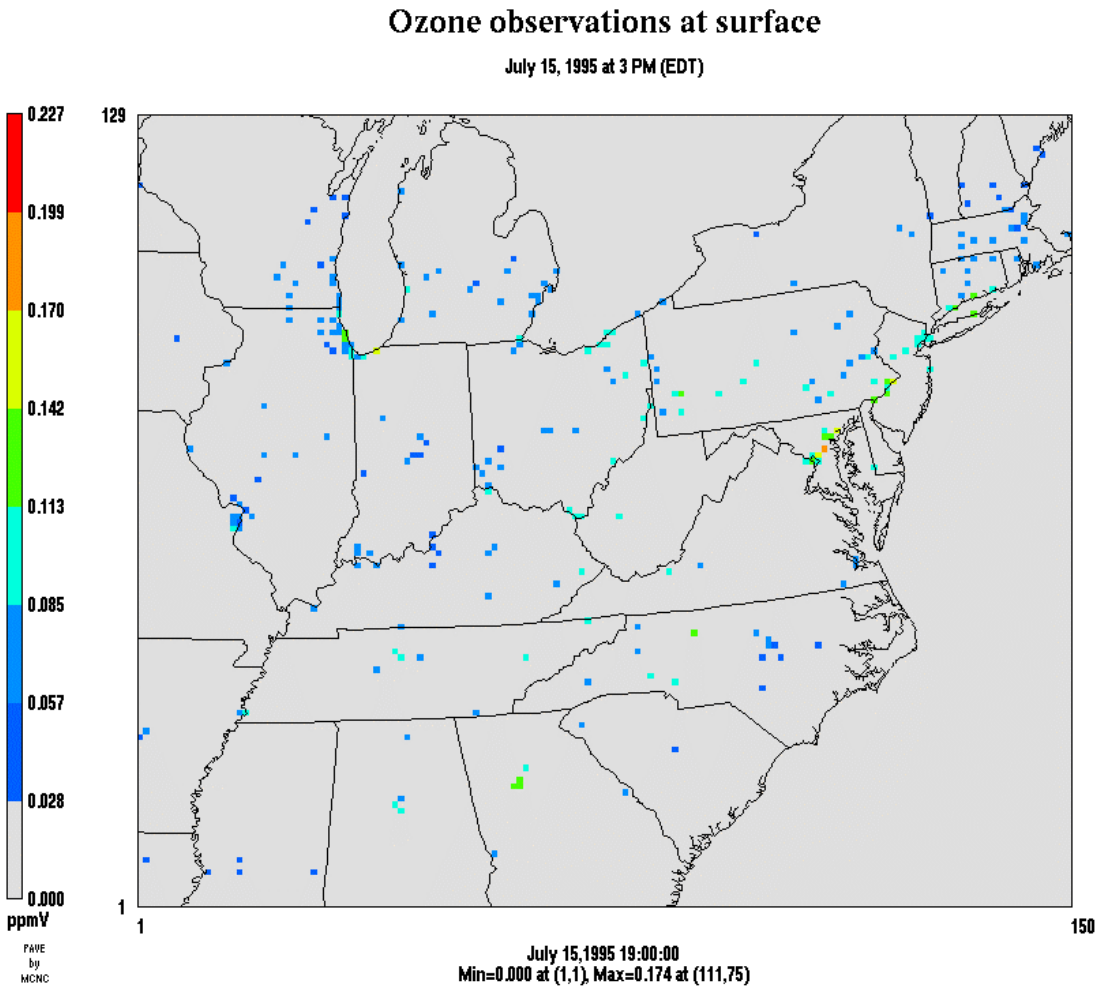

Figure 3-7
Observed surface O_3 concentrations at 3 p.m. EDT on 15 July 1995.

Differences between the observed and simulated patterns of surface O_3 concentrations on July 13 are also seen in northern Illinois and southern Wisconsin and in the region around the Ohio River Valley. In northern Illinois and southern Wisconsin, the observations show generally clean conditions with concentrations ranging from 60 to 100 ppb. The modeled values are higher, ranging from 100 to 140 ppb. As discussed later in Section 3.2.2, some of the discrepancy appears to be associated with transport of NO_x emissions in the base simulation from a large point source in central Illinois to the north and northwest into northern Illinois and southern Wisconsin. This results in an increase in surface O_3 concentrations over the background value of 10 to 20 ppb in the base simulation. When a plume-in-grid approach is used with Models-3/CMAQ-APT, the emissions from the source are primarily transported to the northeast, resulting in O_3 concentrations in the APT simulation that are about 10 ppb lower than the base simulation values, and thus closer to the observed concentrations.

The high observed O_3 concentrations in southern Lake Michigan near Chicago are also comparable with the simulated values. However, the highest observed O_3 concentration of 178 ppb, along the eastern shore of Lake Michigan, is not reproduced by the model. The highest simulated O_3 concentration of 166 ppb occurs in the same region, but about 90 km to the southwest, in southern Lake Michigan.

On July 14 (see Figures 3-3 and 3-6), the observed and simulated spatial patterns in surface O_3 concentrations in the southern portion of the modeling domain are mostly consistent, showing generally clean conditions. However, the model does not reproduce the relatively high O_3 concentrations, ranging from about 130 to 150 ppb, in southern North Carolina and in the tri-state region in southwestern Tennessee. In contrast to July 13, inconsistencies between the observed and simulated spatial patterns are noted in most of Pennsylvania. The base simulation O_3 concentrations in Pennsylvania are generally considerably higher than the observed values. As discussed later in Section 3.2.2, the O_3 concentrations from the APT simulation in western Pennsylvania are lower than the base simulation values by about 10 to 30 ppb, resulting in a better agreement between the APT simulation and observations.

As on July 13, the observed and simulated spatial patterns of O_3 concentrations in the Ohio River Valley region are considerably different. In particular, the high O_3 concentrations predicted by the model in southern Ohio are not seen in the observations. Again, the APT simulation shows lower values than the base simulation in southern Ohio, as discussed later.

In contrast to July 13, both the model and observations show consistent spatial patterns in northern Illinois and southern Wisconsin on July 14, with O_3 concentrations ranging from 60 to 100 ppb. As discussed later, the flows in the region are primarily westerly on July 14, and the NO_x emissions from the large point sources in Illinois are transported to the east in both the base and APT simulations.

As on July 13, the high O_3 concentration (about 130 ppb) observed at the monitoring location along the eastern shore of Lake Michigan is not reproduced in the simulation. The simulated values range from 60 to 100 ppb in the region. The agreement in southern Lake Michigan is better, although the model predicts higher O_3 concentrations than observed.

The maximum observed O_3 concentration of 175 ppb on July 14 occurs in southern Connecticut. The maximum concentration from the base simulation in this region (approximately 25 km to the south of the monitoring location) is about 164 ppb. The maximum concentration in this region from the APT simulation, described in Section 3.2, also occurs at the same location, and is about 166 ppb.

Comparing the simulated and observed O_3 concentration patterns for July 15 (Figures 3-4 and 3-7, respectively), we note that the model reproduces the observed patterns over a large part of the modeling domain. However, the high O_3 concentrations predicted in New Jersey are not seen in the observations. The highest observed and simulated O_3 concentrations are in Maryland on July 15. At the location of the highest observed O_3 concentration of 174 ppb, the simulated values from both the base and APT simulations are also about 174 ppb. The highest O_3 concentrations in the base and APT simulations of 227 and 229 ppb, respectively, occur about 45 km to the southeast of the location of the observed maximum.

The spatial patterns of surface O_3 concentrations in the 4 km resolution domain are presented in Figures 3-8 to 3-10 for July 13 to 15, respectively. These figures show with greater detail the high O_3 concentrations in the northeastern urban corridor. The O_3 concentrations in that domain increase steadily from July 13 to 15, with a maximum O_3 concentration of 133 ppb on July 13 and 183 ppb on July 15.

The temporal variations in O_3 concentrations are presented in Figures 3-11 and 3-12 at three monitoring stations for the 12 km and 4 km resolution domains, respectively. The figures also show the results for the Models-3/CMAQ-APT simulation, discussed in Section 3.2. The model shows poor performance at the Holland, MI station on July 13 and 14, with an underestimation of the peak O_3 concentration on July 13 by about 30 ppb (17%). The model reproduces the O_3 concentration profile well at the Madison, CT station on July 13 but underestimates the peak O_3 concentrations on July 14 and 15 by about 20 to 40 ppb. The O_3 concentrations at the Fort Meade, MD station are well predicted except for an overprediction at midday on July 14 and in the nighttime period on July 15. The peak O_3 concentration on July 15 is well reproduced by the model. The use of a 4 km resolution does not necessarily lead to better performance. For example, the O_3 peak is better predicted at the Fort Meade station on July 14 but not on July 15.

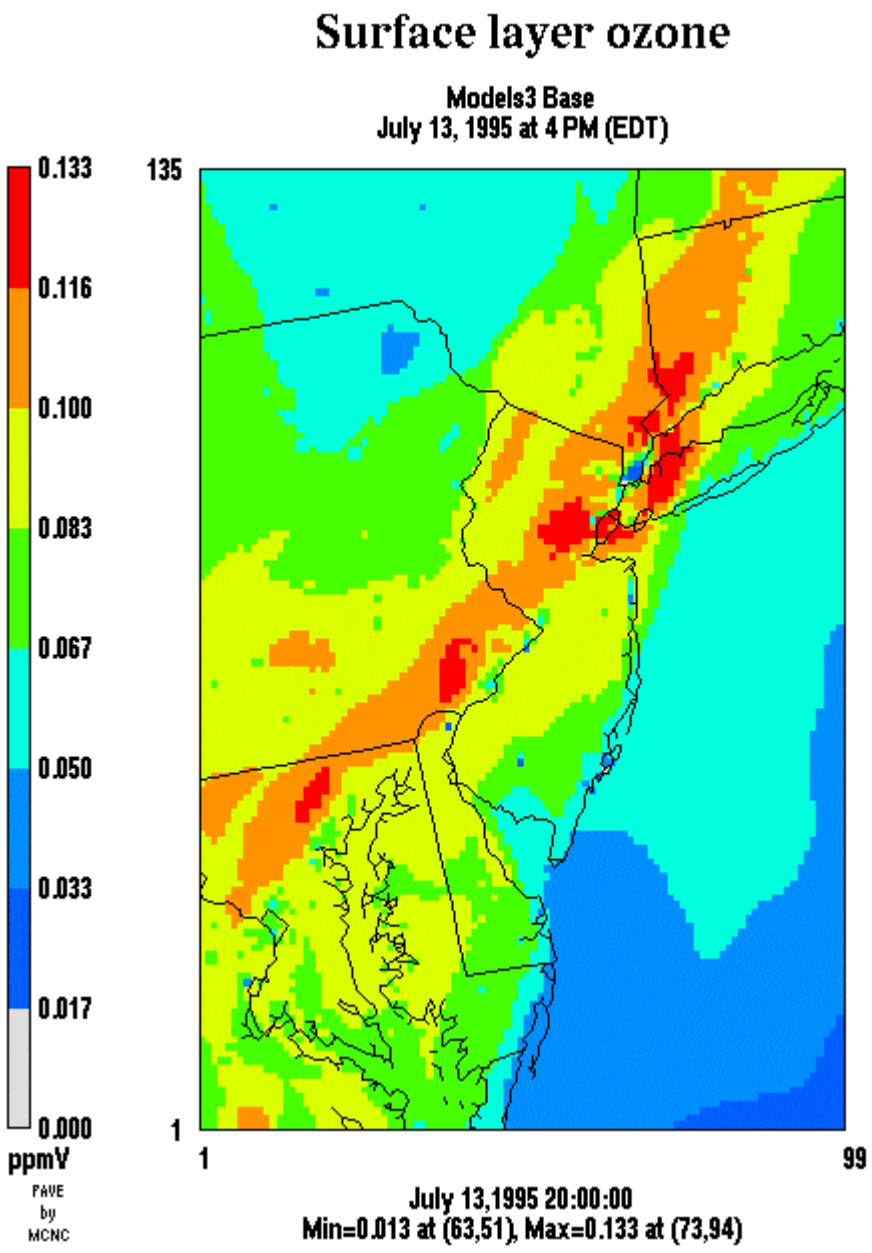

Figure 3-8
Surface O_3 concentrations, Models-3/CMAQ simulation, 4 km resolution domain, 4 p.m. EDT, 13 July 1995.

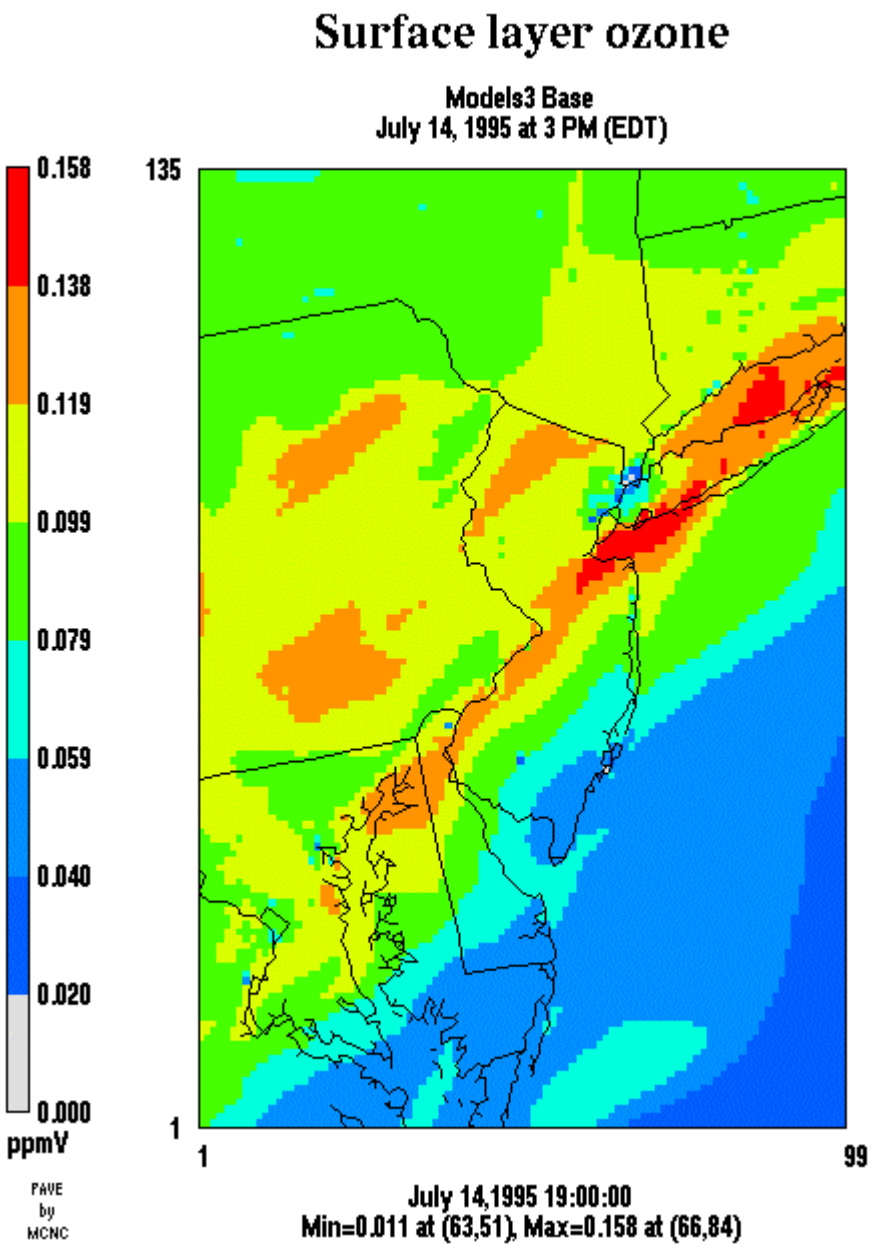

Figure 3-9
Surface O_3 concentrations, Models-3/CMAQ simulation, 4 km resolution domain, 3 p.m. EDT, 14 July 1995.

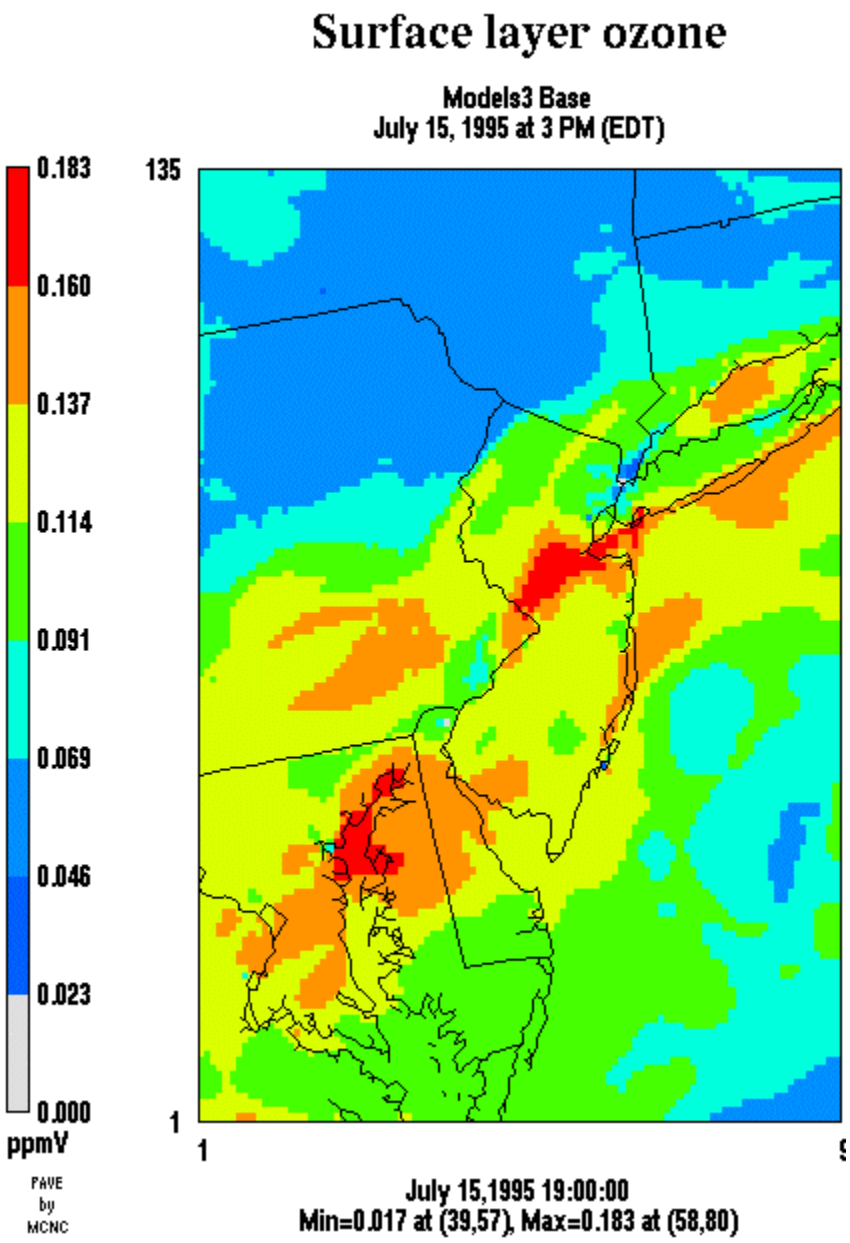

Figure 3-10
Surface O_3 concentrations, Models-3/CMAQ simulation, 4 km resolution domain, 3 p.m. EDT, 15 July 1995.

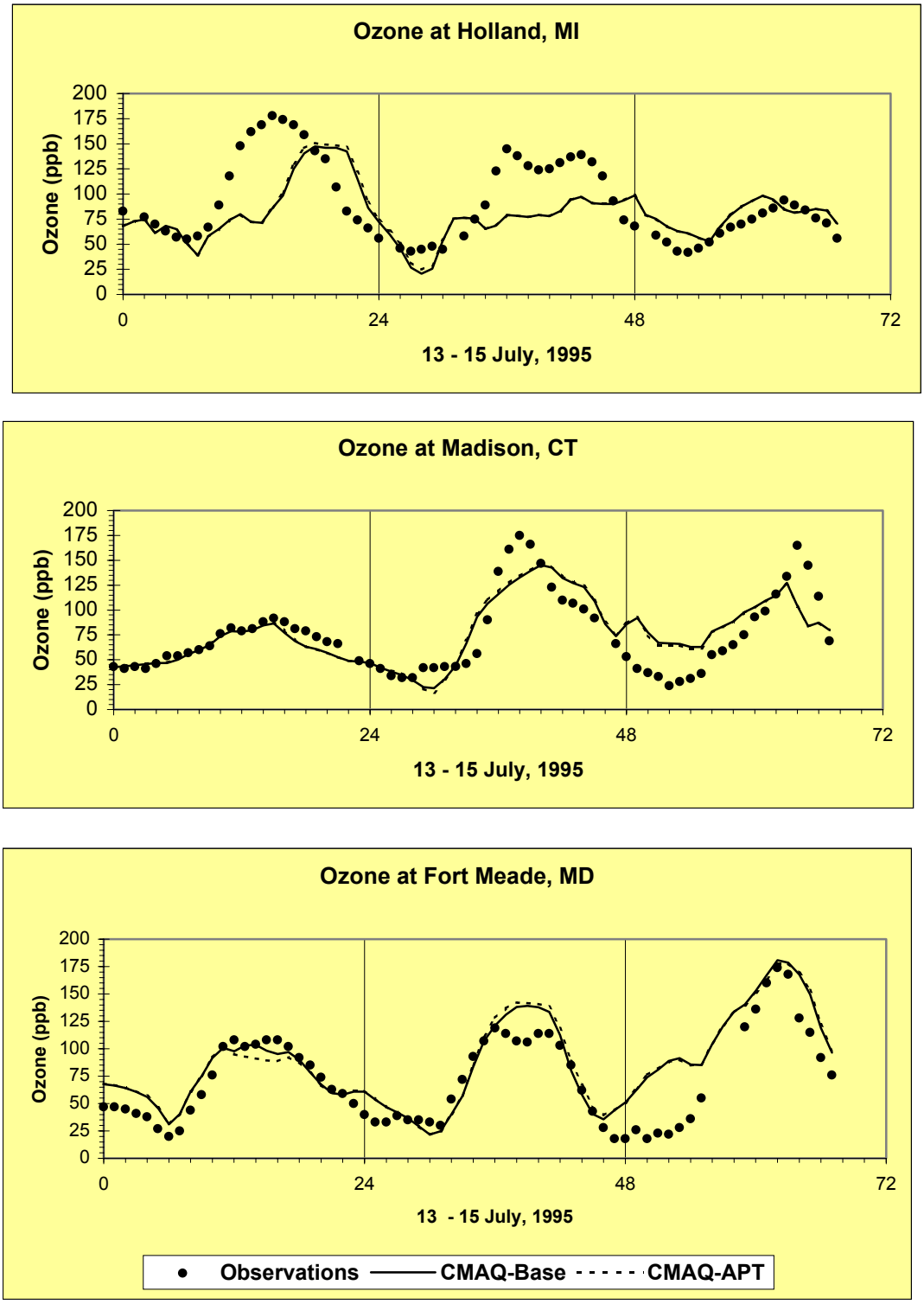

Figure 3-11
Time series of observed and simulated surface O_3 concentrations at three sites, 12 km resolution domain.

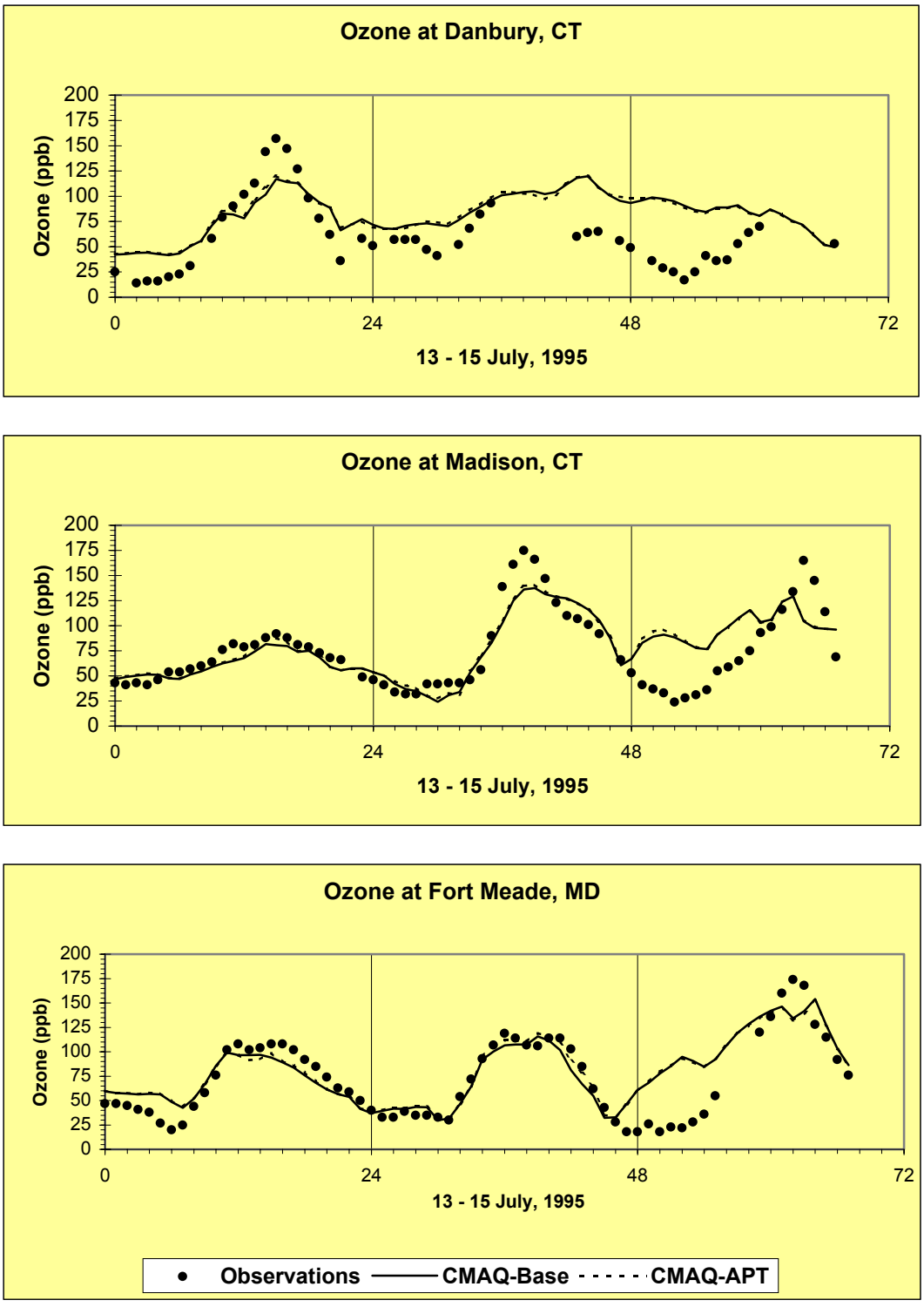

Figure 3-12
Time series of observed and simulated surface O_3 concentrations at three sites, 4 km resolution domain.

The model performance statistics are presented in Tables 3-2 and 3-3 for the 12 km resolution domain and the 4 km resolution domain, respectively. Results are shown for both 1-hour and 8-hour average O_3 concentrations. For the 12 km resolution domain, the error for the peak O_3 concentration paired in space and time is high. The average gross error is of the order of 30% and the average bias is 16%. For the 4 km resolution domain, the performance for the peak O_3 concentration paired in space and time shows an improvement over the 12 km resolution domain results. The gross error and bias are slightly lower than those calculated for the 12 km resolution domain; the gross error is lower by 1 to 2 % and the bias is lower by 8 to 9 %.

3.1.3 HNO_3 Concentrations

The spatial patterns of simulated surface HNO_3 concentrations in the 12 km resolution domain are presented in Figures 3-13 to 3-15 for July 13 to 15, respectively. On July 13, an area located around the Ohio River Valley (Ohio and West Virginia) shows HNO_3 concentrations in the range of 20 to 35 ppb. Most of the HNO_3 concentrations in the rest of the domain are less than 20 ppb. On July 14, an area covering West Virginia and part of Pennsylvania shows HNO_3 concentrations ranging from 15 to 27 ppb. High HNO_3 concentrations (i.e., above 15 ppb) are also predicted near Chicago over southern Lake Michigan and in Connecticut along the Atlantic coast. On July 15, HNO_3 concentrations above 20 ppb are predicted over southern Lake Michigan, in the Ohio River Valley, and in the Maryland/Delaware area.

The spatial patterns of simulated surface HNO_3 concentrations in the 4 km resolution domain are presented in Figures 3-16 to 3-18 for July 13 to 15, respectively. On July 13, the highest HNO_3 concentrations (ranging from 10 to 19 ppb) are predicted near New York City and southwestern Connecticut. On July 14, these high HNO_3 concentrations occur over the Long Island Sound with values ranging up to 22 ppb. A different pattern appears on July 15, with higher HNO_3 concentrations over Maryland (up to 25 ppb); HNO_3 concentrations above 15 ppb are predicted near New York City and on the southern coast of New Jersey.

Table 3-2
Models-3/CMAQ performance statistics for O_3 concentrations for 13-15 July 1995 in the 12 km resolution NARSTO-Northeast domain.

Performance Measure[a]	Performance statistics
1-hour average O_3 concentrations	
Paired peak error[b]	-52%
Gross error	32%
Fractional gross error	0.29
Bias	16%
Fractional bias	0.09
8-hour average O_3 concentrations	
Paired peak error[b]	-37%
Gross error	28%
Fractional gross error	0.25
Bias	16%
Fractional bias	0.10

(a) Performance measures are as defined by Seigneur et al. (2000); statistics are for observed O_3 concentrations greater than 40 ppb at 299 sites.
(b) Paired in both space and time.

Table 3-3
Models-3/CMAQ performance statistics for O_3 concentrations for 13-15 July 1995 in the 4 km resolution NARSTO-Northeast domain.

Performance Measure[a]	Performance statistics
1-hour average O_3 concentrations	
Paired peak error[b]	-22%
Gross error	31%
Fractional gross error	0.31
Bias	7%
Fractional bias	-0.01
8-hour average O_3 concentrations	
Paired peak error[b]	-10%
Gross error	26%
Fractional gross error	0.26
Bias	8%
Fractional bias	0.02

(a) Performance measures are as defined by Seigneur et al. (2000); statistics are for observed O_3 concentrations greater than 40 ppb at 64 sites.
(b) Paired in both space and time.

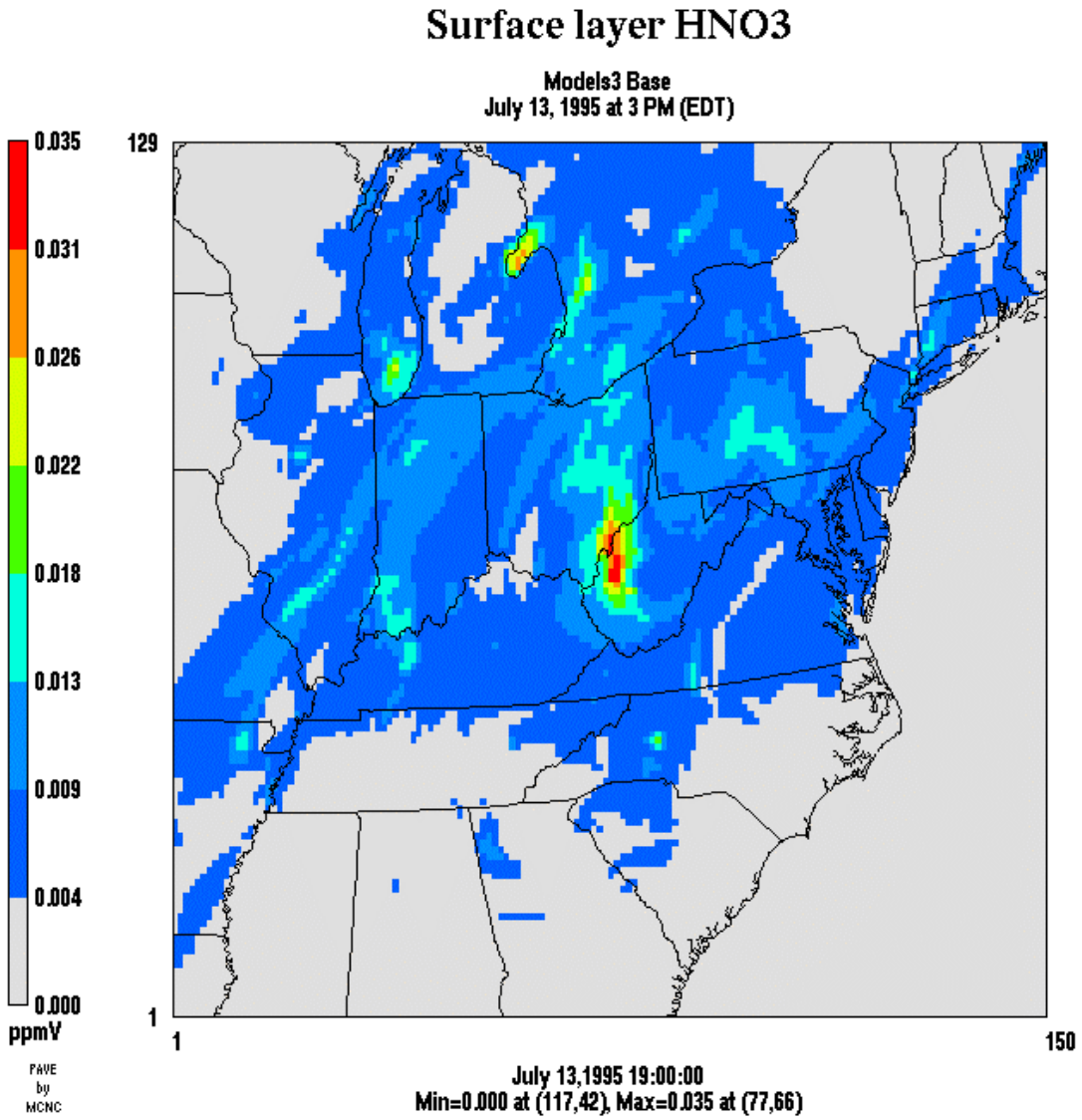

Figure 3-13
Surface HNO_3 concentrations, Models-3/CMAQ simulation, 12 km resolution domain, 3 p.m. EDT, 13 July 1995.

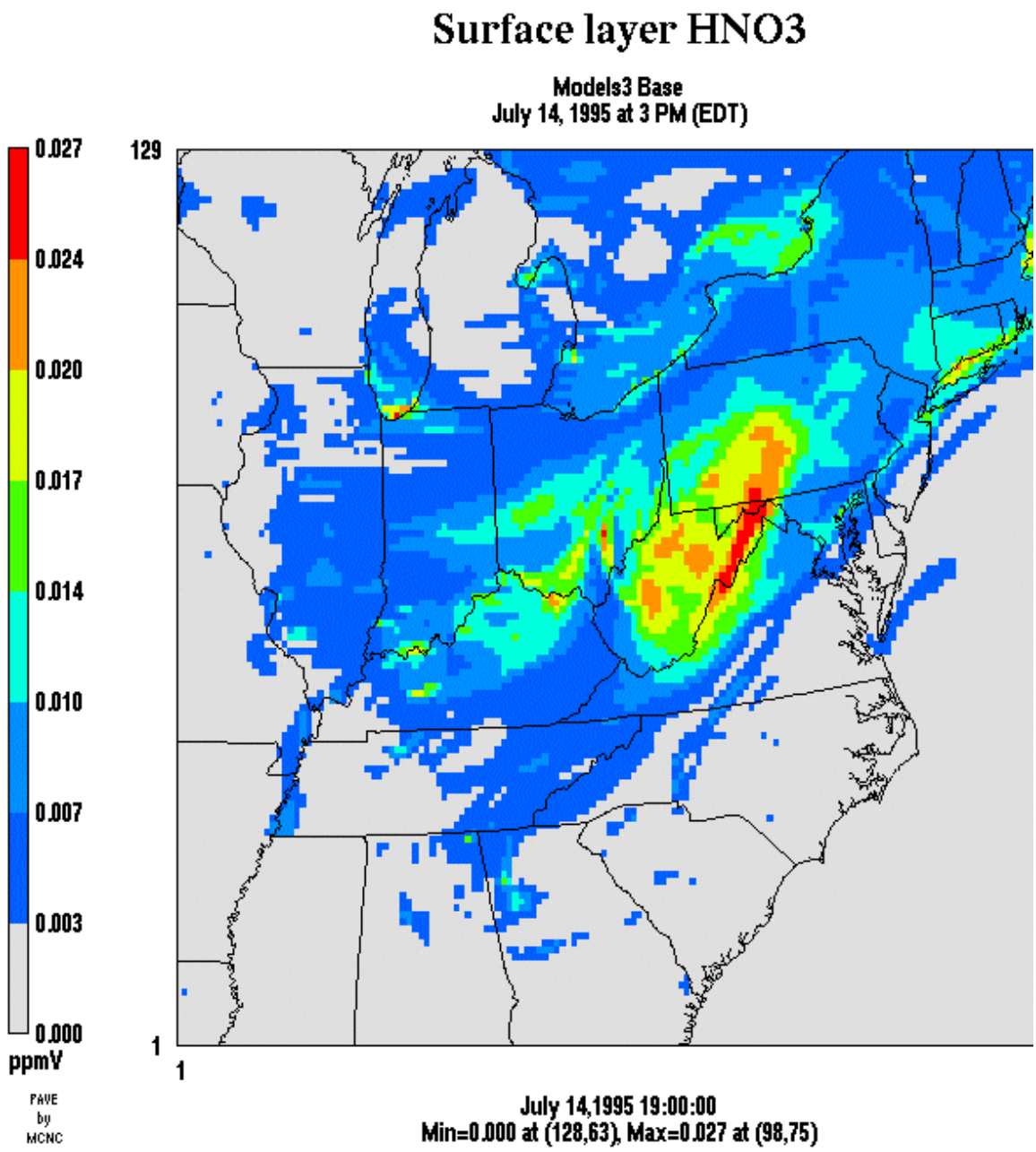

Figure 3-14
Surface HNO_3 concentrations, Models-3/CMAQ simulation, 12 km resolution domain, 3 p.m. EDT, 14 July 1995.

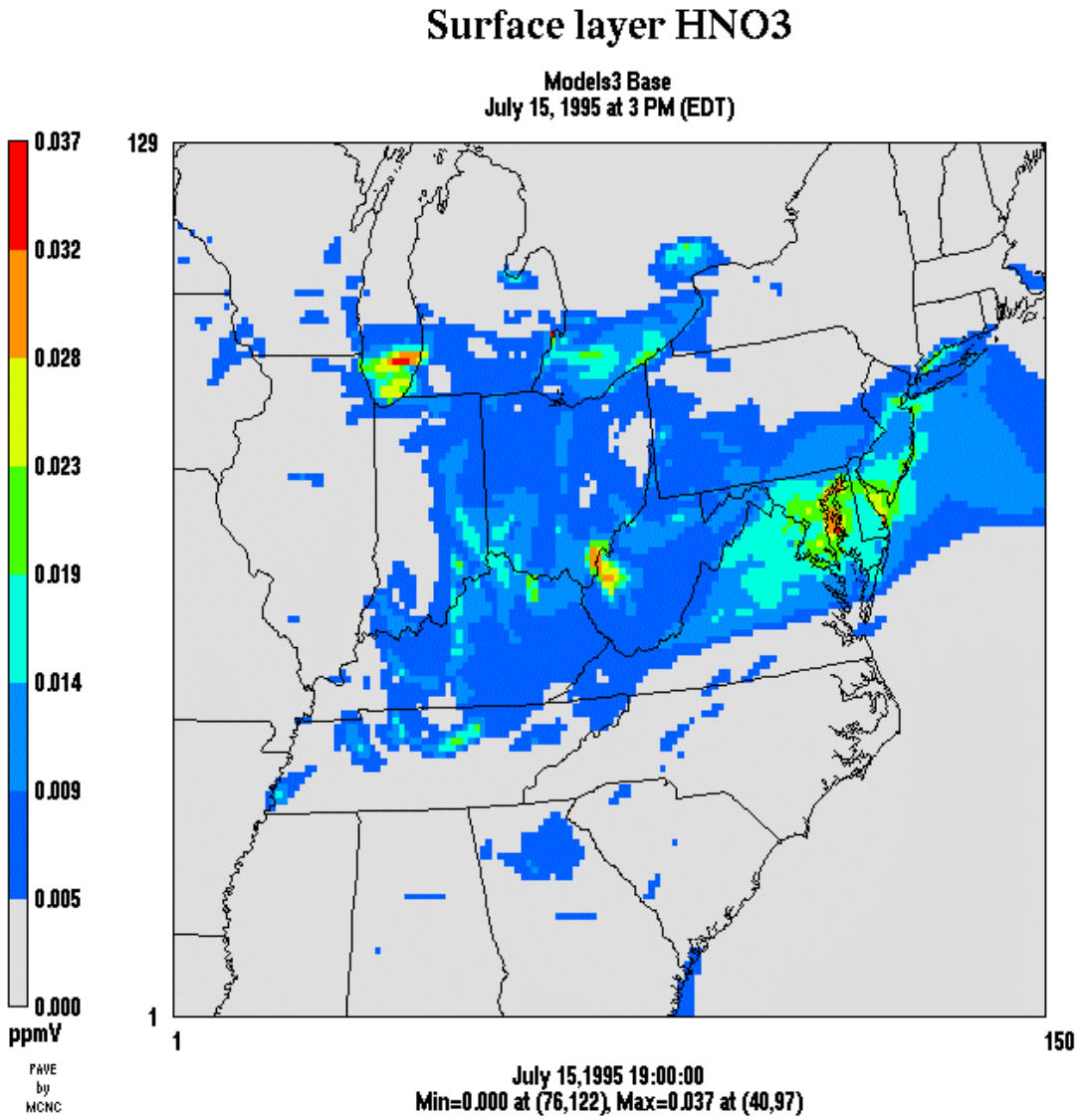

Figure 3-15
Surface HNO_3 concentrations, Models-3/CMAQ simulation, 12 km resolution domain, 3 p.m. EDT, 15 July 1995.

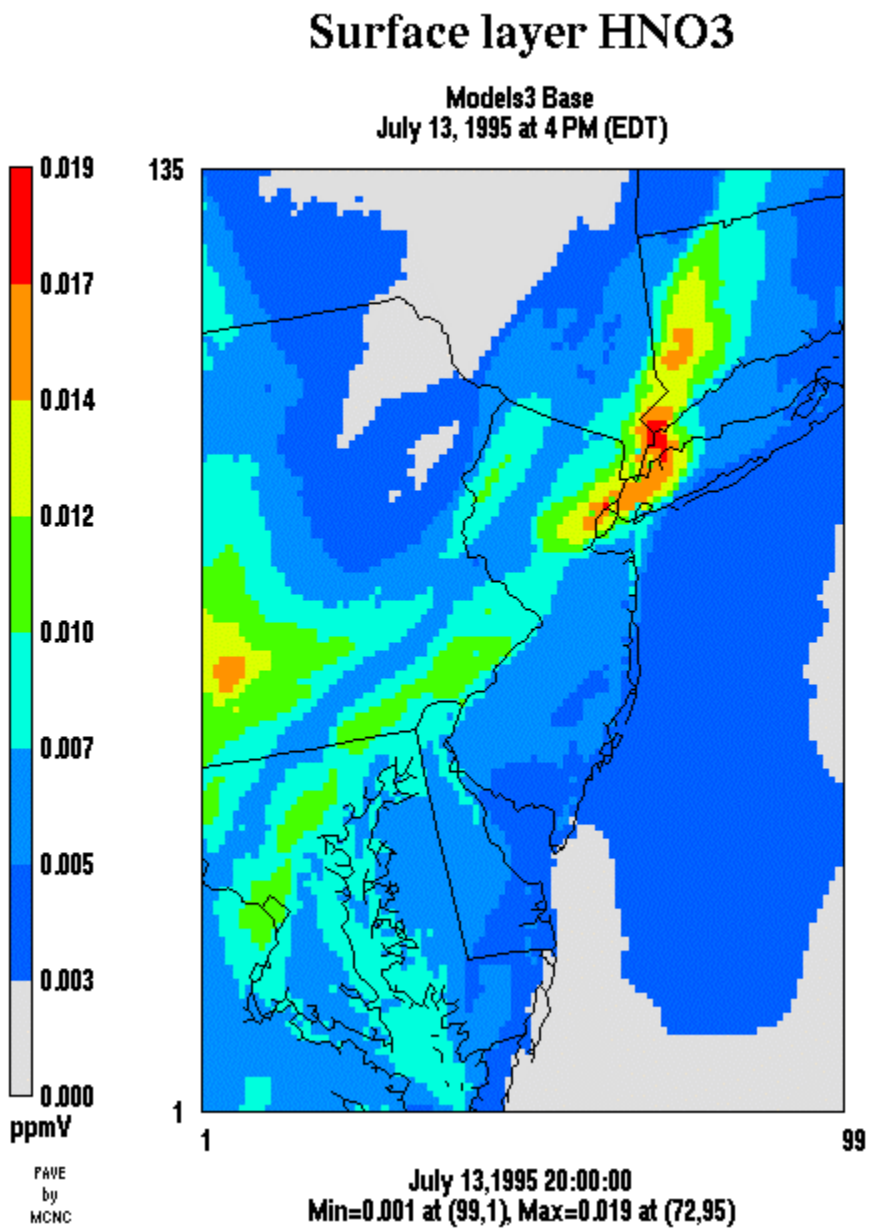

Figure 3-16
Surface HNO_3 concentrations, Models-3/CMAQ simulation, 4 km resolution domain, 4 p.m. EDT, 14 July 1995.

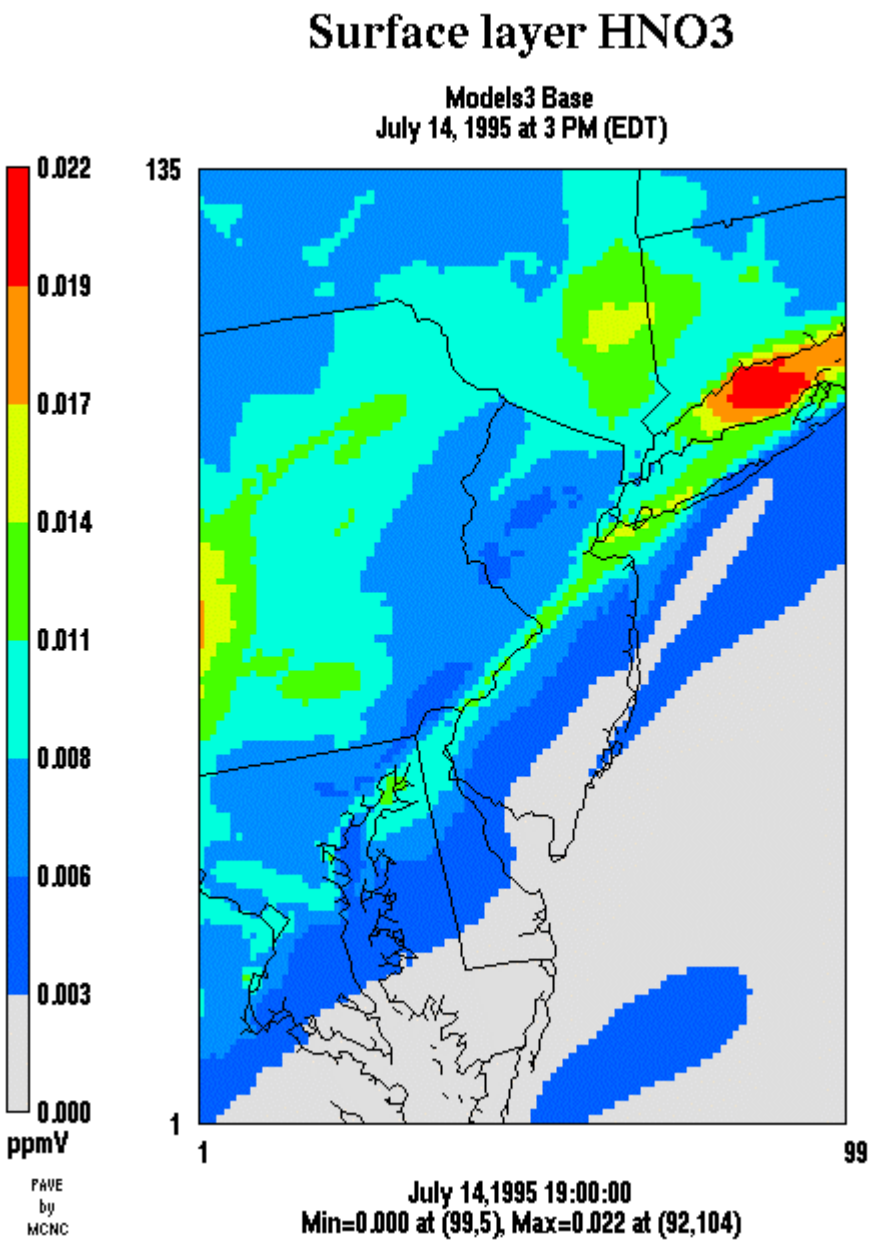

Figure 3-17
Surface HNO_3 concentrations, Models-3/CMAQ simulation, 4 km resolution domain, 3 p.m. EDT, 14 July 1995.

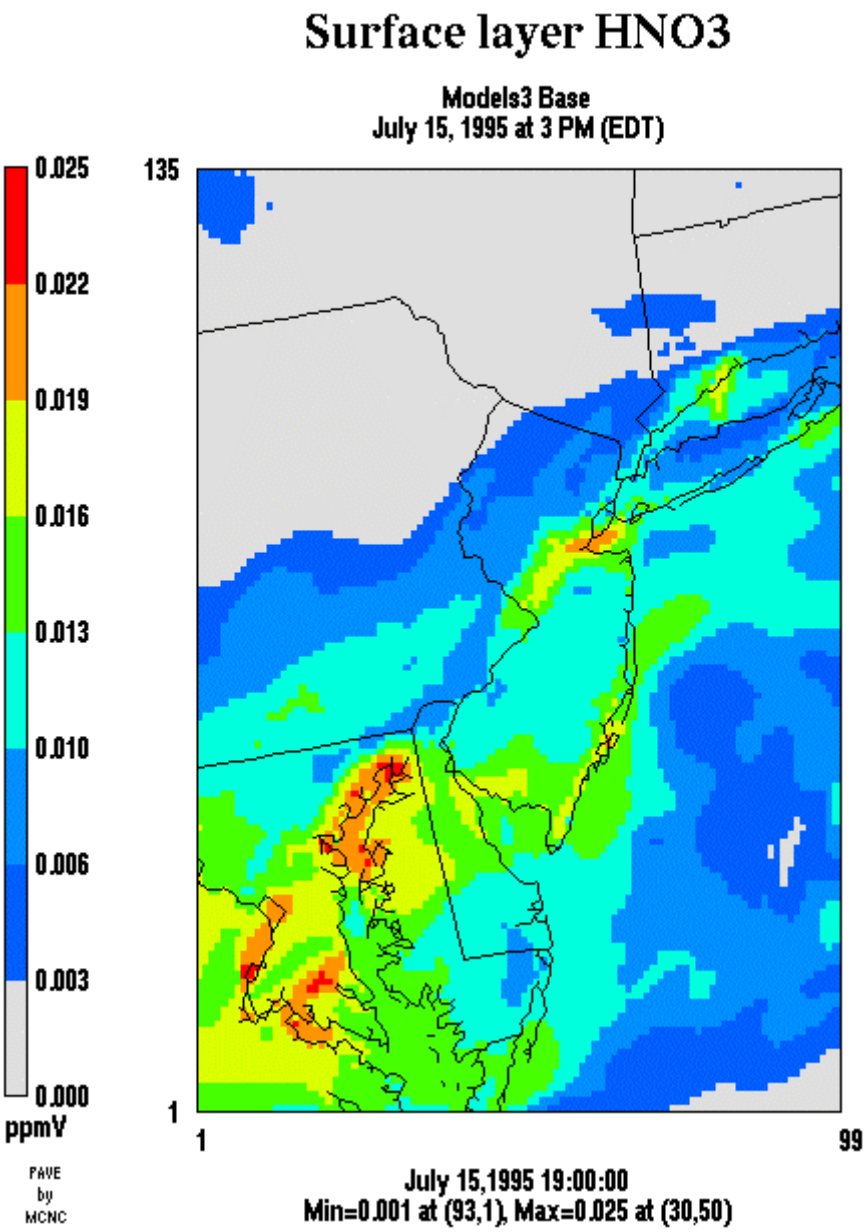

Figure 3-18
Surface HNO_3 concentrations, Models-3/CMAQ simulation, 4 km resolution domain, 3 p.m. EDT, 15 July 1995.

3.2 Models-3/CMAQ – APT Simulation

3.2.1 Overview of the Plume-in-Grid Simulation

Thirty point sources with the highest NO_x emission rates were selected for explicit plume treatment in the Models-3/CMAQ-APT simulation. Figure 3-19 shows the location of these sources (some of these sources are aggregates of stacks in the same grid cell). The 30 point sources selected represent 14% of the total NO_x emission inventory over the modeling domain.

The results of the Models-3/CMAQ-APT simulations are presented in comparison with the Models-3/CMAQ base simulation. The spatial plots are presented as the difference in O_3 or HNO_3 concentrations between the Models-3/CMAQ-APT simulation and the Models-3/CMAQ base simulation. Therefore, a positive value means that the explicit treatment of point sources with the plume-in-grid model leads to a greater concentration of O_3 or HNO_3; a negative value means that the plume-in-grid treatment leads to a lower concentration. The results are presented for the same time periods as in the previous spatial plots from the base Models-3/CMAQ simulation, i.e., at the time of the maximum observed O_3 concentration in the modeling domain for each day from July 13 to July 15.

Small differences between Models-3/CMAQ-APT and the base Models-3/CMAQ are shown in gray (about 4 ppb for O_3 and 1 ppb for HNO_3 in the 12 km resolution domain, 2 ppb for O_3 and 0.3 ppb for HNO_3 in the 4 km resolution domain.) Positive differences are represented by yellow, orange and red colors in order of increasing value. Negative differences are represented by green, light blue and dark blue colors in order of increasing absolute value.

3.2.2 O_3 Concentrations

Figure 3-20 shows the effect of the plume-in-grid treatment on the surface O_3 concentrations for the 12 km resolution domain at 3 p.m. EDT on July 13, 1995. Several distinct patterns are seen in the figure. We discuss these patterns for some selected point sources and regions in the modeling domain.

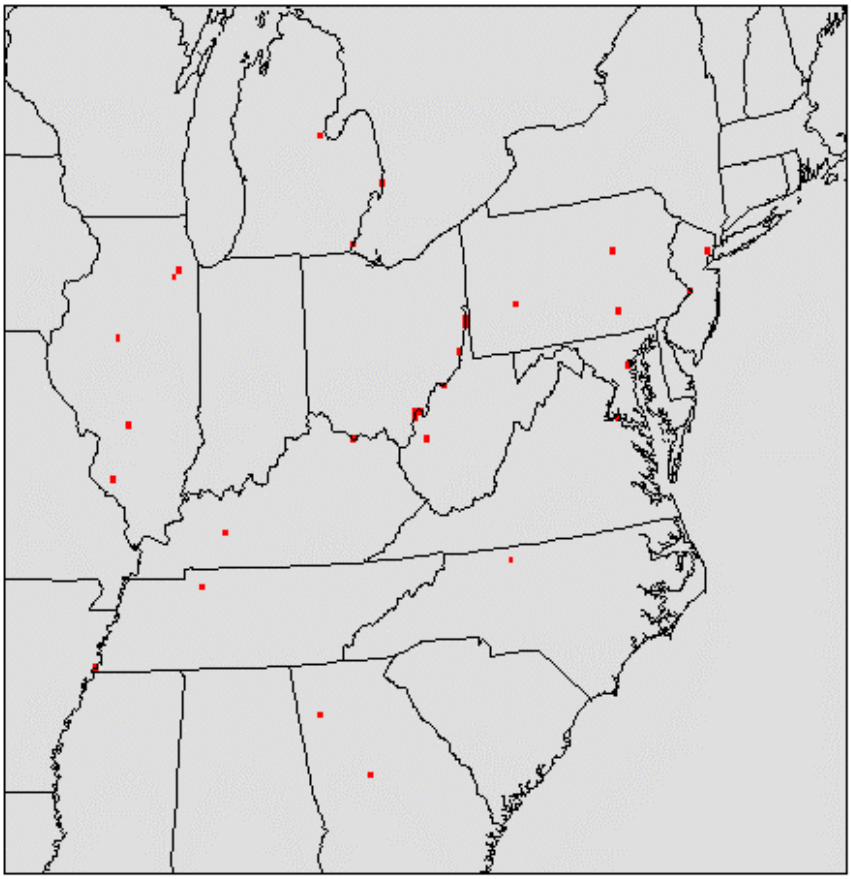

Figure 3-19
Location of point sources with explicit plume-in-grid treatment.

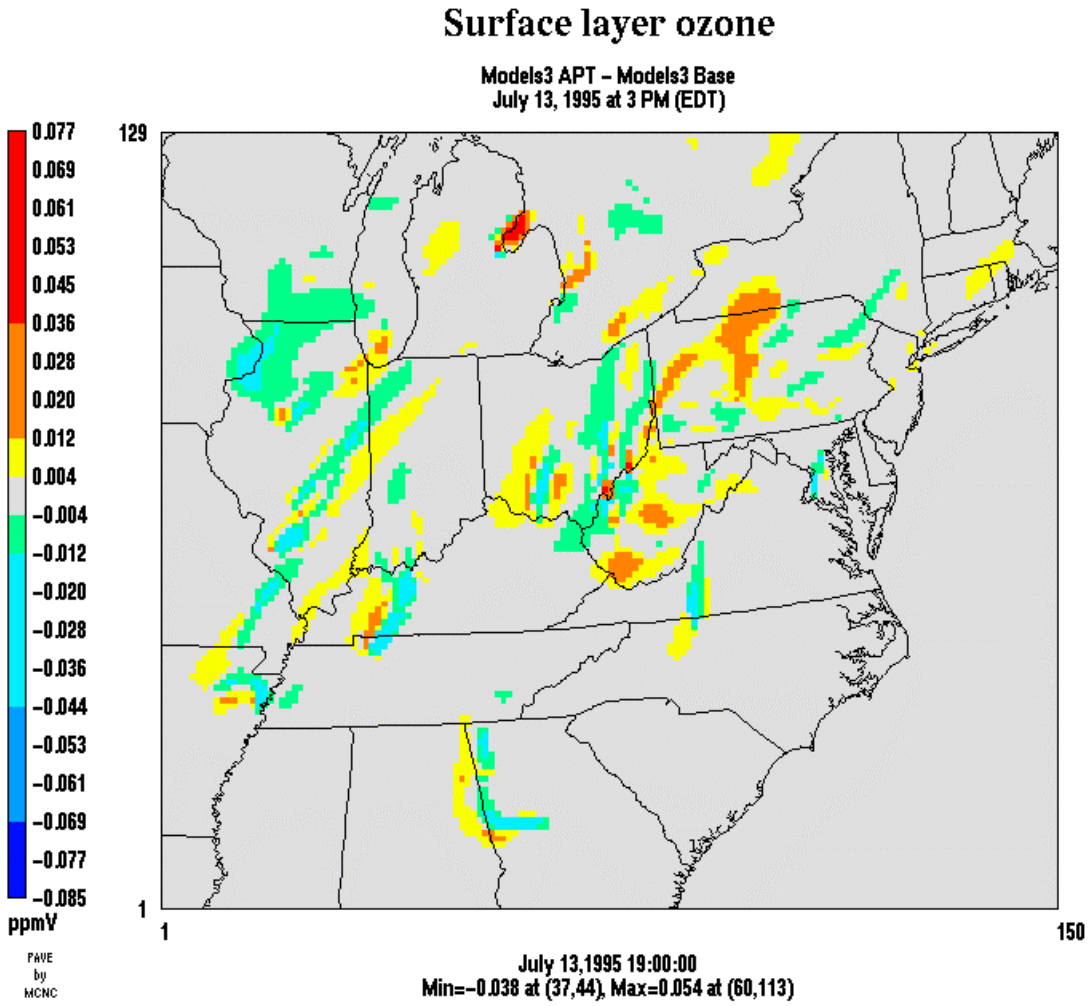

Figure 3-20
Differences (APT – Base) in surface O_3 concentrations, 12 km resolution domain, 3 p.m. EDT, 13 July 1995.

For isolated NO_x point sources that are located in an environment that is primarily NO_x-limited for O_3 formation, the effect of plume-in-grid treatment on O_3 concentrations follows the pattern that was discussed in detail by Karamchandani et al. (2000a) for the Cumberland and Paradise power plants in the Nashville/Tennessee simulation. Here, this pattern is best exemplified by the point source located in North Carolina because it is fairly well isolated from other point sources with plume-in-grid treatment. This source has the fifth highest NO_x emissions of the 30 point sources selected for plume-in-grid treatment for the 12 km resolution domain.

Figure 3-20 shows that, on July 13, the winds are southerly near the vicinity of the North Carolina source, and the plume travels to the north. The plume-in-grid treatment results in small increments in O_3 concentrations (of the order of about 5 to 10 ppb) near and upwind of the source and large decrements in O_3 concentrations (of the order of 20 to 30 ppb) from about 15 to 85 km immediately downwind, as compared to the base simulation. The near-source increment results from the fact that the plume-in-grid treatment prevents the rapid mixing of the plume NO to the surface and, consequently, there is less titration of the existing O_3 by plume NO. Further downwind, the plume-in-grid treatment reduces the formation of O_3 from the point source NO_x emissions by limiting the availability of the plume NO_x. In the base simulation, plume NO_x is rapidly mixed within the grid system and is therefore available for the production of O_3. In the Models-3/CMAQ-APT simulation, the NO_x emitted from the point source is mixed with the background air according to the rate of the plume dispersion and O_3 formation is delayed until the plume has become sufficiently diluted.

Even further downwind, the O_3 decrements become smaller, and the two simulations give identical results at about 170 km downwind. At downwind distances beyond 170 km, the O_3 concentrations from the plume-in-grid simulation are slightly higher (of the order of 2 to 3 ppb) than, or comparable to, the O_3 concentrations from the base simulation. These small increments in O_3 concentrations at very large downwind distances may be due to differences in the VOC/NO_x ratio in those grid cells between the Models-3/CMAQ-APT and Models-3/CMAQ base simulations. Since the plume-in-grid treatment will disperse the plume NO_x more slowly, the NO_x concentrations in the grid cells will be greater than in the base simulation once the plume size becomes commensurate with the grid cell size or the plume is chemically mature. Once O_3 formation starts to take place in the plume, these higher NO_x concentrations will enhance O_3 formation compared to the base simulation if the background environment is NO_x-limited.

The APT simulation also gives small O_3 increments of about 2 to 9 ppb above the base simulation at the eastern edge of the plume up to about 100 km from the source. These increments appear to be due to the scavenging of O_3 in the base simulation by the NO_x emitted from the source, as discussed later below.

To better understand the effect of using a plume-in-grid treatment, we conducted another simulation for the 12 km resolution domain with Models-3/CMAQ without the emissions from the 30 largest NO_x emitting point sources selected for PiG. The concentrations from this simulation can be considered to be "background" values for the point sources. Relative to the results from this "background" simulation, the Models-3/CMAQ-APT simulation and the Models-3/CMAQ base simulation will show the effect of the NO_x emissions from these point sources with and without PiG treatment, respectively. In other words, we can get a measure of

the ozone (and nitric acid) that can be produced (or titrated, in the case of O_3) in the plumes of these point sources with and without PiG treatment, particularly for isolated sources.

Figure 3-21 shows the difference between O_3 concentrations from the base and background simulations at 3 p.m. EDT on July 13, 1995. For many of the point sources, high ozone plumes are clearly visible with increments in downwind surface O_3 concentrations of 30 to 40 ppb over the background value. Figure 3-22 shows the corresponding effect of the 30 point sources on ozone concentrations for the APT simulation. In contrast to the base simulation, the downwind O_3 increments are generally lower (of the order of 10 to 20 ppb) but spread over a larger region.

Focussing on the isolated North Carolina point source, we see from Figure 3-21 that up to 40 ppb of ozone can be produced in the plume due to the NO_x emissions from this source when a PiG treatment is not used. The maximum plume O_3 concentration in the base simulation is about 127 ppb and occurs due north of the source at a downwind distance of about 50 km. This concentration is about 40 ppb higher than the background value of 87 ppb. In contrast, as shown in Figure 3-22, the maximum ozone produced in the North Carolina point source plume in the APT simulation is about 12 ppb at a location about 34 km northwest of the source. The O_3 concentration from the APT simulation at this location is about 105 ppb, the background value is about 93 ppb, and the base simulation O_3 concentration is 109 ppb, about 16 ppb higher than the background value.

Also, as discussed previously, we see from Figure 3-21 that, in the base simulation, the North Carolina point source emissions scavenge the surface ozone directly upwind (south) of the source and downwind along the eastern edge of the plume to a distance of about 100km from the source. This results in small decrements in O_3 concentrations of about 4 ppb south of the source and from 2 to 9 ppb on the eastern edge of the plume. In contrast, in the APT simulation, we see from Figure 3-22 that there is no scavenging of the surface O_3 directly south of the source and along the eastern edge of the plume. However, increments in surface ozone concentrations of up to about 11 to 12 ppb occur upwind to the southwest of the source and downwind along the western edge of the plume to the northwest of the source. The latter increment corresponds to the maximum O_3 produced in the APT simulation for this point source. These results also suggest that there are some differences in wind direction between the surface layer and layers aloft, so that some of the NO_x emitted from the point source travels in slightly different directions in the base and APT simulations.

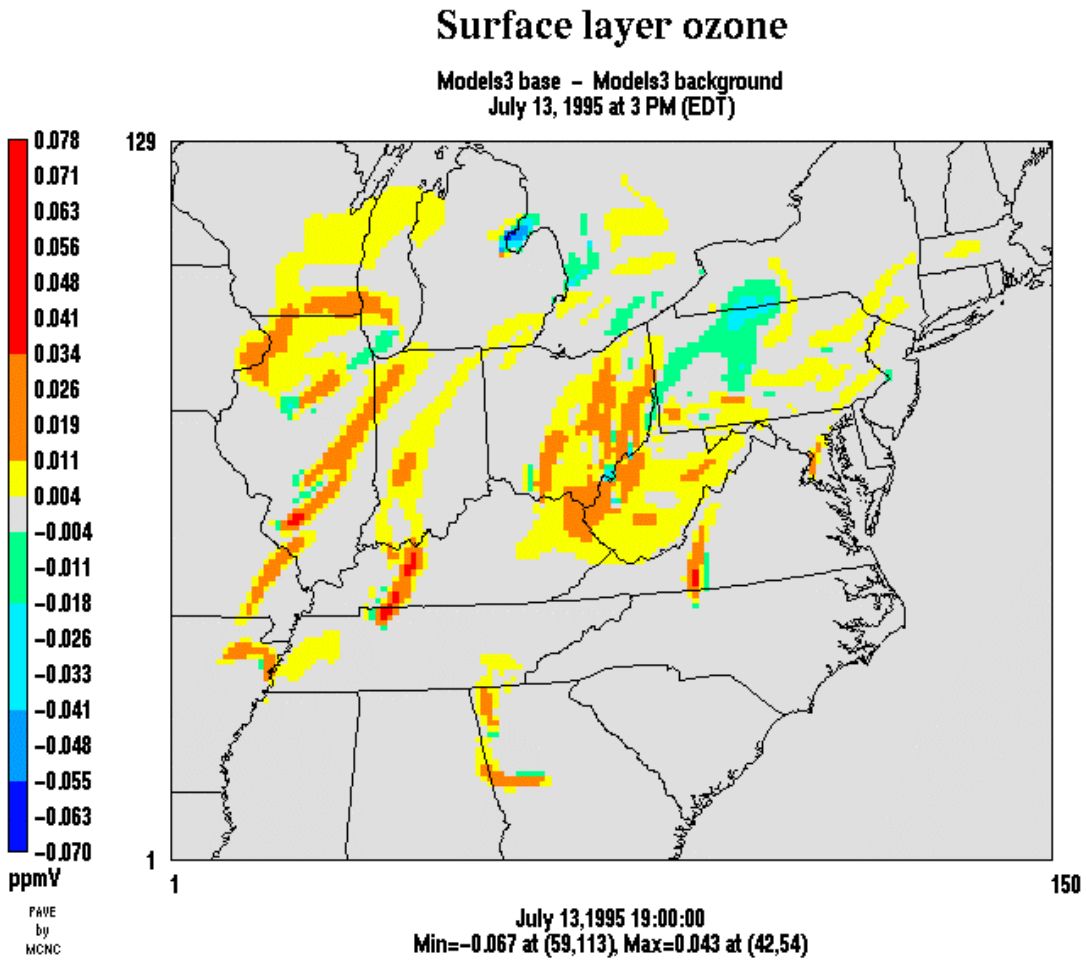

Figure 3-21
Differences (Base – Background) in surface O_3 concentrations, 12 km resolution domain, 3 p.m. EDT, 13 July 1995. The "Background" corresponds to a Models-3/CMAQ simulation without the emissions from the 30 point sources selected for PiG treatment.

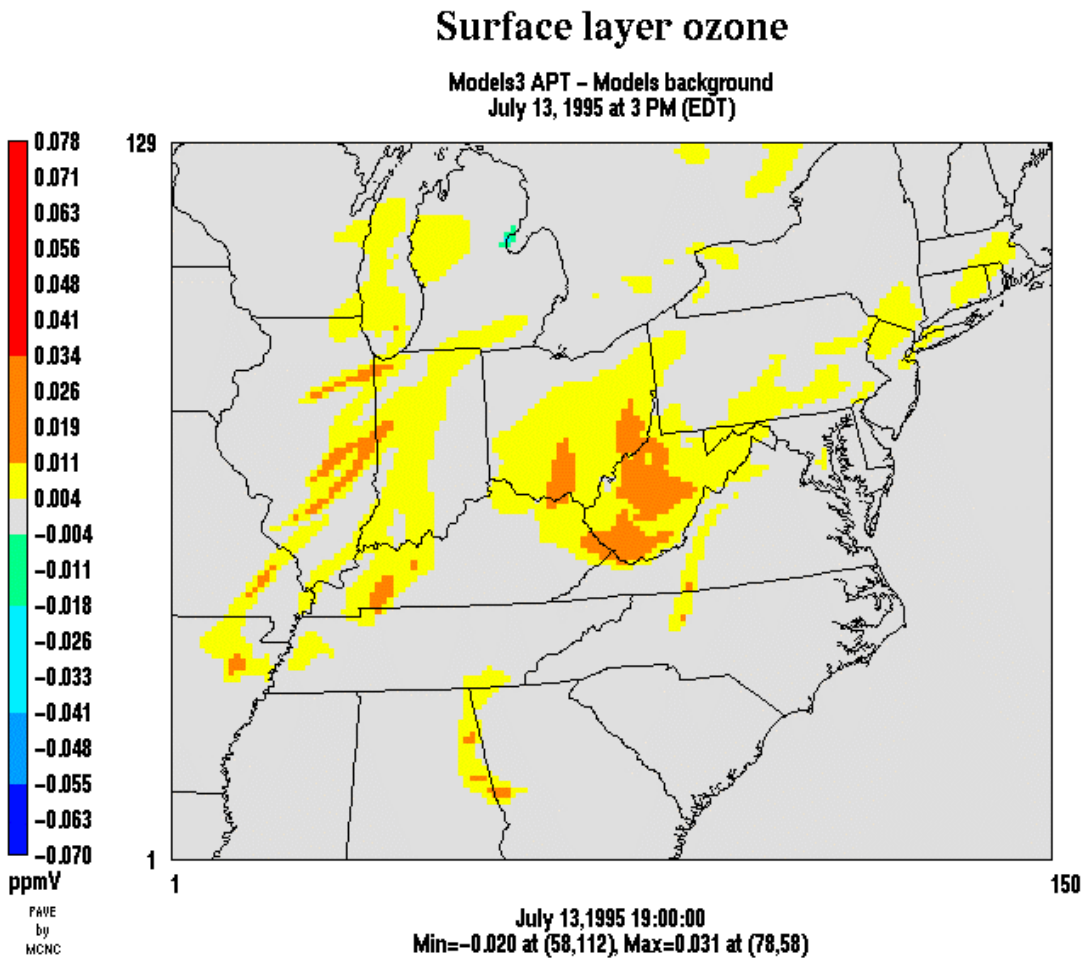

Figure 3-22
Differences (APT – Background) in surface O_3 concentrations, 12 km resolution domain, 3 p.m. EDT, 13 July 1995. The "Background" corresponds to a Models-3/CMAQ simulation without the emissions from the 30 point sources selected for PiG treatment.

Thus, for the North Carolina source, we see that the increases in ozone concentrations due to the source emissions are much smaller when the PiG treatment is used. The maximum ozone that can be attributed to the NO_x emissions from the source in the APT simulation is about 30 ppb lower than that produced in the base simulation on July 13. This is further illustrated by Figure 3-23, which shows the surface ozone concentrations from the background, base, and APT simulations downwind (to the north and north-east) of the North Carolina source at 3 p.m. EDT on July 13, 1995. In the base simulation, shown by the solid line, we note that rapid O_3 production begins immediately downwind of the source. The difference between the O_3 concentrations from the base and background simulations is about 25 ppb at about 20 km downwind from the source. The maximum increase, as noted previously, is about 40 ppb at 50 km downwind. Even at a downwind distance of 120 km, the ozone in the base simulation is about 15 ppb higher than the background value. In contrast, in the APT simulation, the increase in downwind O_3 concentrations above the background value is less than 5 ppb at 25 km from the source and grows to a maximum of about 10 ppb at about 80 to 100 km.

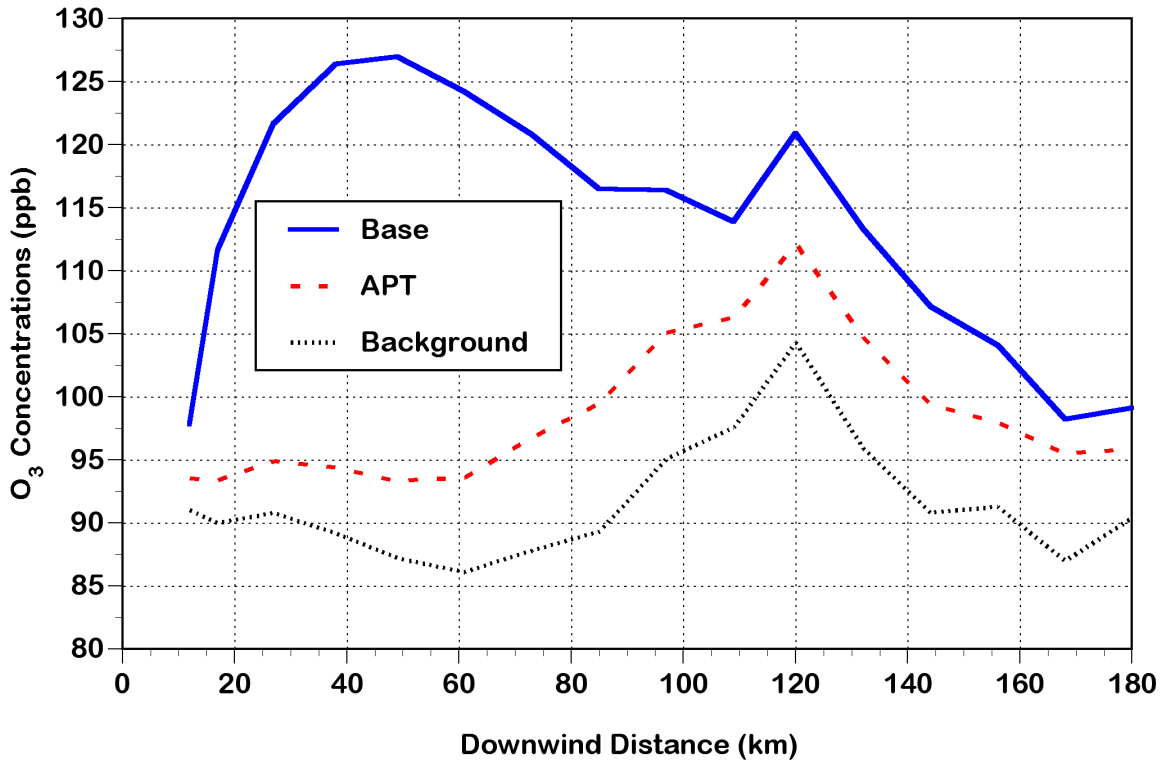

Figure 3-23
Surface O_3 concentrations downwind of the North Carolina point source, 12 km resolution domain, 3 p.m. EDT, 13 July 1995.

We also examine the plume ozone concentrations in more detail for some other selected sources for which it is easy to discern the effect of the plume-in-grid treatment. The TVA Cumberland power plant was the largest NO_x emitter in the modeling domain for the period simulated. It is situated in a rural location in northern Tennessee, near the border with Kentucky, and approximately 80 km west of Nashville. The TVA Paradise power plant was the third largest NO_x emitter and is located in Kentucky approximately 107 km NNE of the Cumberland power plant.

The results for the Cumberland and Paradise power plants are qualitatively similar to the results for the North Carolina point source. From Figure 3-20, we see that, on July 13, the Cumberland plume travels towards the NNE, and ultimately merges with the Paradise power plant plume. We also see that the APT simulation gives O_3 concentrations that are significantly lower (by about 20 to 40 ppb) than the base simulation downwind of the Cumberland power plant along the plume centerline. The APT simulation gives higher O_3 concentrations (by about 5 to 20 ppb) than the base simulation upwind of the source and along the western edge of the plume.

Figure 3-21 shows that, in the base simulation, there is initial scavenging of the surface O_3 of about 4 ppb upwind of the Cumberland power plant and of up to about 7 ppb along the western edge of the plume. However, rapid O_3 production begins immediately downwind of the source. The peak O_3 production in the Cumberland plume in the base simulation is about 41 ppb over the background value of 101 ppb and occurs at about 43 km northeast of the power plant. The O_3

concentration at this location from the APT simulation is about 106 ppb, lower than the base simulation value by 37 ppb, and higher than the background value by about 5 ppb. In contrast, the peak O_3 production in the Cumberland plume in the APT simulation occurs further downwind at about 70 km north of the power plant and is about 15 ppb over the background value of about 109 ppb (Figure 3-22). The base simulation O_3 concentration at this location is 105 ppb, lower than the background value by about 4 ppb.

Similarly, Figure 3-20 shows that the APT simulation downwind O_3 concentrations in the combined Cumberland-Paradise plume are significantly lower (by as much as 30 ppb) than the base simulation downwind O_3 concentrations on July 13. The maximum downwind O_3 production in the base simulation in the combined plume is about 43 ppb over the background value of about 100 ppb (Figure 3-21) and occurs northeast of the Paradise power plant a distance of about 43 km from the plant. This is also the location of the maximum downwind O_3 production in the APT simulation (Figure 3-22). The APT simulation O_3 concentration at this location is about 112 ppb, higher than the background simulation value by about 12 ppb and lower than the base simulation value by about 31 ppb.

Similar patterns are noted for the two point sources in southwestern and south-central Illinois, and the point source in north-central Illinois. The plumes from these sources travel towards the northeast on July 13. The plume from the southwestern Illinois source eventually merges with that from the south-central Illinois source. The maximum ozone produced in the base simulation in the plume is about 38 ppb over the background value of 105 ppb (Figure 3-21). This maximum occurs northeast of the source at a distance of approximately 50 km. The APT simulation O_3 concentration at this location is about 115 ppb, 10 ppb above the background value and 28 ppb below the base simulation value. The maximum ozone produced in the APT simulation is about 16 ppb over the background value of 115 ppb (Figure 3-22), and occurs to the northeast of the source at a much larger distance (approximately 140 km) than the base simulation. The base simulation O_3 concentration at this location is 127 ppb, 12 ppb higher than the background value and 4 ppb lower than the APT simulation value. Similarly, the base simulation gives a maximum ozone production northeast from the south-central Illinois point source of 23 ppb above the background value of 131 ppb, at a distance of approximately 34 km. The O_3 concentration from the APT simulation at this location is 144 ppb, 13 ppb above the background value and 10 ppb below the base simulation value. The corresponding APT maximum ozone production from the south-central Illinois source also occurs northeast of the source, but at a larger downwind distance of approximately 85 km (Figure 3-22). The APT O_3 concentration at this location is 125 ppb, 18 ppb above the background value of 107 ppb, and 5 ppb below the base simulation value of 130 ppb.

For the north-central Illinois point source, the maximum increase in O_3 concentrations over the background values in the base simulation is about 24 ppb on July 13, and occurs northeast of the source at a distance of approximately 70 km (Figure 3-21). The base simulation O_3 concentration at this location is 111 ppb, the background value is 87 ppb, and the APT simulation value is 98 ppb, 11 ppb above the background and 13 ppb below the base simulation value. The maximum ozone produced in the APT simulation from this source occurs to the NNE at a much larger downwind distance (approximately 190 km). The O_3 concentration from the APT simulation at this location is about 118 ppb, about 17 ppb over the background value of 101 ppb, and 10 ppb higher than the base simulation value of 108 ppb (Figure 3-22). Also note that some of the emissions from this source are transported north into Wisconsin in the base

simulation, leading to O_3 formation of 5 to 17 ppb above the background value in northern Illinois and southern Wisconsin (Figure 3-21). On the other hand, Figure 3-22 shows that there is little transport in this direction in the APT simulation. Thus, the O_3 concentrations from the APT simulation in northern Illinois and southern Wisconsin are comparable to the background value, resulting in the APT simulation giving lower O_3 concentrations in the region compared to the base simulation (Figure 3-20).

Somewhat different patterns are seen in the comparison of the APT and base simulations in other regions of the modeling domain, possibly due to differences in the VOC/NO_x ratios as well as to differences in the meteorology and configurations of major point sources treated with plume-in-grid. For example, although the eastern U.S. is primarily NO_x-limited with respect to O_3 formation during summertime (Jacob et al., 1995), some urban areas such as Chicago, Illinois are VOC-limited (Pun et al., 2001). On July 13, the plumes of the two point sources located in northeastern Illinois are transported over the Chicago area. Since the background environment is VOC-limited, the effect of the plume-in-grid treatment is primarily to limit titration of O_3 by NO and we see from Figure 3-20 that the APT simulation results in higher O_3 concentrations than the base simulation over the Chicago area and over the southern part of Lake Michigan. This is confirmed by Figures 3-21 and 3-22, which show that the O_3 concentrations downwind of the two northeastern Illinois point sources in the base simulation are up to 20 ppb lower than the background value, while the APT simulation O_3 concentrations are the same as or within 5 ppb of the background value. Similar patterns are noted for the two point sources in eastern Michigan, one on the shore of Lake Huron at Saginaw Bay and the other to the southeast near Detroit. Figure 3-20 indicates that the APT simulation gives much larger surface O_3 concentrations (up to about 50 ppb) than the base simulation downwind (northeast) of the Saginaw Bay point source. However, as Figures 3-21 and 3-22 show, this increase is a direct result of the relatively larger titration of surface O_3 concentrations by the NO_x emissions from the point source in the base simulation as compared to the APT simulation. In the base simulation, as much as 67 ppb of the background O_3 concentration of approximately 109 ppb are titrated, while only 15 to 20 ppb of the background O_3 are titrated in the APT simulation.

The patterns observed near the Ohio River Valley and in its downwind areas are more complex because of the large number of point sources with explicit plume-in-grid treatment (9 point sources along the borders of Ohio, Kentucky and West Virginia; see Figure 3-19) and the complex wind flow around the Appalachian Mountains. Thus, some point source plumes are transported north and northeast over Ohio and Pennsylvania whereas other point source plumes are transported south and east over the Appalachian Mountains into West Virginia. The effect of the plume-in-grid treatment on downwind O_3 concentrations is a complex mixture of O_3 decrements and increments between the APT and base simulations.

On July 13, we see from Figure 3-20 that the APT simulation gives lower O_3 concentrations than the base simulation north of the two point sources in southern Ohio, one located along the border with Kentucky, and the other located along the border with West Virginia. On the other hand, the APT simulation gives higher surface O_3 concentrations than the base simulation in most of West Virginia as well as over western and northern Pennsylvania northeast of the Ohio River Valley. To understand the reasons for these differences, we again refer to Figures 3-21 and 3-22, which show the change in O_3 concentrations from the base and APT simulations, respectively, relative to the background simulation. Figures 3-21 and 3-22 show that the decrements (in the APT simulation with respect to the base simulation) in central and northern Ohio, as well as in

the western portion of West Virginia (immediately to the east and southeast of the point sources in southeastern Ohio and West Virginia) are associated with higher production of ozone in the base simulation than in the APT simulation. On the other hand, the increments in western and northern Pennsylvania are primarily associated with larger titration of surface O_3 by the NO_x emitted from the Ohio River Valley sources in the base simulation as compared to the APT simulation, rather than with higher O_3 production in the APT simulation compared to the base simulation. These results are qualitatively similar to the results for the other point sources discussed so far and for most of the point sources selected for PiG treatment in our study.

In contrast, the increments in the central portion of West Virginia are associated with increased production of O_3 in the APT simulation as compared to the base simulation. As discussed later in Section 3.2.3, a possible explanation for this result is that the NO_x in the plumes from the sources in southeastern Ohio and in West Virginia undergo rapid mixing as they are transported over complex terrain into West Virginia. In the base simulation, this results in enhanced production of both HNO_3 and some O_3 immediately downwind of the sources, leading to a depletion of NO_x in the plumes by the time they arrive in central West Virginia. In the APT simulation, the production of both HNO_3 and O_3 in the plumes also begins occurring immediately downwind but at a slower rate than in the base simulation, resulting in the peak production occurring later downwind, when the plumes reach central West Virginia.

The results for the other days are generally similar to those for July 13 with some differences as discussed below. Figure 3-24 shows the difference in surface O_3 concentrations between the APT and base simulations for the 12 km resolution domain on July 14, at 3 p.m. EDT. The plume from the North Carolina point source travels towards the northeast. Surface ozone concentrations in the plume are generally lower than those on July 13 for both the base and APT simulations. The O_3 concentrations in the APT simulation directly downwind of the source are about 5 to 10 ppb lower than the corresponding base case values at all downwind distances to which the plume is discernible in the figure (up to about 300 km downwind, where the base simulation O_3 concentration is about 88 ppb and the APT simulation concentration is about 85 ppb). At the eastern edge of the plume, the APT simulation gives higher (10 to 15 ppb) O_3 concentrations than the base simulation.

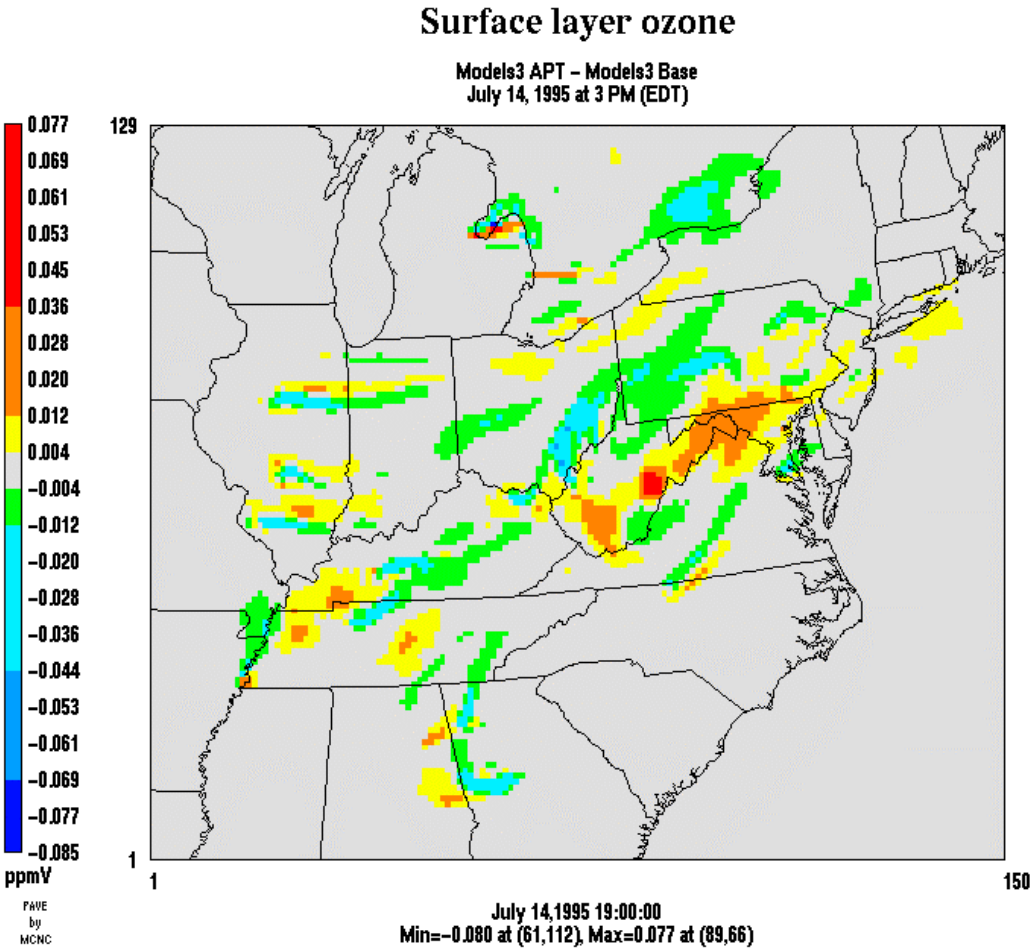

Figure 3-24
Differences (APT – Base) in surface O_3 concentrations, 12 km resolution domain, 3 p.m. EDT, 14 July 1995.

Figures 3-25 and 3-26, which show the O_3 concentration differences on July 14 relative to the background values for the base and APT simulations, respectively, shed more light on these results. As on July 13, more ozone is produced in the base simulation than in the APT simulation directly downwind of the source. We also note more titration of the background O_3 in the base simulation upwind of the source and for a small distance downwind along the eastern edge of the plume. The maximum O_3 produced in the plume in the base simulation is about 17 ppb over the background value of 70 ppb and occurs to the NNE immediately downwind (within 27 km) of the source. The APT simulation O_3 concentration at this location is 71 ppb, only 1 ppb higher than the background value. The maximum O_3 produced in the North Carolina point source plume in the APT simulation is about 16 ppb over the background value of 54 ppb and occurs to the ENE of the source along the eastern edge of the plume at a distance of about 100 km. The base simulation O_3 concentration at this location is about 60 ppb, 6 ppb higher than the background value and 10 ppb lower than the APT simulation value. Thus, on July 14, the maximum O_3 produced in the base and APT simulations from the North Carolina point source emissions are almost identical, although they occur at different locations, and for generally clean conditions in the vicinity of the source.

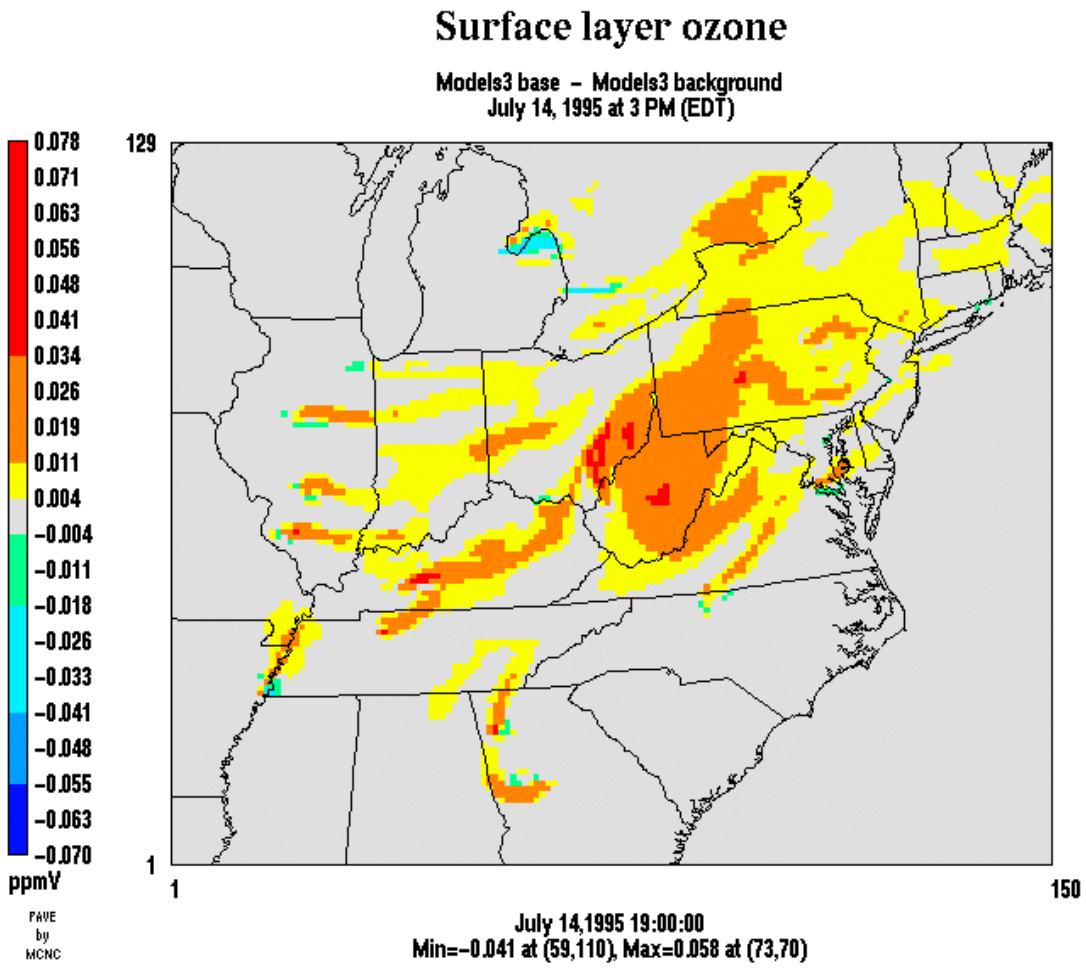

Figure 3-25
Differences (Base – Background) in surface O_3 concentrations, 12 km resolution domain, 3 p.m. EDT, 14 July 1995. The "Background" corresponds to a Models-3/CMAQ simulation without the emissions from the 30 point sources selected for PiG treatment.

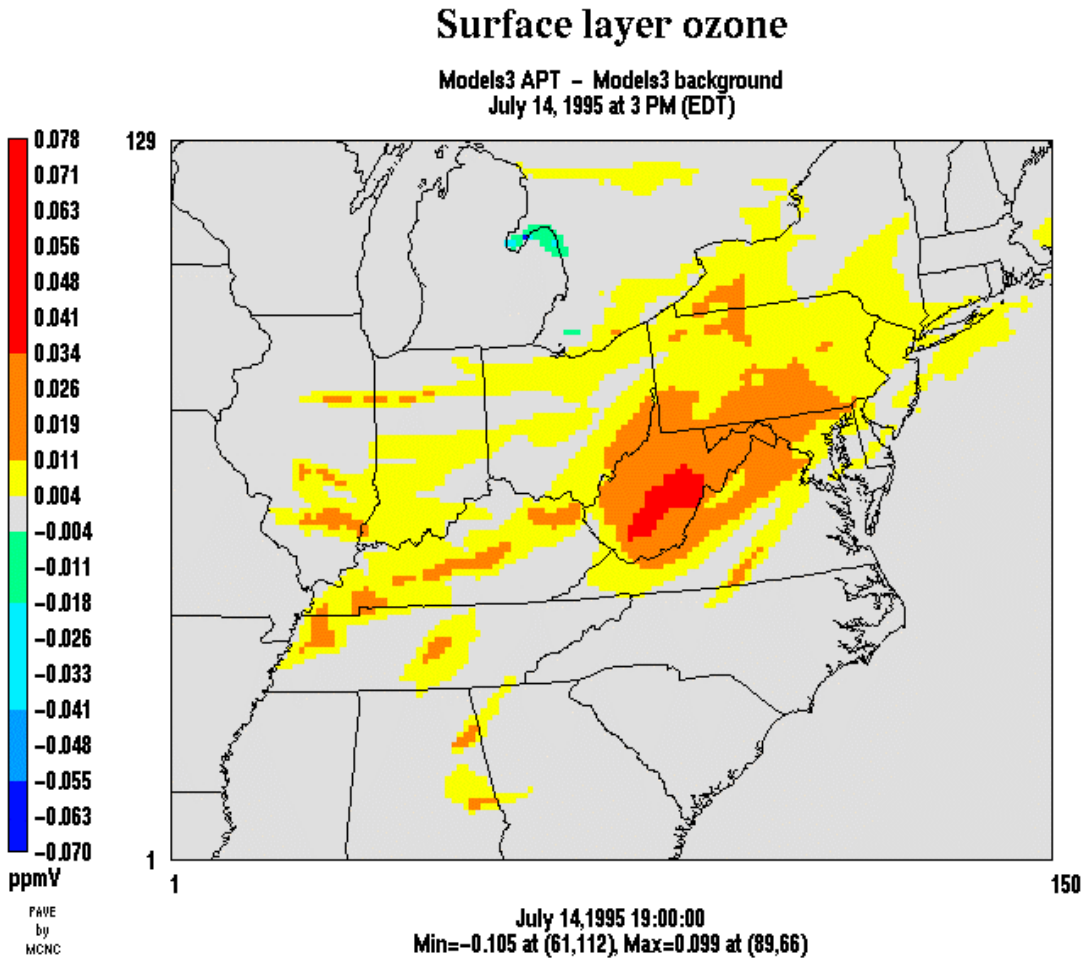

Figure 3-26
Differences (APT – Background) in surface O_3 concentrations, 12 km resolution domain, 3 p.m. EDT, 14 July 1995. The "Background" corresponds to a Models-3/CMAQ simulation without the emissions from the 30 point sources selected for PiG treatment.

The results for the Cumberland and Paradise power plants on July 14 are also qualitatively similar to those on July 13. Again, more O_3 is produced by the NO_x emitted from these sources in the base simulation than in the APT simulation. One important difference in the results is that the Cumberland plume appears to be transported in different directions in the two simulations. Figure 3-25 shows that, in the base simulation, the plume initially travels to the southeast and then to the ENE, producing O_3 concentrations up to 34 ppb over the background value of 63 ppb immediately downwind of (within 17 km) and to the southeast of Cumberland. The APT simulation O_3 concentration at this location is 63 ppb, the same as the background value. In the APT simulation, the emissions from the power plant are transported in a more southerly direction and the maximum ozone produced in the plume is 14 ppb over the background value of 73 ppb ESE of the source at a distance of approximately 134 km. The base simulation O_3 concentration at this location is the same as the background concentration.

The results for the Paradise power plant for July 14 dramatically illustrate the effect of using a PiG treatment for large NO_x sources. Figure 3-24 shows that the downwind O_3 concentrations from the APT simulation are considerably lower than those from the base simulation. In both simulations, the plumes are being transported to the east, as shown in Figures 3-25 and 3-26. The maximum ozone production in the Paradise plume in the base simulation is 53 ppb above the background value of about 99 ppb (Figure 3-25). This occurs to the east of the power plant at about 50 km downwind. The O_3 concentration from the APT simulation at this location is 111 ppb, about 12 ppb higher than the background concentration, and 41 ppb lower than the base simulation value. Moreover, the maximum O_3 produced in the plume in the APT simulation is only 17 ppb above the background value of 94 ppb, again occurring to the east of the power plant further downwind at a distance of about 70 km (Figure 3-26). At this location, the base simulation O_3 concentration is 128 ppb, about 34 ppb higher than the background value and 17 ppb higher than the APT simulation value.

The results for the point sources located in southern and central Illinois show that the plumes from these sources are generally transported to the east and southeast on July 14, and that the O_3 produced in the APT simulation is generally lower than that produced in the base simulation. The effects of PiG treatment on O_3 production in these plumes are generally similar to those on July 13, and are not discussed in more detail here. The results for the two point sources located in northeastern Illinois are more interesting and show some important differences from the July 13 results. On July 13, the plumes from these sources were transported over the VOC-limited Chicago area and over the southern part of Lake Michigan (see earlier discussion) whereas on July 14, they are transported toward Indiana into an environment that is likely to be NO_x-limited. The July 13 results showed that in the base simulation, the NO_x emissions from the two sources titrated the background surface O_3 to large downwind distances, while the NO_x in the plumes was transported aloft in the APT simulation, resulting in downwind O_3 concentrations that were comparable to the background values. Thus, the APT simulation gave higher surface O_3 concentrations downwind of the sources than the base simulation. For both simulations, there was negligible ozone production downwind of the sources on July 13. On the other hand, we see from Figure 3-25 that, in the base simulation on July 14, there is some initial titration of background O_3, followed by some production of O_3 in the plumes from these sources. In contrast, the downwind O_3 concentrations from the APT simulation on July 14 are comparable to the background values. This results in the APT simulation giving lower surface O_3 concentrations downwind of the sources than the base simulation.

As on July 13, we note more complex patterns near the Ohio River Valley and in its downwind areas on July 14. As shown in Figure 3-26, surface O_3 concentrations from the APT simulation are lower than the base simulation values to the north and northeast (central and eastern Ohio and western Pennsylvania) of the major sources in southern Ohio. Figures 3-25 and 3-26 show that this is primarily due to lower production of O_3 in the APT simulation than in the base simulation. From Figure 3-25, we note large increases (greater than 30 ppb) in surface O_3 concentrations over the background value to the north of the cluster of sources in southeastern Ohio in the base simulation. The largest O_3 production in this region of 58 ppb over the background value occurs about 17 km to the northwest of the second largest NO_x source in the modeling domain (a source in southeastern Ohio, near the border with West Virginia). This increase also corresponds to the largest increase anywhere in the modeling domain on July 14 in the base simulation. The background O_3 concentration at this location is about 106 ppb, while the base simulation value is 164 ppb, the second largest O_3 concentration predicted in the base simulation. The APT

simulation O_3 concentration at this location is 112 ppb, 6 ppb above the background value and 52 ppb below the base simulation value. As shown in Figure 3-3, the highest O_3 concentration of 171 ppb predicted in the base simulation on July 14 occurs further north of the Ohio River Valley sources. At this location, the background value is about 123 ppb, 48 ppb lower than the base simulation value. The APT simulation concentration at this location is about 130 ppb, 7 ppb higher than the background value. Furthermore, in contrast to July 13, Figure 3-25 shows that the transport of the Ohio River Valley emissions to the northeast into Pennsylvania results in increases of surface O_3 concentrations of up to 30 ppb over background values on July 14 in the base simulation. Figure 3-26 shows that O_3 is also produced in the APT simulation as the Ohio River Valley emissions are transported into Pennsylvania, but in lower amounts than in the base simulation.

In contrast, the APT simulation gives higher surface O_3 concentrations than the base simulation in most of West Virginia, particularly in the southern and eastern portions, as well as in Maryland, as shown in Figure 3-24. The reason for the higher APT concentrations is elucidated in Figures 3-25 and 3-26, which show that while O_3 is produced in both the base and APT simulations to the east and southeast of the cluster of point sources in southeastern Ohio and the point source in West Virginia, the O_3 produced in the APT simulation is generally higher than that produced in the base simulation. The maximum O_3 produced in the APT simulation occurs about 155 km to the east of the West Virginia point source and about 185 km to the ESE of the cluster of sources in southeastern Ohio. The increase in surface O_3 concentrations over the background value of 79 ppb at this location is about 99 ppb, resulting in the highest O_3 concentration of 178 predicted in the modeling domain in the APT simulation at 3 p.m. EDT on July 14. The base simulation O_3 concentration at this location is 102 ppb, 23 ppb above the background value. The largest increase in O_3 concentrations over background values in West Virginia in the base simulation is about 35 ppb, approximately 70 km to the east of the West Virginia point source. In the APT simulation, the increase at this location is about 42 ppb. The background value at this location is 80 ppb, and the base simulation and APT simulation O_3 concentrations are about 115 ppb and 122 ppb, respectively. One possible reason for the higher O_3 formation in the APT simulation is that significantly more HNO_3 is produced immediately downwind of the sources in the base simulation than in the APT simulation, as discussed later in Section 3.2.3, leading to a depletion of NO_x further downwind in the base simulation.

The O_3 concentration differences for July 15 are shown in Figures 3-27 through 3-29. Figure 3-27 shows the difference between the APT and base simulation values, while Figures 3-28 and 3-29 show the differences from the background values of the base and APT simulation values, respectively. In general, the prevailing flow in the entire modeling domain on July 15 appears to be primarily westerly, transporting most of the point source plumes to the east and NNE.

The results for July 15 for many of the sources (the point source in North Carolina, the Cumberland and Paradise power plants, the point sources in southern and central Illinois) follow the same general patterns discussed earlier for July 13 and 14, and are not discussed in more detail here. The patterns for the regions downwind of the Ohio River Valley sources on July 15 are generally similar to those for July 13 and 14, with some differences, as discussed below.

On July 15, the Ohio River Valley emissions are primarily transported to the east into West Virginia and southern Pennsylvania. Recall that, on the previous two days, the winds were from the south and the southwest, so that the emissions were primarily transported to the north and

northeast, into central Ohio and western Pennsylvania. Figure 3-27 shows that the O_3 concentrations in West Virginia in the base simulation are generally larger than those in the APT simulation immediately downwind of the sources. Further downwind, the APT simulation O_3 concentrations are larger than the base simulation values. Figures 3-28 and 3-29 show that these differences are primarily due to differences in the rate of O_3 production downwind of the sources in the two simulations.

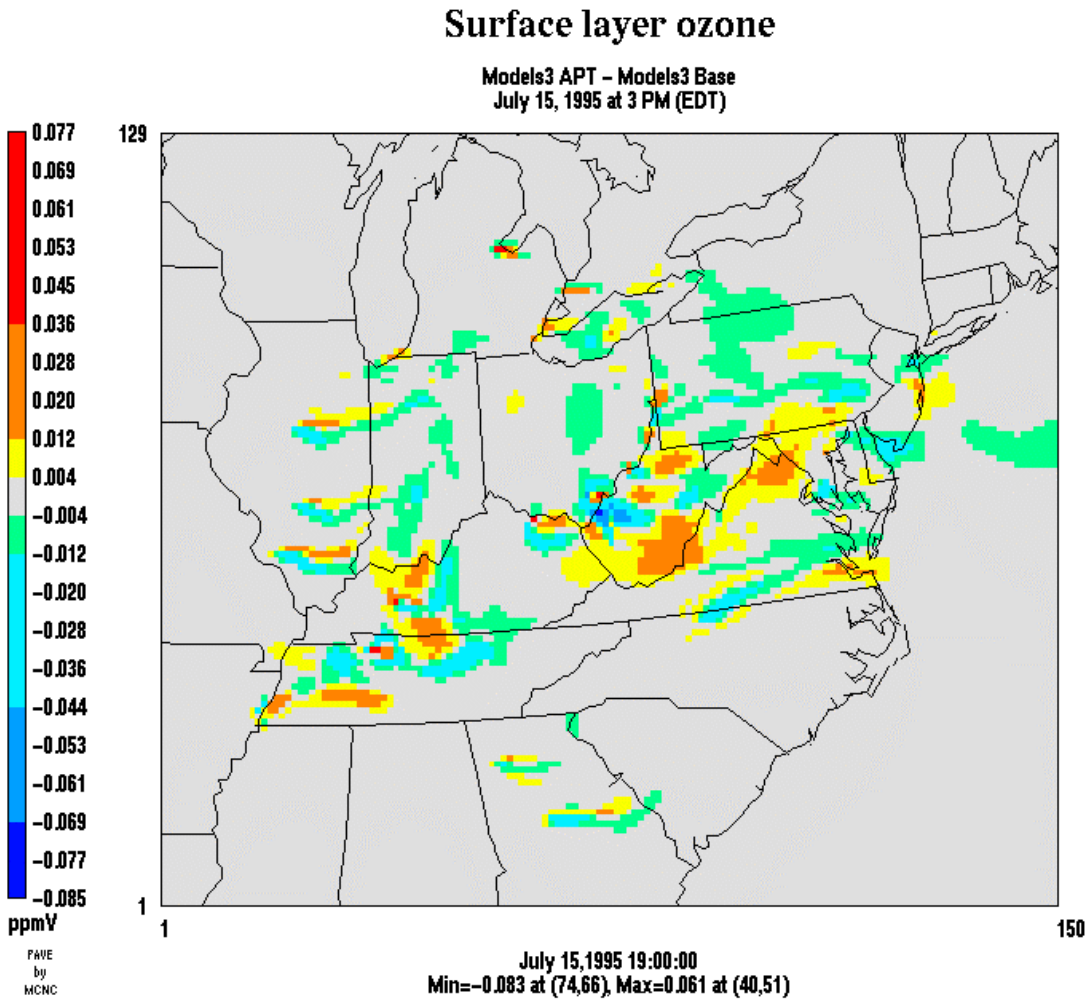

Figure 3-27
Differences (APT – Base) in surface O_3 concentrations, 12 km resolution domain, 3 p.m. EDT, 15 July 1995.

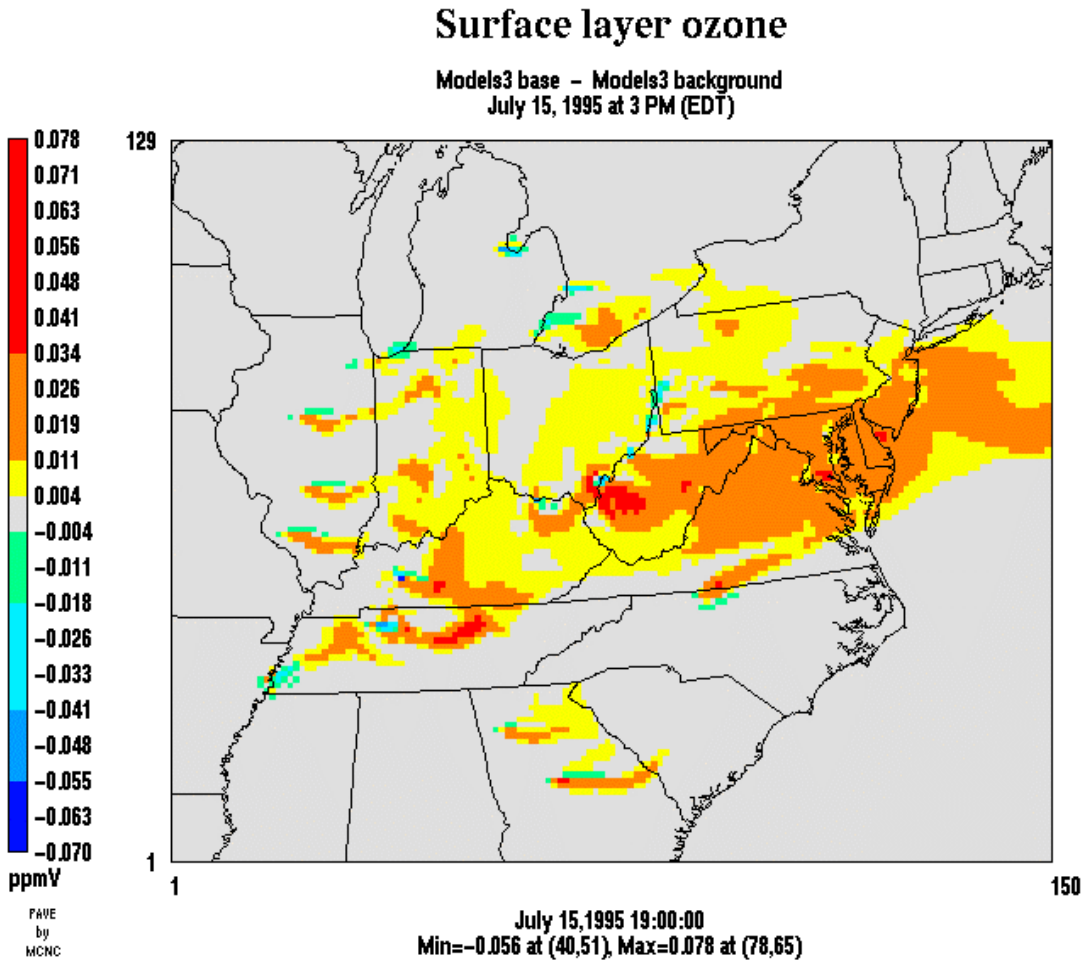

Figure 3-28
Differences (Base – Background) in surface O_3 concentrations, 12 km resolution domain, 3 p.m. EDT, 15 July 1995. The "Background" corresponds to a Models-3/CMAQ simulation without the emissions from the 30 point sources selected for PiG treatment.

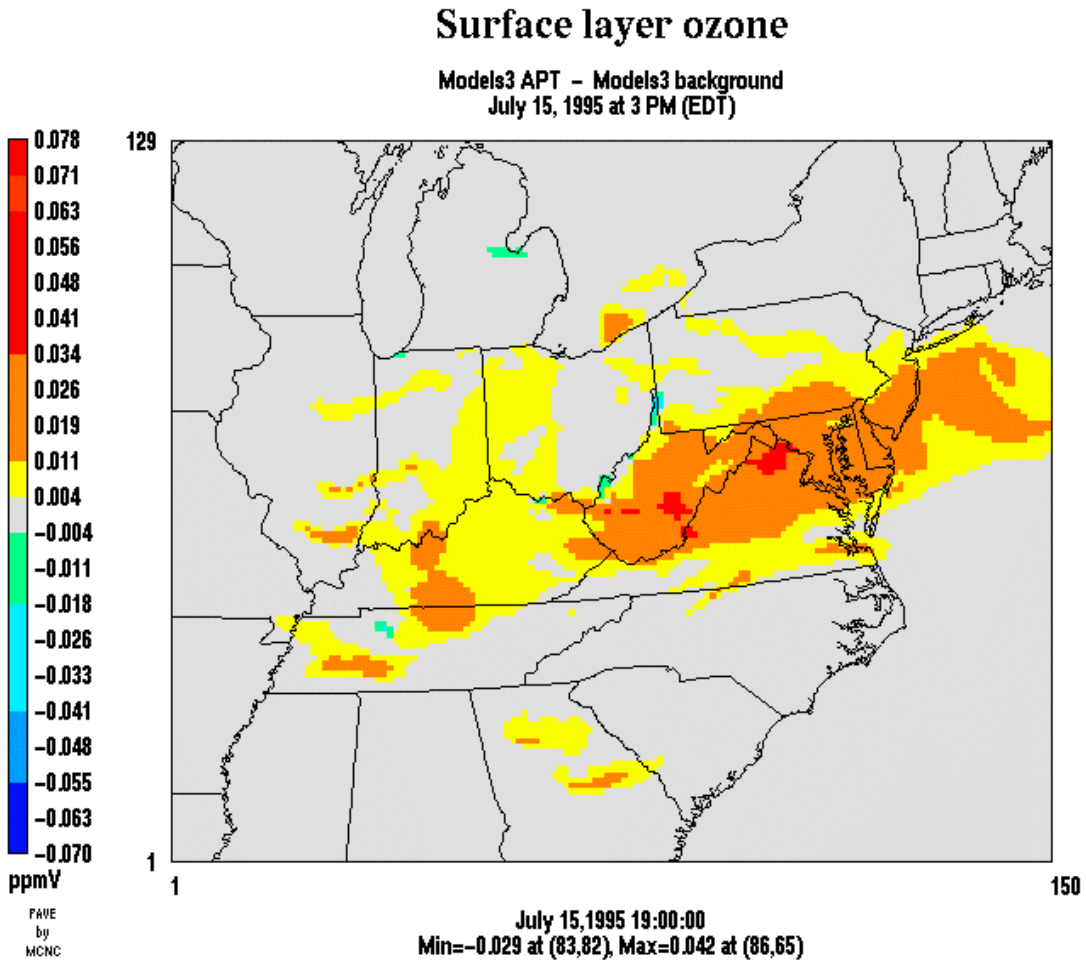

Figure 3-29
Differences (APT – Background) in surface O_3 concentrations, 12 km resolution domain, 3 p.m. EDT, 15 July 1995. The "Background" corresponds to a Models-3/CMAQ simulation without the emissions from the 30 point sources selected for PiG treatment.

The maximum O_3 produced in the base simulation is about 78 ppb above the background value of 97 ppb at a location 24 km directly east of the West Virginia point source located near the border with Ohio and about 70 km to the southeast of the cluster of sources in southeastern Ohio (see Figure 3-28). The base simulation O_3 concentration at this location is 175 ppb, and the APT simulation value is 116 ppb, about 19 ppb above the background value.

The maximum increase in surface O_3 concentrations in West Virginia in the APT simulation on July 15 is about 42 ppb above the background value of 75 ppb, as shown in Figure 3-29. This increase occurs much further downwind, at about 95 km to the east of the corresponding maximum O_3 increase location in the base simulation, from the Ohio River Valley sources. The base simulation O_3 concentration at this location is about 98 ppb, 23 ppb higher than the background value and 19 ppb lower than the APT simulation value.

We now briefly discuss the results for the 4 km resolution domain. Figures 3-30 to 3-32 show the differences in surface O_3 concentrations between the APT and base simulations for the 4 km domain for July 13 to 15, 1995. O_3 "plumes" are closely associated with the six point sources with a plume-in-grid treatment within the 4 km resolution domain. However, these plumes differ among the six point sources. For example, Figure 3-30 shows that, immediately downwind of the two point sources located in Pennsylvania, the APT simulation gives generally lower O_3 concentrations than the base simulation on July 13, except at the lower edge of the plume from the northern Pennsylvania source, where the APT simulation gives higher O_3 concentrations than the base simulation. The latter increase is possibly associated with titration of the surface O_3 in the base simulation. Further downwind, the plume from the northern Pennsylvania source gives higher O_3 concentrations in the APT simulation than in the base simulation. These results are generally consistent with those obtained for the North Carolina point source and the Cumberland and Paradise power plants in the 12 km resolution domain, which are located in NO_x-limited environments. Ozone formation in these plumes generally occurs at a slower rate and further downwind in the APT simulation than in the base simulation.

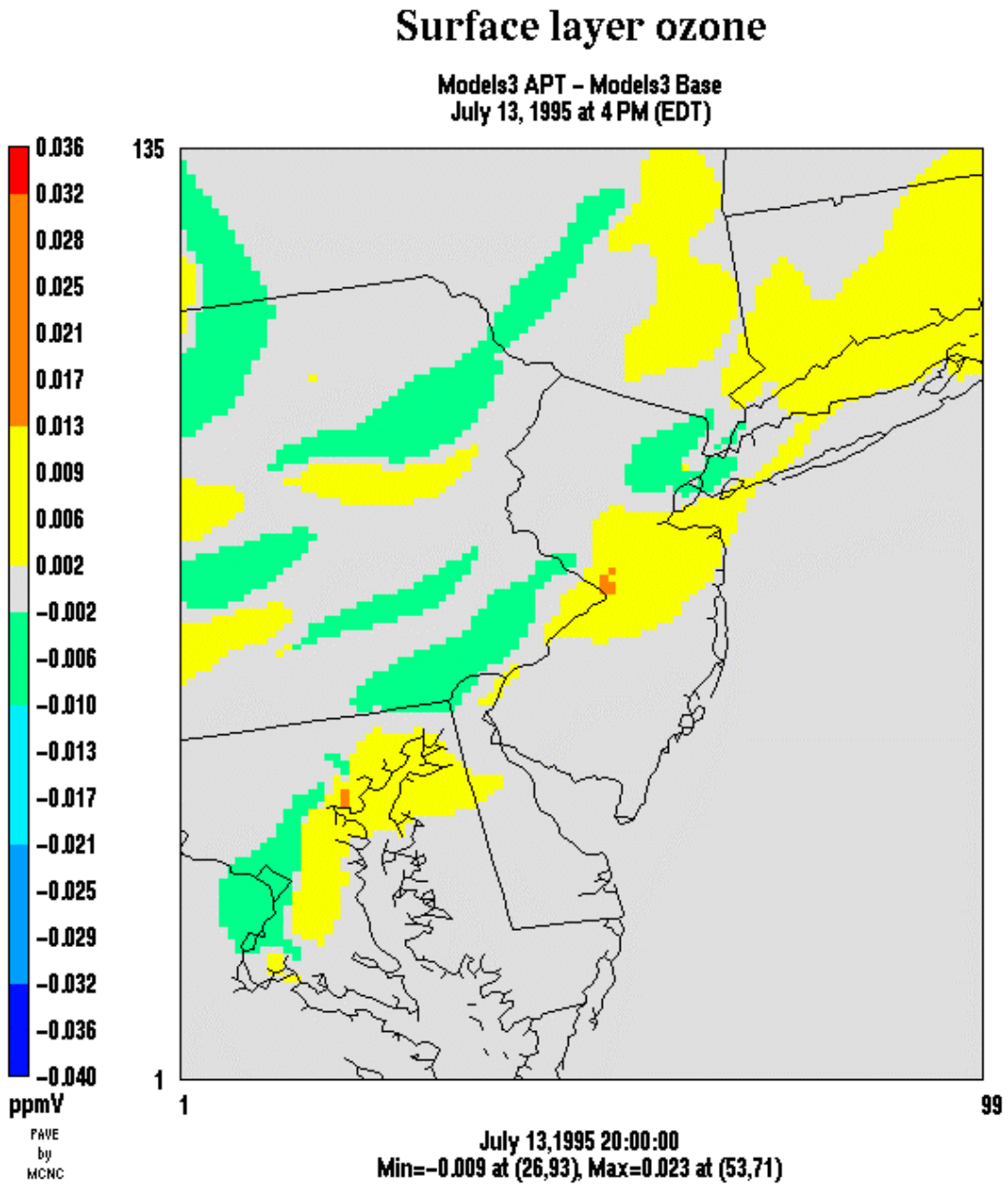

Figure 3-30
Differences (APT – Base) in surface O_3 concentrations, 4 km resolution domain, 4 p.m. EDT, 13 July 1995.

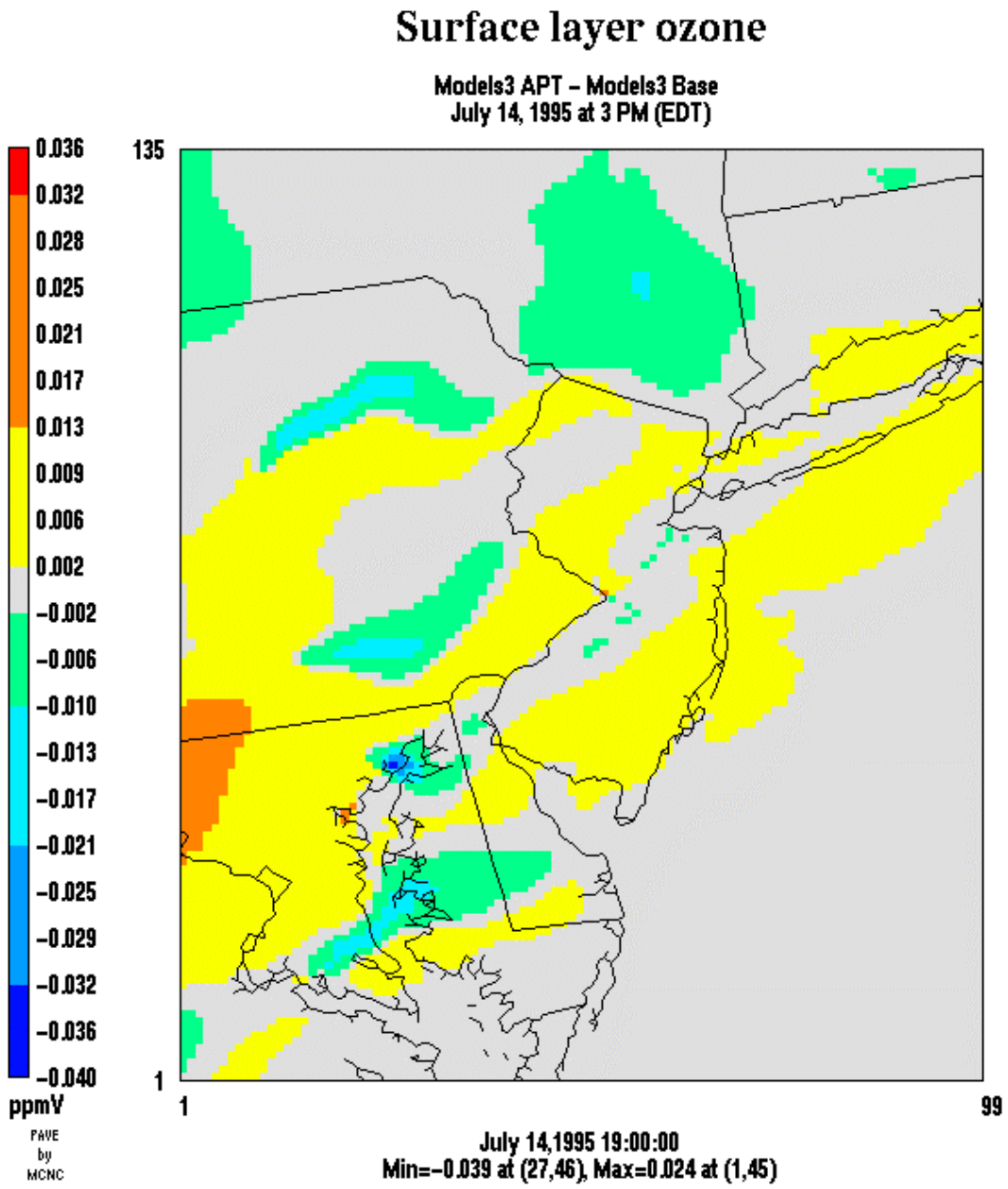

Figure 3-31
Differences (APT – Base) in surface O_3 concentrations, 4 km resolution domain, 3 p.m. EDT, 14 July 1995.

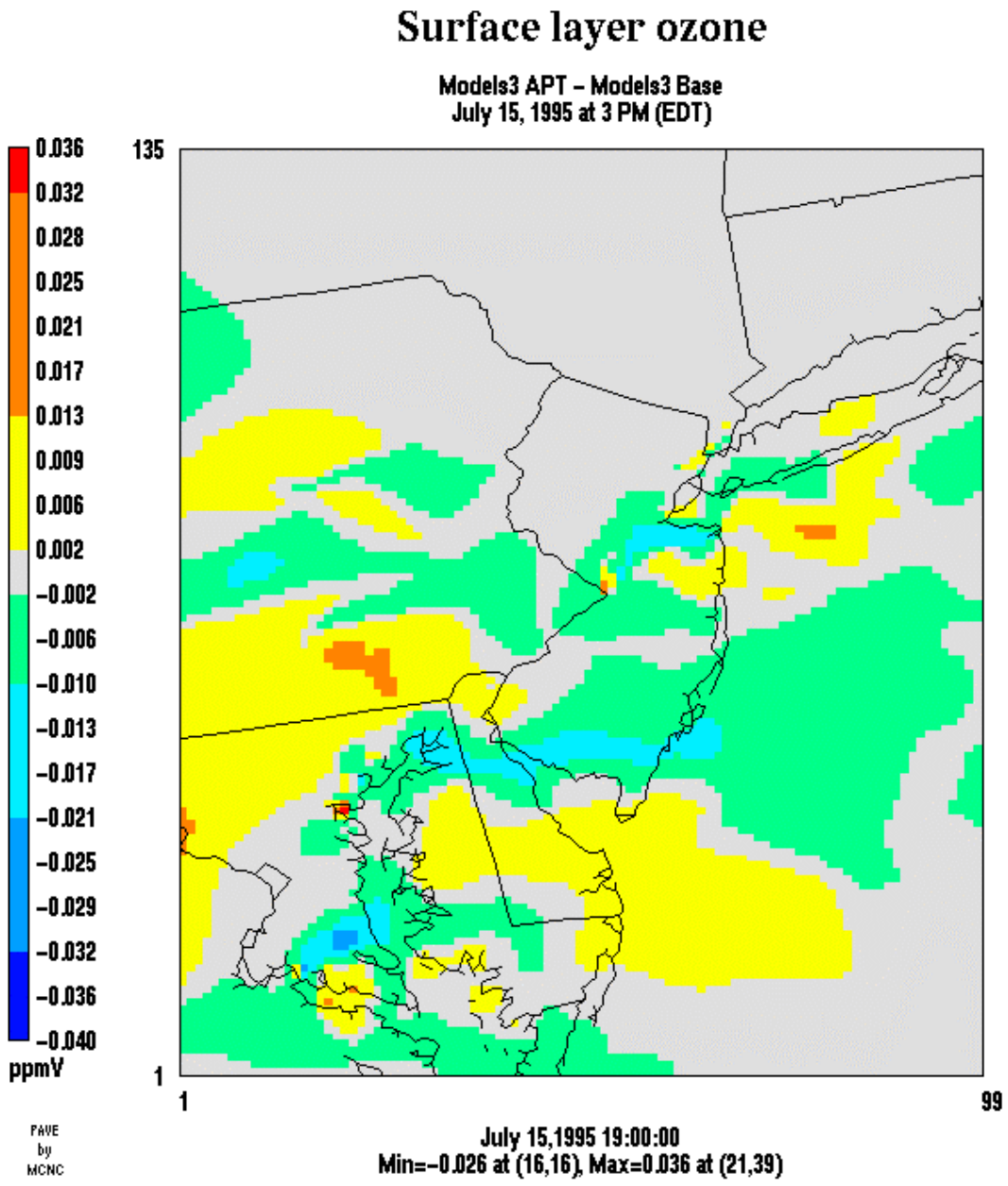

Figure 3-32
Differences (APT – Base) in surface O_3 concentrations, 4 km resolution domain, 3 p.m. EDT, 15 July 1995.

For the point source located at the border of New Jersey and Pennsylvania, the APT simulation gives higher surface O_3 concentrations than the base simulation at the source location as well as downwind of the source on July 13. This behavior is similar to that seen in the 12 km resolution domain results for July 13 for the point source located near Saginaw Bay in eastern Michigan and the two point sources located in northeastern Illinois near Chicago. The plumes from these sources are transported over areas that are likely to be primarily VOC-limited and the NO_x in these plumes titrate the background O_3 instead of producing more O_3. For these sources, the plume-in-grid treatment reduces the amount of O_3 titration by plume NO leading to larger O_3 concentrations in the APT simulation than in the base simulation.

The patterns are similar, albeit to different extents, on July 14 and 15. We also note the influence of the western and southern boundary conditions on O_3 concentrations predicted in the 4 km resolution domain as the episode progresses from July 13 to 15 and the wind direction changes from southerly to southwesterly to westerly. Recall that these boundary conditions are obtained from the 12 km resolution domain simulation results.

The temporal profiles of O_3 concentrations predicted by Models-3/CMAQ-APT have already been compared to the observed concentrations and the concentrations predicted by the base Models-3/CMAQ in Figures 3-11 and 3-12. At the sites considered here, the plume-in-grid treatment does not show a large influence except at the Fort Meade, Maryland site on July 15.

Performance statistics for the Models-3/CMAQ-APT simulation are presented in Tables 3-4 and 3-5 for the 12 km resolution domain and the 4 km resolution domain, respectively. If we compare these statistics with those presented in Tables 3-2 and 3-3 for Models-3/CMAQ, we see that the performance for the peak O_3 concentrations paired in space and time is the same as or slightly better for Models-3/CMAQ-APT. The fractional gross error statistics are also the same or slightly better for Models-3/CMAQ-APT versus Models-3/CMAQ. The fractional bias for the 1-hour average O_3 concentrations from the Models-3/CMAQ-APT simulation is the same as or slightly better than that from the Models-3/CMAQ simulation, while the fractional bias for the 8-hour average concentrations is slightly worse for Models-3/CMAQ-APT.

Table 3-4
Models-3/CMAQ-APT performance statistics for O_3 concentrations for 13-15 July 1995 in the 12 km resolution NARSTO-Northeast domain.

Performance Measure[a]	Performance statistics
1-hour average O_3 concentrations	
Paired peak error[b]	-51%
Gross error	31%
Fractional gross error	0.28
Bias	17%
Fractional bias	0.09
8-hour average O_3 concentrations	
Paired peak error[b]	-36%
Gross error	27%
Fractional gross error	0.24
Bias	16%
Fractional bias	0.11

(a) Performance measures are as defined by Seigneur et al. (2000); statistics are for observed O_3 concentrations greater than 40 ppb at 299 sites.
(b) Paired in both space and time.

Table 3-5
Models-3/CMAQ-APT performance statistics for O_3 concentrations for 13-15 July 1995 in the 4 km resolution NARSTO-Northeast domain.

Performance Measure[a]	Performance statistics
1-hour average O_3 concentrations	
Paired peak error[b]	-20%
Gross error	31%
Fractional gross error	0.31
Bias	8%
Fractional bias	0.0
8-hour average O_3 concentrations	
Paired peak error[b]	-9%
Gross error	27%
Fractional gross error	0.26
Bias	9%
Fractional bias	0.03

(a) Performance measures are as defined by Seigneur et al. (2000); statistics are for observed O_3 concentrations greater than 40 ppb at 64 sites.
(b) Paired in both space and time.

Overall, the total O_3 mass integrated across the 12 km resolution modeling domain over all model layers is slightly higher (0.4%) in the APT simulation than in the base simulation. In the surface layer, the total O_3 mass integrated across the modeling domain is also slightly higher (0.5%) in the APT simulation than in the base simulation. This result, and the results presented earlier in this section, indicate that the generally lower production of O_3 downwind of major NO_x point sources in the APT simulation is more or less compensated by the unrealistically large titration of existing surface O_3 by the NO_x emissions in the base simulation without PiG treatment.

3.2.3 HNO_3 Concentrations

Spatial patterns of surface HNO_3 concentration differences between the Models-3/CMAQ-APT and Models-3/CMAQ base simulations are shown in Figure 3-33 for the 12 km resolution domain at 3 p.m. EDT on July 13. The patterns for the HNO_3 concentration differences show some similarities with those obtained for the O_3 concentration differences but also some discrepancies.

The HNO_3 results for the isolated North Carolina source, the Cumberland and Paradise power plants, and the point sources located in southern and central Illinois are qualitatively similar to the O_3 results discussed earlier. For all these sources, the APT simulation gives lower HNO_3 concentrations than the base simulation immediately downwind of the sources, but gives higher concentrations at the plume edges and further downwind of the sources. As in the discussion of the ozone results, we use the background simulation to determine the extent of HNO_3 formation in the plumes with and without PiG treatment. Figures 3-34 and 3-35 present the differences in HNO_3 concentrations between the base and background simulations and between the APT and background simulations , respectively, for July 13.

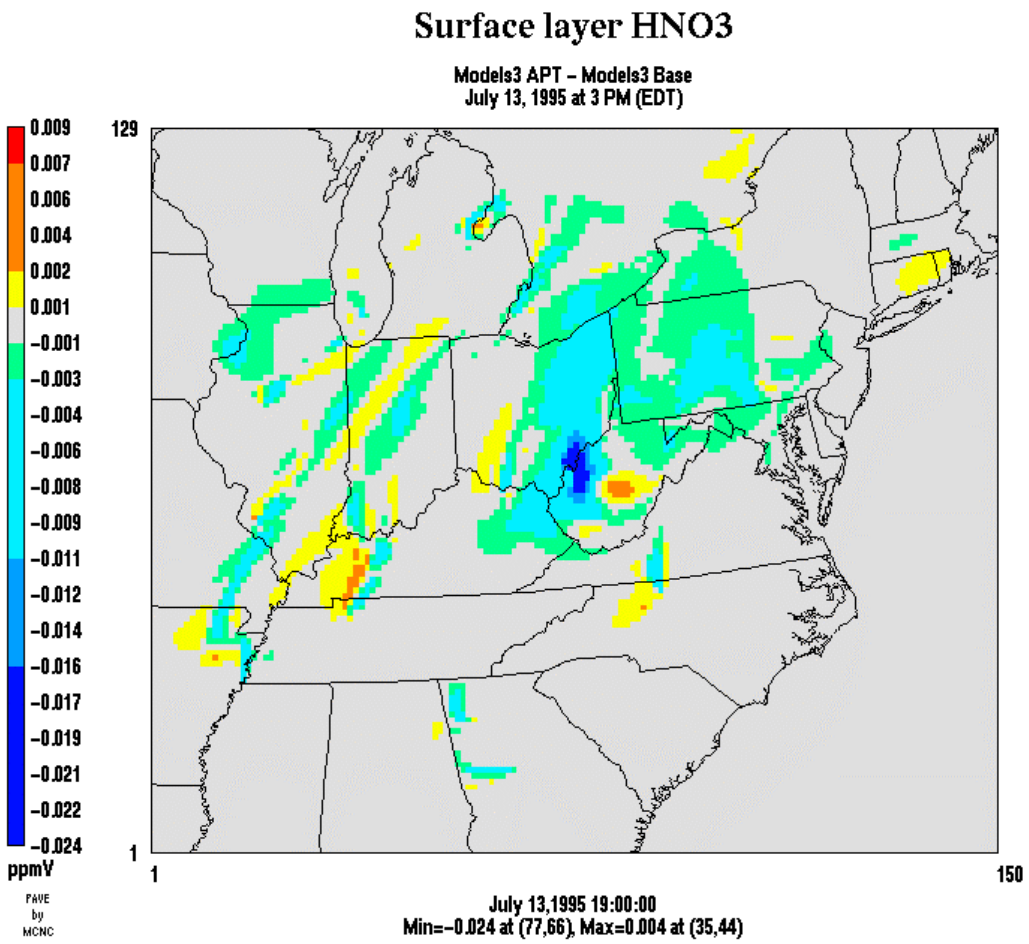

Figure 3-33
Differences (APT – Base) in surface HNO_3 concentrations, 12 km resolution domain, 3 p.m. EDT, 13 July 1995.

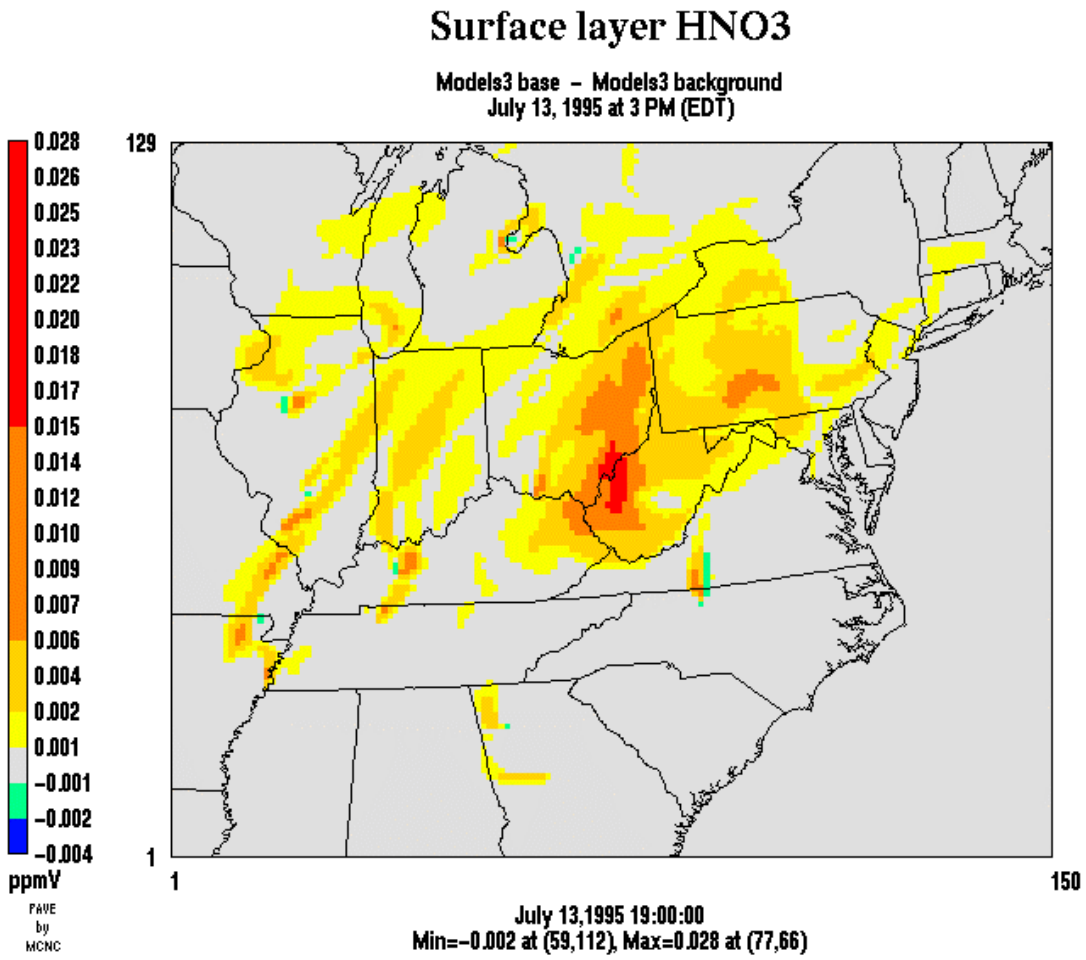

Figure 3-34
Differences (Base – Background) in surface HNO_3 concentrations, 12 km resolution domain, 3 p.m. EDT, 13 July 1995. The "Background" corresponds to a Models-3/CMAQ simulation without the emissions from the 30 point sources selected for PiG treatment.

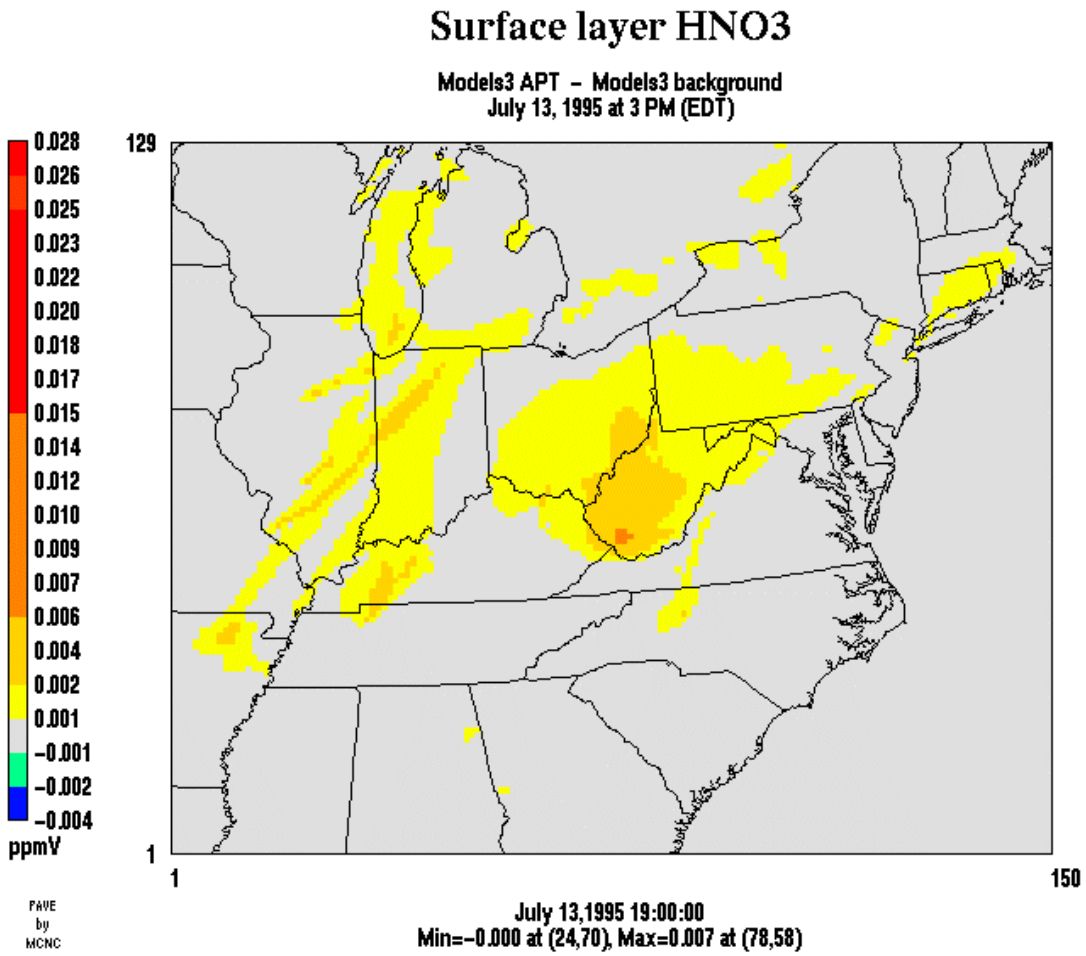

Figure 3-35
Differences (APT – Background) in surface HNO_3 concentrations, 12 km resolution domain, 3 p.m. EDT, 13 July 1995. The "Background" corresponds to a Models-3/CMAQ simulation without the emissions from the 30 point sources selected for PiG treatment.

Figure 3-34 shows that, downwind of the North Carolina point source, more than 6 ppb of HNO_3 is produced in the plume (above the background value) in the base simulation. However, upwind of the source and along the eastern edge of the plume, where the plume NO_x scavenges the background O_3 (see Figure 3-21), we see that the effect of the point source emissions is a reduction in HNO_3 concentrations when a PiG treatment is not used. In contrast, Figure 3-35 shows that, when a PiG treatment is used, small amounts of HNO_3 (generally less than 2 ppb) are formed in the plume up to about 220 km downwind of the source. An investigation of the actual HNO_3 concentrations shows that a maximum of 11 ppb is produced in the North Carolina point source plume in the base simulation over the background value of 6 ppb at about 40 km downwind (NNW) of the source. The HNO_3 production in the APT simulation at this location is less than 1 ppb. The maximum HNO_3 produced in the APT simulation is about 2 ppb over the background value of 7 ppb.

In the Cumberland plume, a maximum of about 6 ppb of HNO_3 is formed over the background value of 4 ppb in the base simulation. In the APT simulation, the maximum HNO_3 produced is less than 4 ppb over a background value of 5 ppb. Similarly, the maximum HNO_3 produced in the plume of the southern Illinois source is more than 7 ppb over the background value of 9 ppb in the base simulation, while the maximum HNO_3 produced in the APT simulation is about 4 ppb over a background value of 8 ppb.

Some differences between the O_3 and HNO_3 patterns are apparent in the results for the eastern Michigan point source located near Saginaw Bay and for the regions downwind of the Ohio River Valley for July 13. Figure 3-34 shows that there is some formation of HNO_3 in the plume (up to about 4 ppb over the background value of 16 ppb) downwind of the Saginaw Bay point source in the base simulation. In the APT simulation, small amounts of HNO_3 are produced downwind of the source (the maximum production is about 2 ppb over a background value of about 26 ppb), as shown in Figure 3-35. However, as discussed earlier, large reductions in background O_3 concentrations (see Figure 3-21) are obtained downwind of the source due to titration by the NO_x in the plume in the base simulation, while the corresponding reductions in the APT simulation (Figure 3-22) are much smaller. Thus, the downwind O_3 concentrations in the APT simulation are higher than those in the base simulation (because less background O_3 is titrated with PiG treatment), but the downwind HNO_3 concentrations in the APT simulation are lower than the base simulation (because less HNO_3 is produced with PiG treatment).

Also, we see from Figure 3-33 that the HNO_3 concentrations from the APT simulation in the region around the Ohio River Valley are significantly lower than the base simulation values on July 13, except over the central portion of West Virginia. For the O_3 concentrations we had noted an increase in O_3 concentrations over most of West Virginia in the APT simulation as compared to the base simulation (note, however, that the HNO_3 and O_3 increments between the APT and base simulations over the central portion of West Virginia are qualitatively similar).

To understand the similarities and discrepancies in the O_3 and HNO_3 patterns discussed above, it is useful to briefly review the chemistry of HNO_3 and O_3 formation in NO_x plumes. In a plume rich in NO_x, oxidants are depleted initially and formation of oxidation products such as HNO_3 and H_2SO_4 is suppressed. As the plume becomes more dilute, these oxidation products will start to form, albeit at a rate slower than the rate in the background air (i.e., outside the plume). Farther downwind, in a NO_x-sensitive environment, the formation of oxidants such as O_3 may

exceed that of the background. The formation rate of HNO_3 farther downwind in the plume will differ depending on whether the background is NO_x- or VOC-limited (Karamchandani and Seigneur, 1999). In a VOC-limited environment, the HNO_3 plume concentration will increase steadily as the VOC/NO_x ratio approaches that of the background. In a NO_x-limited environment, the HNO_3 formation rate will increase rapidly as the VOC-limited plume environment is more conducive to HNO_3 formation than the background; as the plume becomes more dilute, the HNO_3 formation rate will decrease toward that of the background. Although O_3 and HNO_3 concentrations in a plume follow similar trends as the plume becomes dispersed, it is important to note that in a NO_x-sensitive environment, HNO_3 formation occurs earlier than O_3 formation in the plume and, farther downwind, plume HNO_3 concentrations decrease more rapidly than plume O_3 concentrations.

Thus, in the base simulation, we note from Figure 3-34 that a significant amount of HNO_3 is produced in the western portion of West Virginia near the border with Ohio due to the emissions from the point sources located in southeastern Ohio and in West Virginia. The maximum HNO_3 produced is about 28 ppb (over a background value of only 6 ppb) in the grid cell immediately to the northeast of the West Virginia point source. At this location, the HNO_3 production in the APT simulation is only about 5 ppb over the background value. Further downwind, the production of HNO_3 in the base simulation decreases, but production in the APT simulation continues.

The HNO_3 results for July 14 are shown in Figures 3-36 through 3-38. These results are generally similar to those for July 13, showing significantly lower production of HNO_3 in the APT simulation than in the base simulation over most of the modeling domain, resulting in generally lower HNO_3 concentrations in the APT simulation than in the base simulation.

Figures 3-39 through 3-41 show the HNO_3 results for July 15. Again, the results are generally similar to the results for the previous days. One important difference is that higher HNO_3 concentrations are predicted in the APT simulation than in the base simulation over a large portion of central West Virginia, as shown in Figure 3-39. This is explained by Figures 3-40 and 3-41 that show the HNO_3 concentrations over the background values in the two simulations. Figure 3-40 shows that a significant amount of HNO_3 (up to 24 ppb above the background value) is produced in the point source plumes in the base simulation immediately downwind of the sources in the Ohio River Valley, while less than 6 ppb is produced further downwind. On the other hand, Figure 3-41 shows that this production is delayed in the APT simulation, occurring further downwind over central West Virginia. The maximum HNO_3 production in the APT simulation is about 11 ppb over the background value. Thus, immediately downwind of the sources, the base simulation HNO_3 concentrations are considerably higher (by up to about 20 ppb) than the APT simulation values. Further downwind, the APT simulation HNO_3 concentrations are higher (by up to about 6 ppb) than the base simulation values.

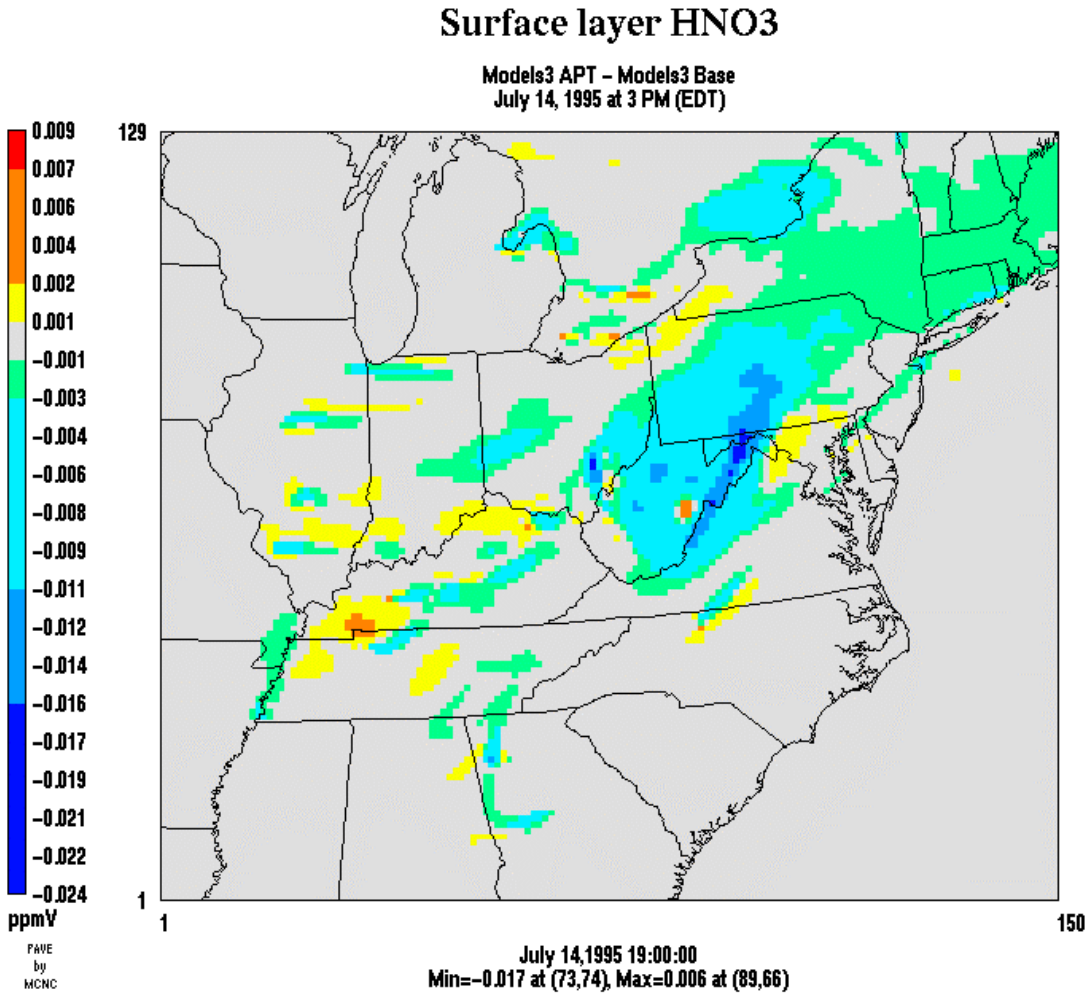

Figure 3-36
Differences (APT – Base) in surface HNO_3 concentrations, 12 km resolution domain, 3 p.m. EDT, 14 July 1995.

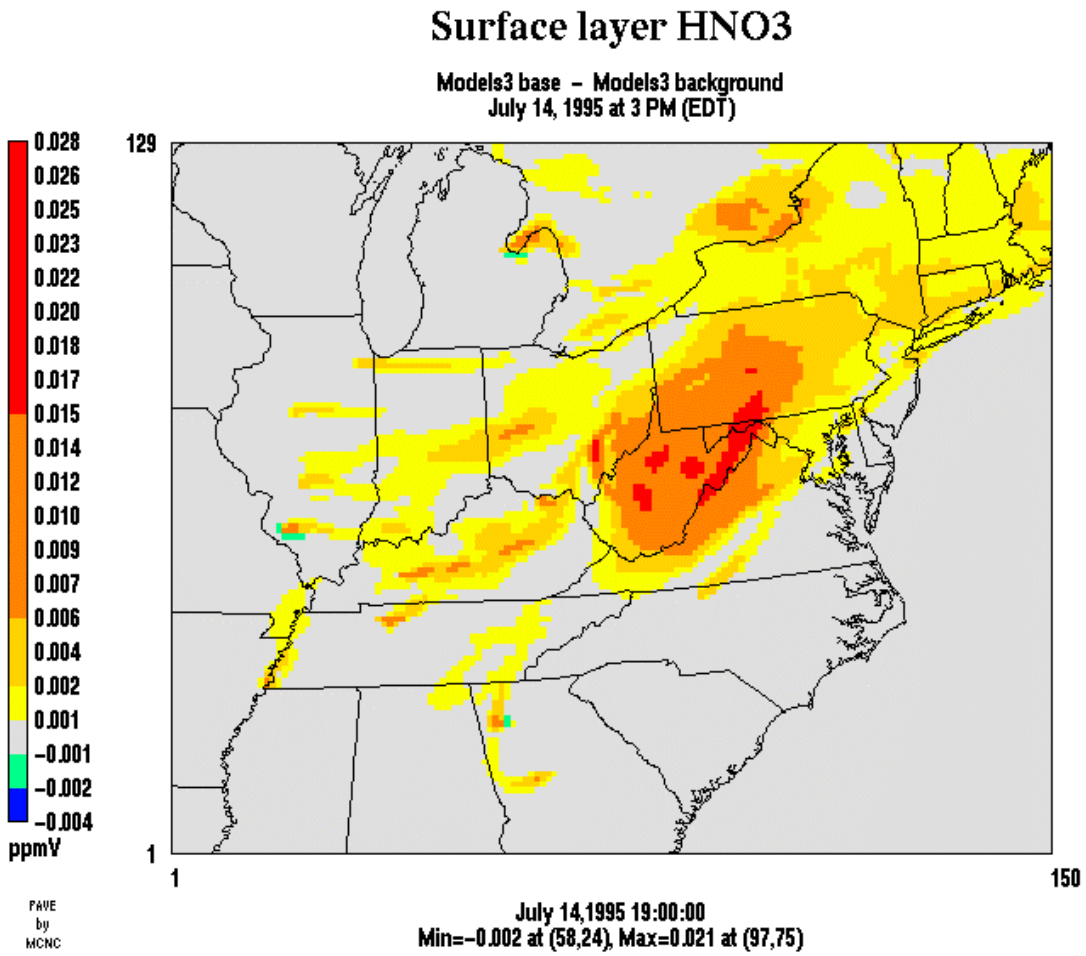

Figure 3-37
Differences (Base – Background) in surface HNO_3 concentrations, 12 km resolution domain, 3 p.m. EDT, 14 July 1995. The "Background" corresponds to a Models-3/CMAQ simulation without the emissions from the 30 point sources selected for PiG treatment.

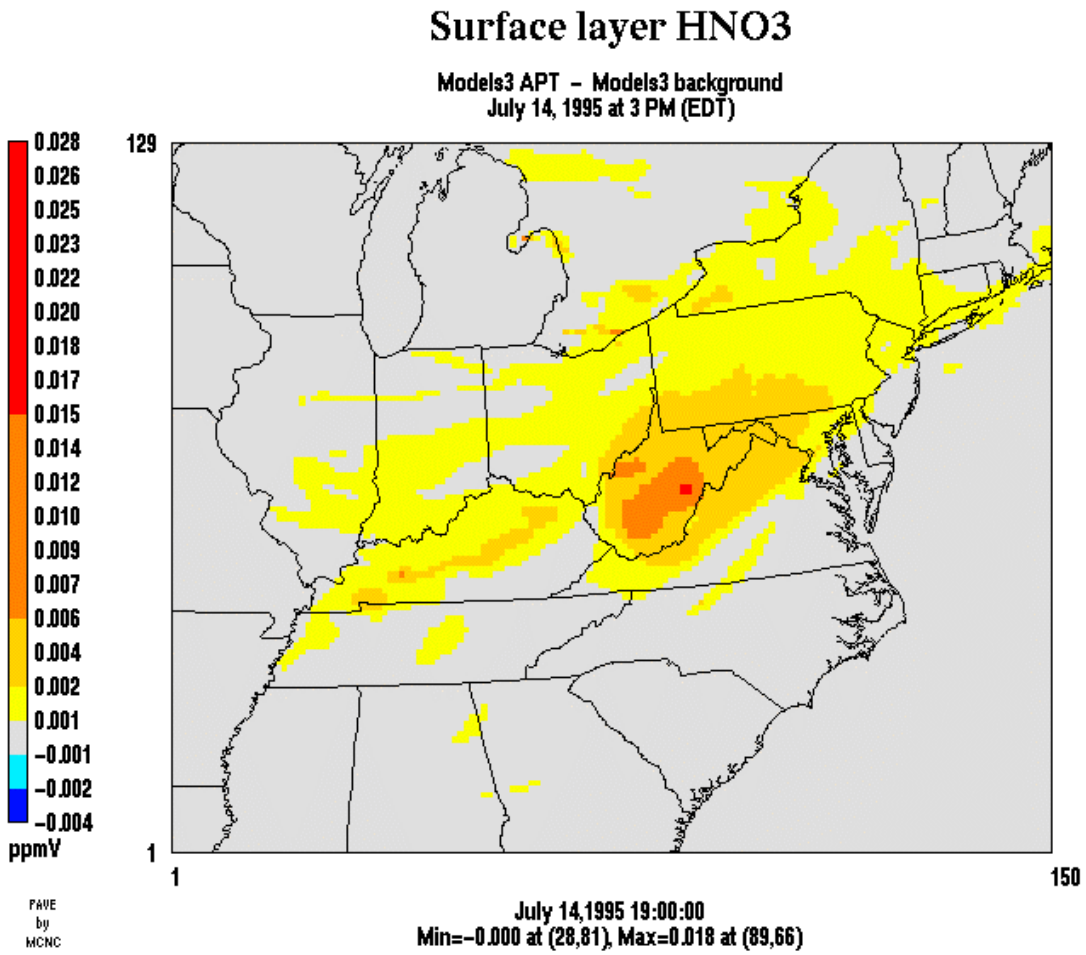

Figure 3-38
Differences (APT – Background) in surface HNO_3 concentrations, 12 km resolution domain, 3 p.m. EDT, 14 July 1995. The "Background" corresponds to a Models-3/CMAQ simulation without the emissions from the 30 point sources selected for PiG treatment.

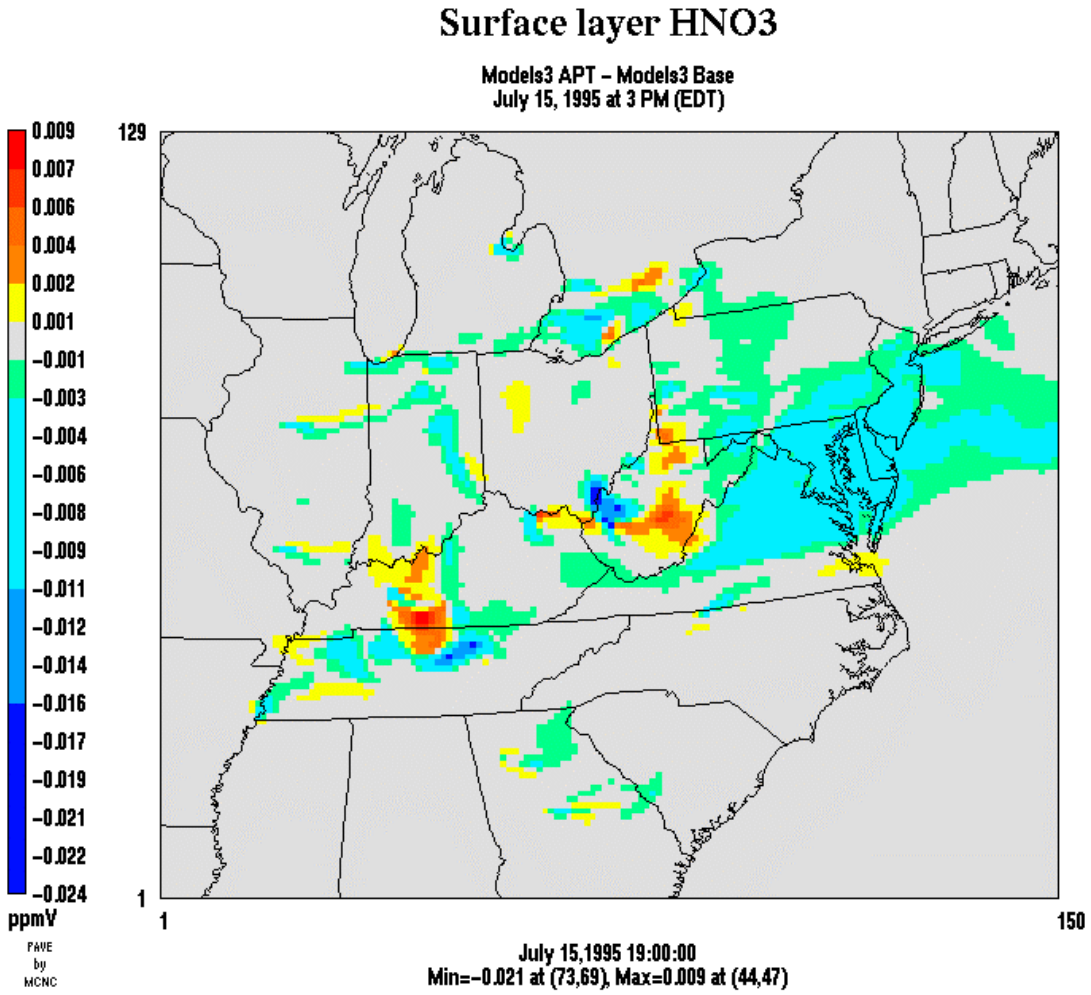

Figure 3-39
Differences (APT – Base) in surface HNO_3 concentrations, 12 km resolution domain, 3 p.m. EDT, 15 July 1995.

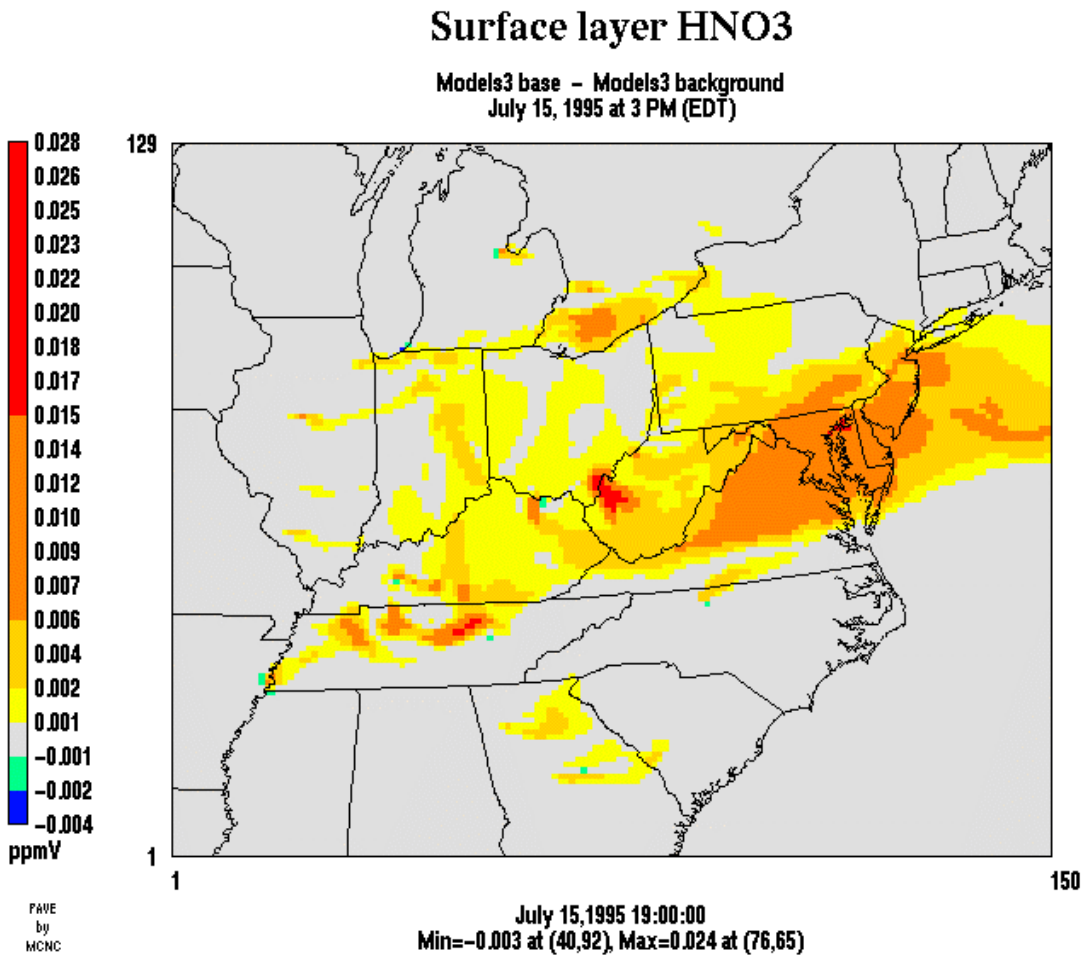

Figure 3-40
Differences (Base – Background) in surface HNO_3 concentrations, 12 km resolution domain, 3 p.m. EDT, 15 July 1995. The "Background" corresponds to a Models-3/CMAQ simulation without the emissions from the 30 point sources selected for PiG treatment.

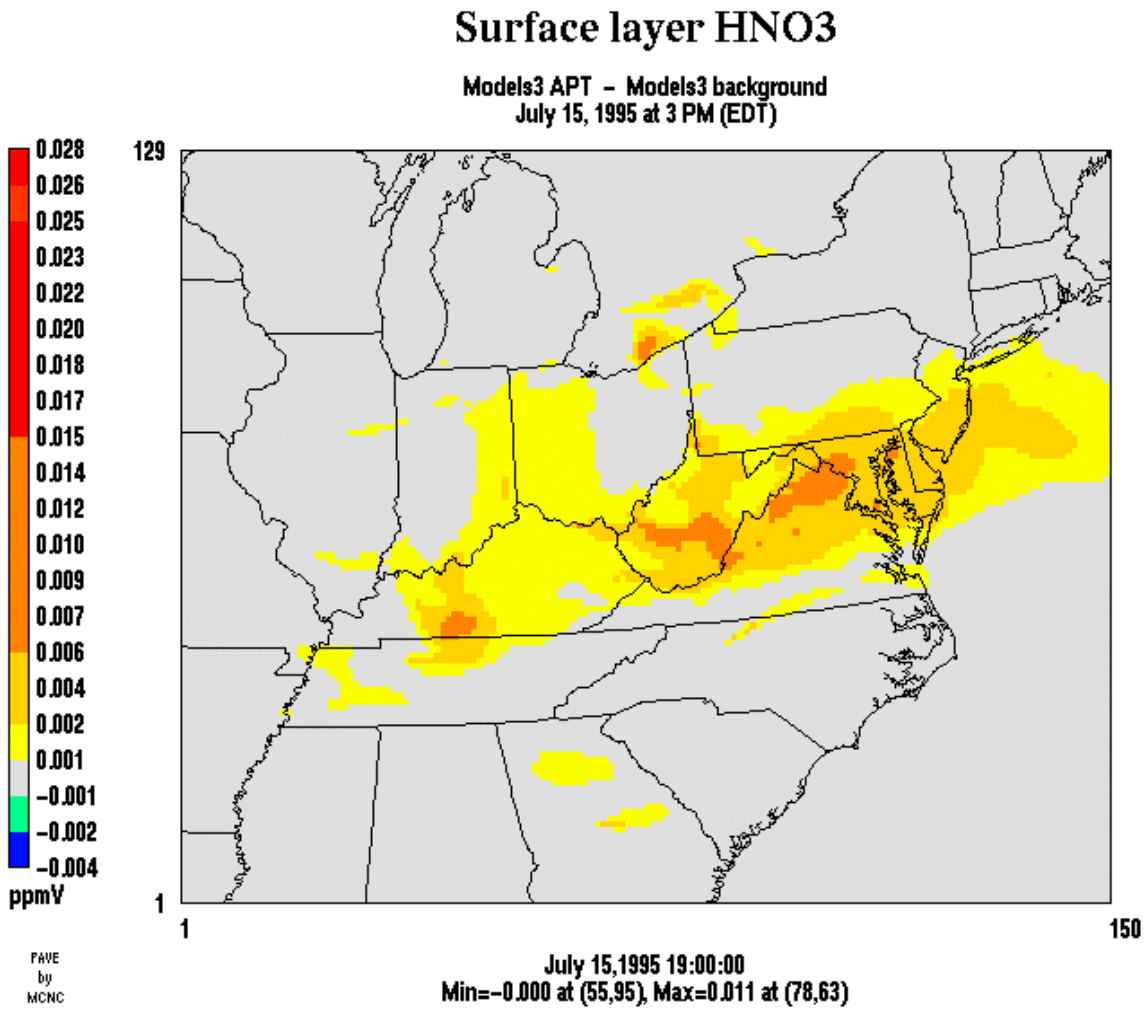

Figure 3-41
Differences (APT – Background) in surface HNO_3 concentrations, 12 km resolution domain, 3 p.m. EDT, 15 July 1995. The "Background" corresponds to a Models-3/CMAQ simulation without the emissions from the 30 point sources selected for PiG treatment.

Figures 3-42 to 3-44 show the surface HNO_3 concentration difference plots between the APT and base simulations for July 13 to 15, 1995 for the 4 km resolution domain. Over most of the domain, the APT simulation HNO_3 concentrations are lower than the base simulation values by up to 4 ppb on July 13 to about 10 ppb on July 15. On July 15, the base simulation HNO_3 concentrations are higher than the APT simulation values over almost the entire domain. In some parts of the domain on July 13 and 14, the APT simulation HNO_3 concentrations are higher than the base values. These increments are generally 1.6 ppb or lower on July 13 and 3.4 ppb or lower on July 14.

The HNO_3 concentration patterns are governed by the inflow from the western boundary as well as the plume-in-grid treatment for the six point sources located within the 4 km resolution

domain. The effect of some of those point sources appears more or less clearly depending on the day. For example, on July 15, the point source located in western New Jersey (see Figure 3-44) shows a distinct HNO_3 decrement plume that extends northeast to New York City.

Over the five-day simulation and the entire 12 km resolution modeling domain, the Models3/CMAQ-APT simulation leads to 11% less HNO_3 than the Models-3/CMAQ base simulation. In the surface layer, the Models3/CMAQ-APT simulation leads to 8% less HNO_3 than the Models-3/CMAQ base simulation. This difference is primarily due to the generally lower production of HNO_3 downwind of the major NO_x point sources in the APT simulation as compared to the base simulation.

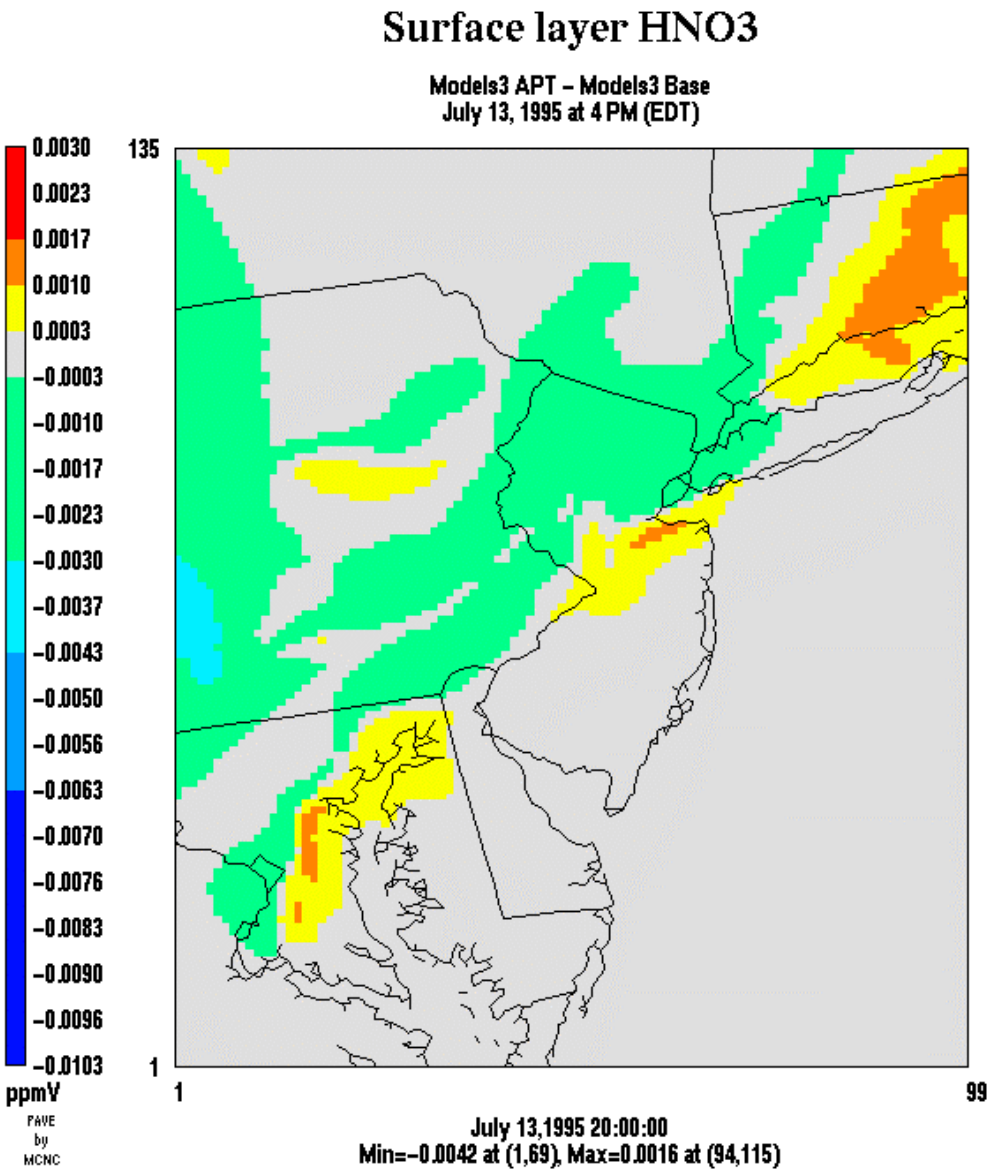

Figure 3-42
Differences (APT – Base) in surface HNO_3 concentrations, 4 km resolution domain, 4 p.m. EDT, 13 July 1995.

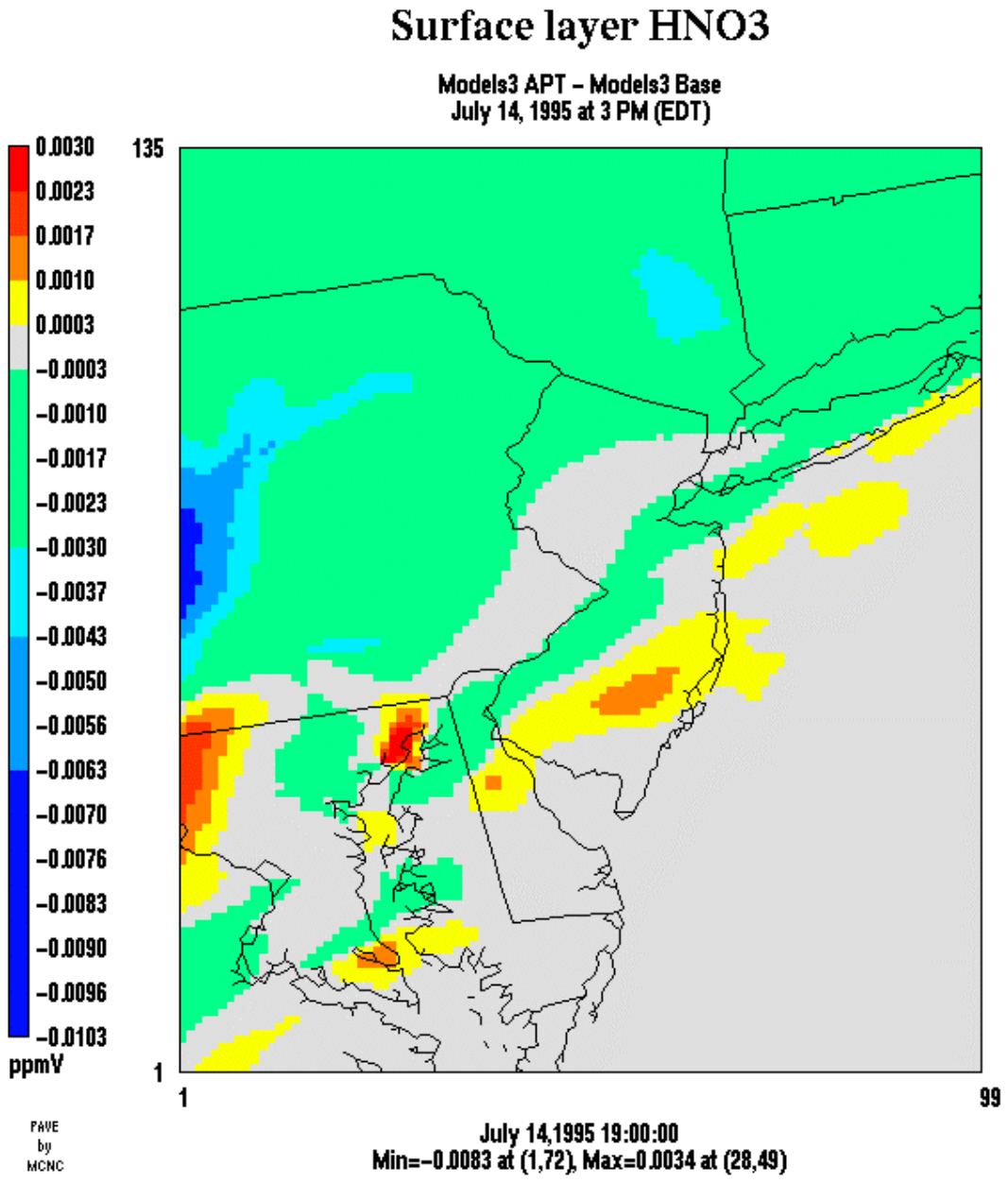

Figure 3-43
Differences (APT – Base) in surface HNO_3 concentrations, 4 km resolution domain, 3 p.m. EDT, 14 July 1995.

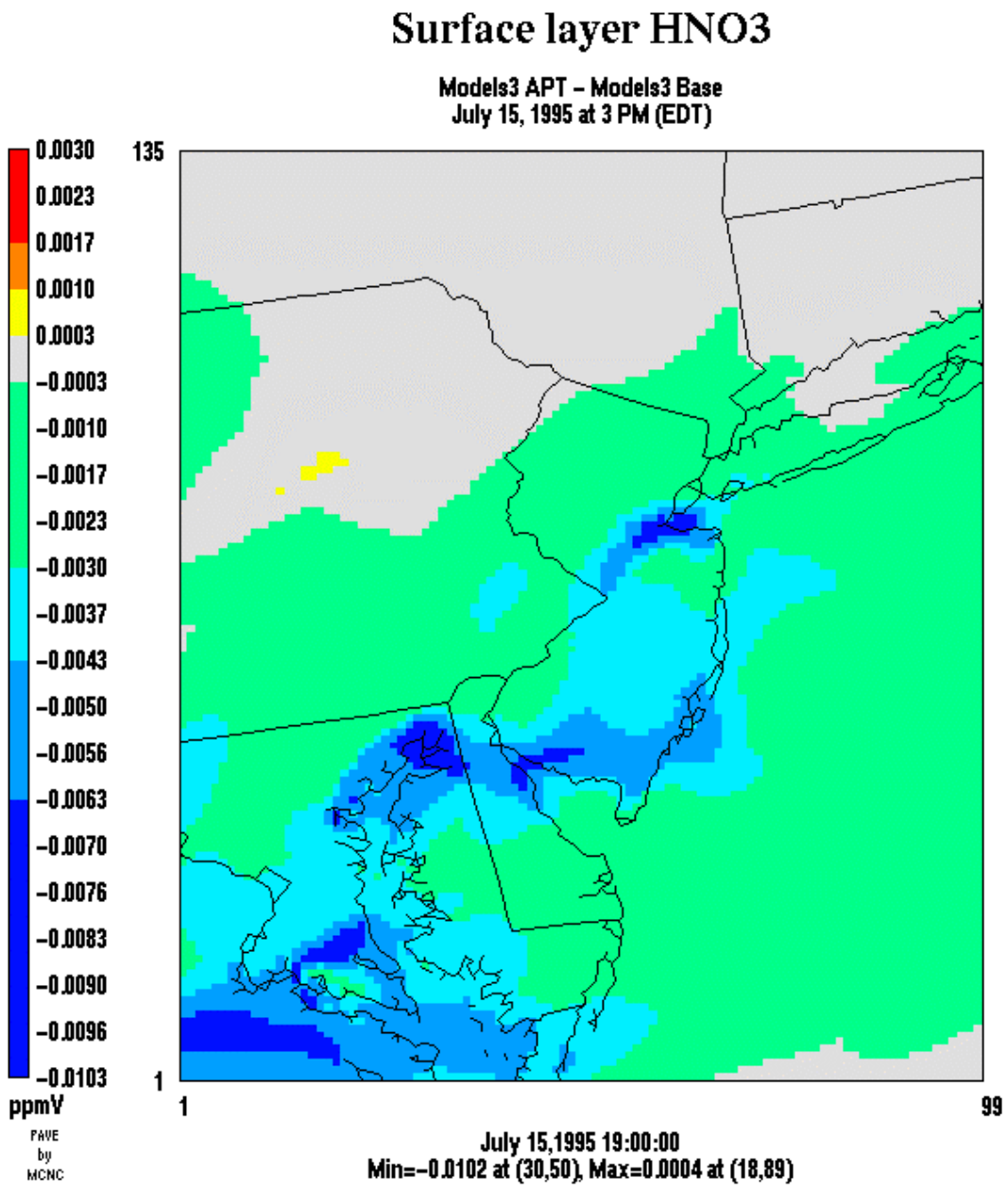

Figure 3-44
Differences (APT – Base) in surface HNO_3 concentrations, 4 km resolution domain, 3 p.m. EDT, 15 July 1995.

4
MODELS-3/CMAQ-PING APPLICATION TO THE NARSTO-NORTHEAST DOMAIN

4.1 Models-3/CMAQ Base Simulation

This Models-3/CMAQ base simulation is identical to the one presented in Section 3.1 except that a different numerical solver was used for the gas-phase chemical kinetics. As discussed in Section 2.4.2, we used the Young & Boris numerical solver for the simulations presented in Section 3. Using the Young & Boris solver led to about a 30 to 35% reduction in computational time compared to using the QSSA solver. However, since the original plume-in-grid (PinG) module of Models-3/CMAQ uses QSSA (or SMVGEAR) as the numerical solver for chemical kinetics, it was necessary for consistency to use the QSSA solver for both a Models-3/CMAQ base simulation and the Models-3/CMAQ-PinG simulation.

The Models-3/CMAQ base simulations conducted with the Young & Boris solver and the QSSA solver are very similar although some local differences are apparent. Figures 4-1 and 4-2 present the July 14 surface concentrations of O_3 and HNO_3, respectively, simulated with the QSSA solver for the 12 km resolution domain. These figures can be compared with the corresponding results from the simulation conducted with the Young & Boris solver, shown in Figures 3-3 and 3-14.

The performance statistics for the Models-3/CMAQ simulation with the QSSA solver are presented in Table 4-1 for the 12 km resolution domain and in Table 4-2 for the 4 km resolution domain. The 1-hour and 8-hour performance statistics obtained with the QSSA solver show slightly worse peak predictions but lower gross error and bias for the 12 km resolution domain, compared to the statistics obtained with the Young & Boris solver (see Table 3-2). For the 4 km resolution domain, the statistics obtained with the QSSA solver show similar performance for the peak predictions and gross error and slightly lower bias compared to the statistics obtained with the Young & Boris solver (see Table 3-3).

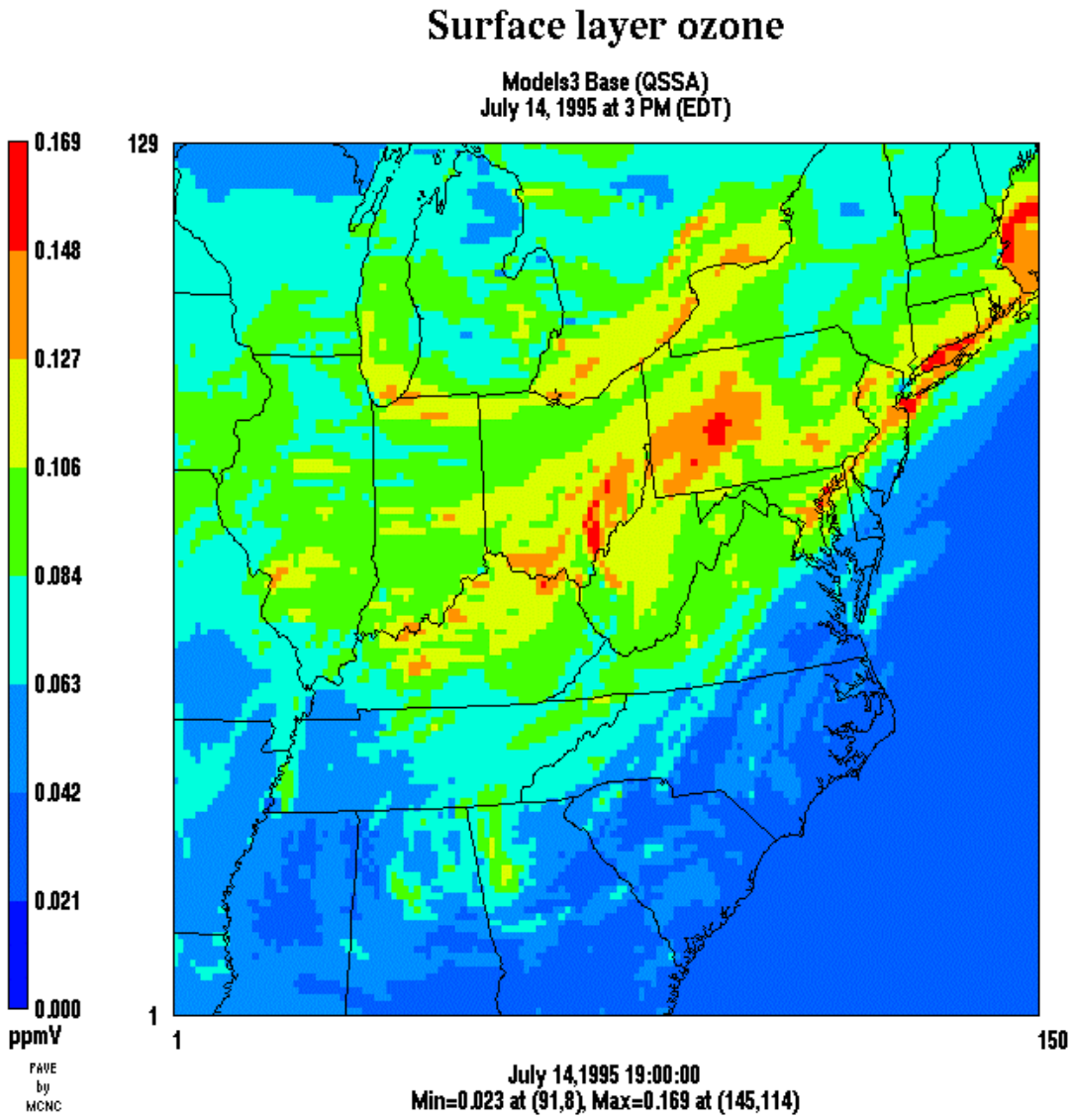

Figure 4-1
Surface O_3 concentrations, Models-3/CMAQ simulation with QSSA solver, 12 km resolution domain, 3 p.m. EDT, 14 July 1995.

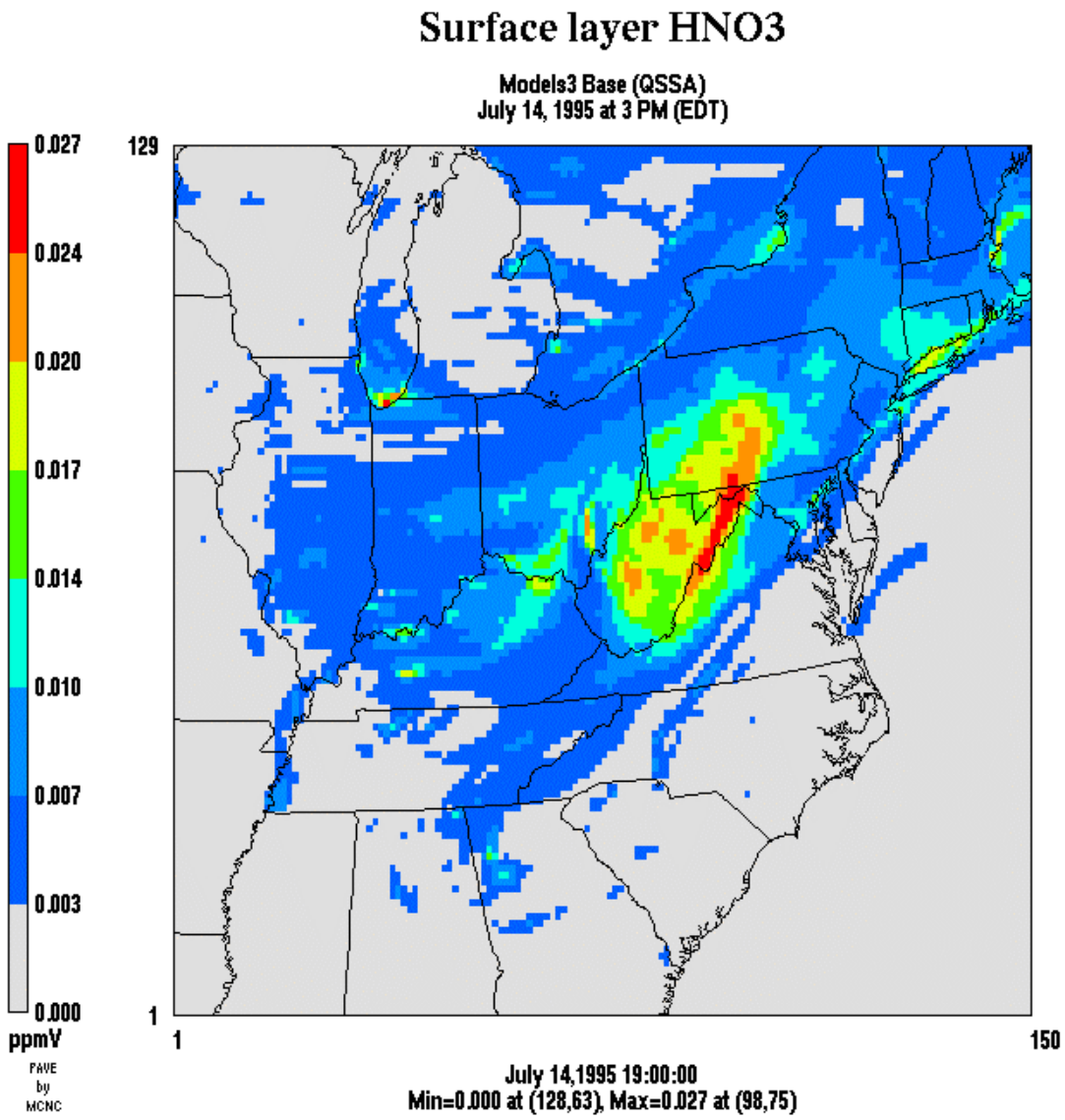

Figure 4-2
Surface HNO_3 concentrations, Models-3/CMAQ simulation with QSSA solver, 12 km resolution domain, 3 p.m. EDT, 14 July 1995.

Table 4-1
Models-3/CMAQ (QSSA) performance statistics for O_3 concentrations for 13-15 July 1995 in the 12 km resolution NARSTO-Northeast domain.

Performance Measure[a]	Performance statistics
1-hour average O_3 concentrations	
Paired peak error[b]	-53%
Gross error	30%
Fractional gross error	0.28
Bias	14%
Fractional bias	0.07
8-hour average O_3 concentrations	
Paired peak error[b]	-39%
Gross error	26%
Fractional gross error	0.24
Bias	13%
Fractional bias	0.08

(a) Performance measures are as defined by Seigneur et al. (2000); statistics are for observed O_3 concentrations greater than 40 ppb at 299 sites.
(b) Paired in both space and time.

Table 4-2
Models-3/CMAQ (QSSA) performance statistics for O_3 concentrations for 13-15 July 1995 in the 4 km resolution NARSTO-Northeast domain.

Performance Measure[a]	Performance statistics
1-hour average O_3 concentrations	
Paired peak error[b]	-22%
Gross error	30%
Fractional gross error	0.31
Bias	4%
Fractional bias	-0.04
8-hour average O_3 concentrations	
Paired peak error[b]	-11%
Gross error	25%
Fractional gross error	0.25
Bias	6%
Fractional bias	0

(a) Performance measures are as defined by Seigneur et al. (2000); statistics are for observed O_3 concentrations greater than 40 ppb at 64 sites.
(b) Paired in both space and time.

The temporal profiles of surface O_3 concentrations at the 3 stations with peak O_3 values in the 12 km resolution domain and in the 4 km resolution domain are shown in Figures 4-3 and 4-4, respectively. These results are quite similar to those obtained with the Young & Boris solver (see Figures 3-11 and 3-12).

4.2 Models-3/CMAQ-PinG Simulation

4.2.1 Overview of the Plume-in-Grid Simulation

The same point sources were selected for plume-in-grid simulation as in the Models-3/CMAQ-APT simulation. The presentation of the results follows a similar format to that in Section 3. Spatial plots are presented as the difference in O_3 or HNO_3 concentrations between the Models-3/CMAQ-PinG simulation and the Models-3/CMAQ base simulation. As in Section 3, small differences between the two simulations are shown in gray (about 4 ppb for O_3 and 2 ppb for HNO_3 in the 12 km resolution domain, 3 ppb for O_3 and 0.4 ppb for HNO_3 in the 4 km resolution domain). Positive differences are shown in yellow, orange and red while negative differences are shown in green, light blue and dark blue. Results are also presented for temporal profiles of O_3 concentrations at three sites each in the 12 km and 4 km resolution domains. However, unlike the results presented in Section 3, we do not present results showing the differences from the "background" of the base and PinG concentrations, since we did not perform a background simulation using the QSSA solver.

4.2.2 O_3 Concentrations

Figures 4-5 to 4-7 show the effect of the plume-in-grid treatment on the surface O_3 concentrations for the 12 km resolution domain for July 13 to 15, respectively. These figures can be compared with the corresponding results for Models-3/CMAQ-APT (Figures 3-20, 3-24, and 3-27). Some clear patterns emerge when comparing these two sets of figures. For example, on July 13, we see similarities in the plumes from the two point sources on the shore of Lake Huron in Michigan, with O_3 "plumes" near the point sources and some slight O_3 decrement at the edges of those O_3 "plumes". The plume of the point source located in the northern part of North Carolina is transported northward into Virginia on July 13. In the Models-3/CMAQ-APT simulation, the plume over Virginia results primarily in an O_3 decrement with only a slight O_3 increment on the eastern edge of the plume (Figure 3-20). In the Models-3/CMAQ-PinG simulation, the plume area with an O_3 decrement is reduced and there are larger areas on both edges of the plume and farther downwind that show O_3 increments.

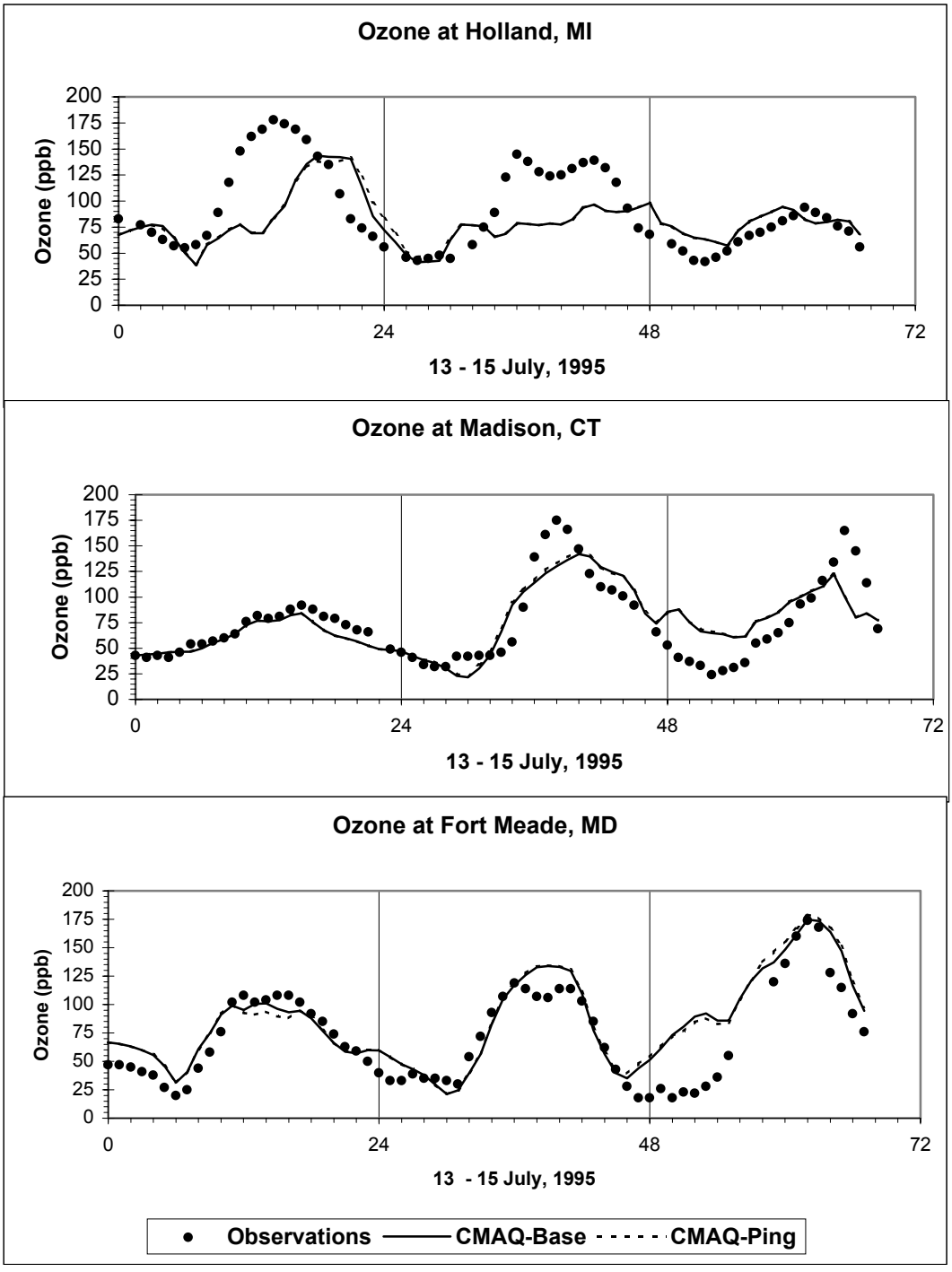

Figure 4-3
Time series of observed and simulated surface O_3 concentrations at three sites, 12 km resolution domain.

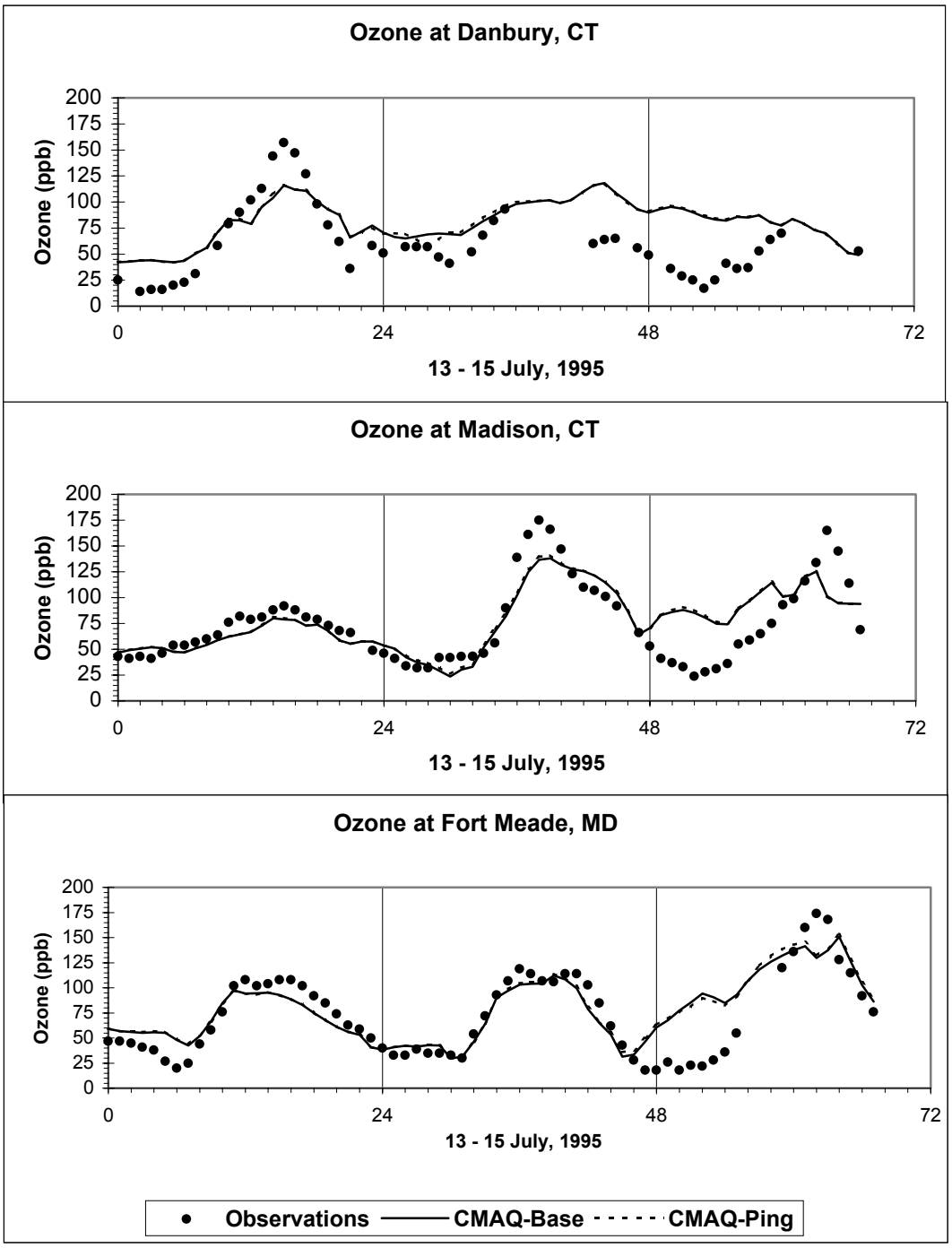

Figure 4-4
Time series of observed and simulated surface O_3 concentrations at three sites, 4 km resolution domain.

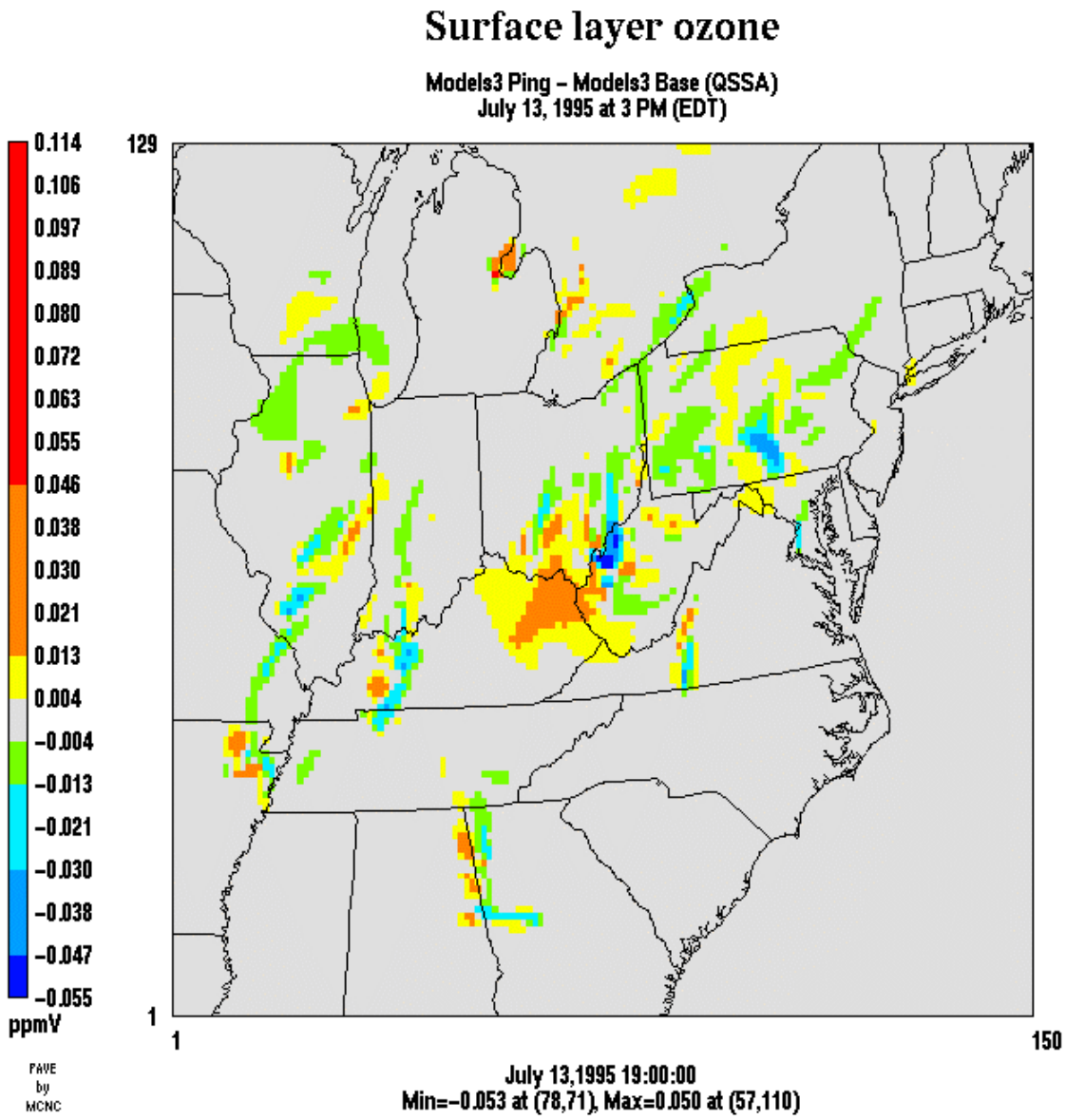

Figure 4-5
Differences (PinG – Base) in surface O_3 concentrations, 12 km resolution domain, 3 p.m. EDT, 13 July 1995.

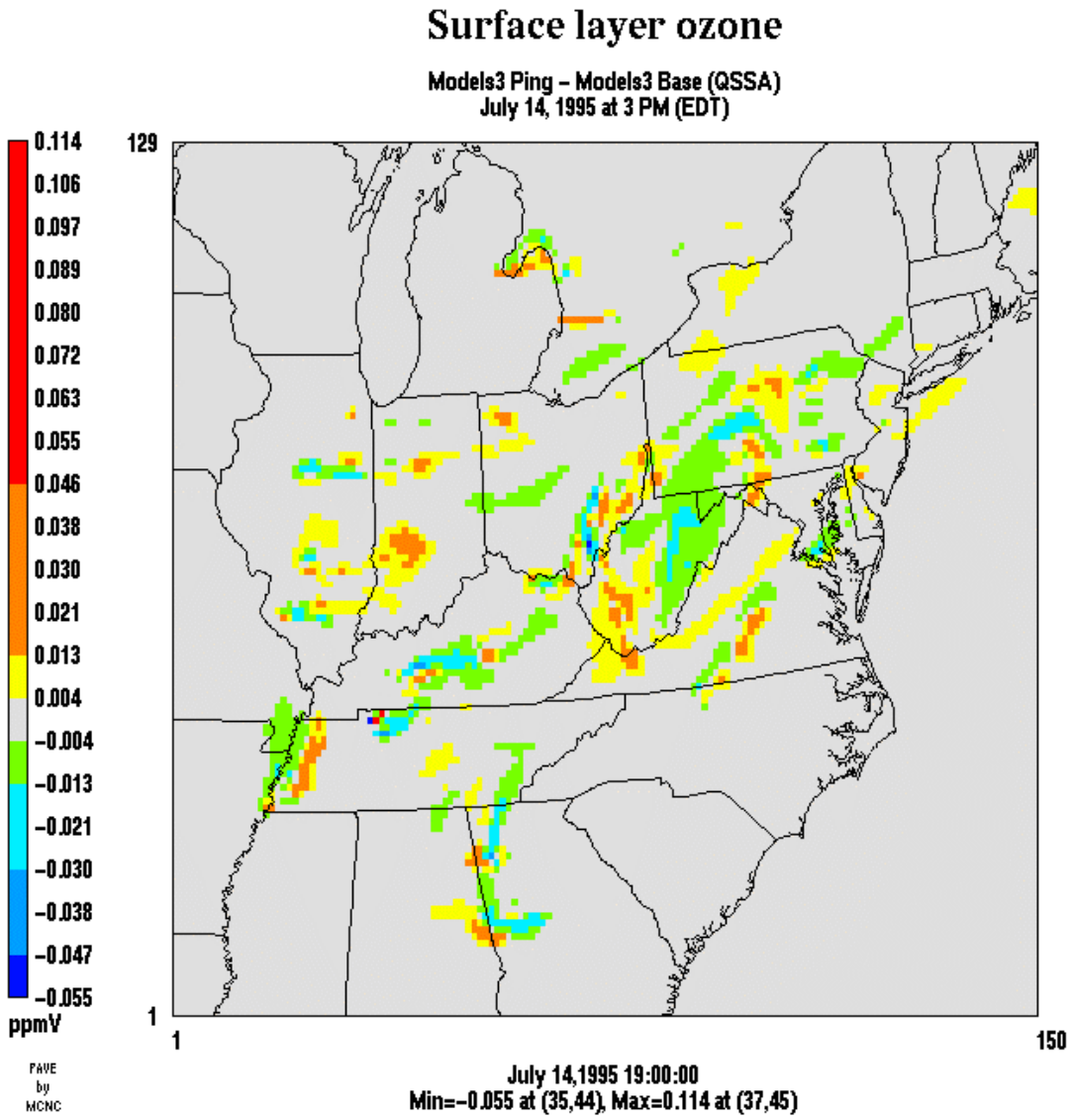

Figure 4-6
Differences (PinG – Base) in surface O_3 concentrations, 12 km resolution domain, 3 p.m. EDT, 14 July 1995.

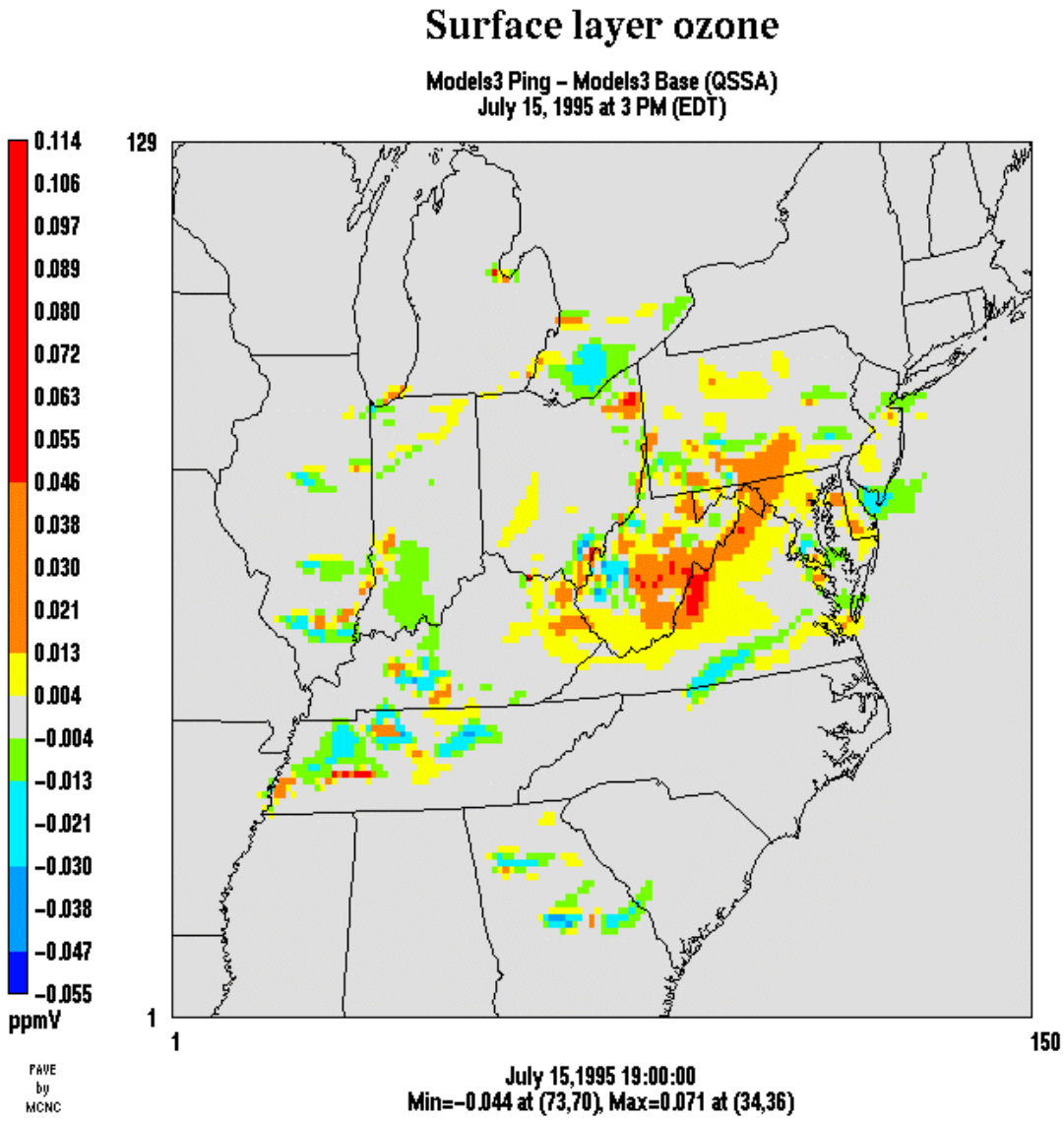

Figure 4-7
Differences (PinG – Base) in surface O_3 concentrations, 12 km resolution domain, 3 p.m. EDT, 15 July 1995.

The PinG O3 results near the Cumberland power plant on July 14 (Figure 4-6) are anomalous. The 114 ppb O_3 increment about 25 km NNE of Cumberland in the PinG simulation appears to be unrealistic. In the base simulation with the Y&B solver (Figure 3-3), the concentrations in the region range from about 55 ppb to a maximum of about 108 ppb. In the base simulation with the QSSA solver (Figure 4-1), the concentrations range from about 55 ppb to a maximum of 105 ppb (at the same location as the Y&B maximum). In the APT simulation, the concentrations range from 55 to 98 ppb. However, in the PinG simulation, there is a large decrement in O_3 concentration (to almost zero) in the grid cell immediately NW of the Cumberland source, and two large increments in the adjacent cells (to 136 ppb in the cell immediately north of Cumberland and to 180 ppb about 25 km NNE of Cumberland, 114 ppb above the QSSA base simulation value of 66 ppb).

Differences between the Models-3/CMAQ-APT and Models-3/CMAQ-PinG simulations are more prevalent in the area surrounding the Ohio River Valley (i.e., Ohio, West Virginia and Kentucky). In the Models-3/CMAQ-PinG simulation, both decrements and increments in O_3 concentrations appear around the Ohio River Valley and the downwind areas. However, these areas of O_3 increments and decrements do not always match those obtained in the Models-3/CMAQ-APT simulation

The Models-3/CMAQ-APT and Models-3/CMAQ-PinG simulation results can be summarized as follows:

- Similar results for the plumes located in VOC-limited environments on July 13 (i.e., the two point sources near Chicago and the point source in northern Michigan).
- Similar results but with O_3 increments appearing at the plumes edges and farther downwind in the Models-3/CMAQ-Ping simulation for isolated point sources in the Southeast and the upper Midwest.
- Significant differences in the Ohio River Valley and downwind areas where Models-3/CMAQ-APT and Models-3/CMAQ-Ping show different patterns of O_3 decrements and increments.

The similar results in the upper Midwest on July 13 occur in areas that are VOC-limited. In such areas, both plume-in-grid treatments show O_3 increments in the vicinity of the point sources because NO_x titration is postponed until farther downwind.

The point sources in the Midwest and the Southeast are located in an environment that is typically NO_x-limited in summertime (Jacob et al., 1995). Therefore, the plume-in-grid treatment leads to decrements in O_3 formation as NO_x is less available for O_3 formation compared to the base simulation. As the plume becomes more dilute and/or plume material gets transferred to the host model, the increases in NO_x concentrations may then lead to O_3 increments. Comparing the results of the two sets of simulations, these results suggest that the plumes are transferred to the host model earlier in the Models-3/CMAQ-PinG simulation than in the Models-3/CMAQ-APT simulation. This difference may be explained by the fact that the PinG plume module assumes a vertically well-mixed plume (i.e., more dispersed vertically than the APT plume) and uses different algorithms for plume dispersion than the APT plume module. Also, although the primary criteria for plume-to-grid transfer are similar in both models, Models-3/CMAQ-Ping has additional criteria that will lead to early plume-to-grid transfer (these criteria

are designed to promote plume-to-grid transfer in cases of strong wind speed shear or interacting plumes).

The larger discrepancies that appear in the Ohio River Valley and in the areas located downwind are likely due to a combination of factors. The possible earlier release of plume material to the host model in the Model-3/CMAQ-PinG simulation mentioned above will contribute to O_3 increments in areas that are locally NO_x-sensitive. For example, on July 14 the Models-3/CMAQ-APT simulation shows a well-defined area of O_3 decrements in southeastern Ohio, north and downwind of several point sources with explicit plume-in-grid treatment. On the other hand, the Models-3/CMAQ-PinG simulation shows some areas of O_3 decrements intertwined with areas of O_3 increments, thereby suggesting that plume material may have been released to the host grid system more rapidly than in the Models-3/CMAQ-APT simulation. The lack of treatment for overlapping plumes in the Models-3/CMAQ-PinG formulation may also contribute to this discrepancy since the Ohio River Valley includes several major point sources (see Figure 3-19) that are likely to have overlapping plumes. Finally, the early release of plume material to the host grid system may lead to faster conversion of NO_2 to HNO_3 (see next section). As NO_2 is removed from the photochemical cycle, it is no longer available for O_3 formation and O_3 decrements should result farther downwind. Such an area of O_3 decrements is seen in the Models-3/CMAQ-PinG simulation on July 14 in the northeastern part of West Virginia and southwestern Pennsylvania. In contrast, the Models-3/CMAQ-APT simulation shows O_3 increments in those areas.

Figures 4-8 to 4-10 show the effect of the plume-in-grid treatment on the surface O_3 concentrations for the 4 km resolution domain for July 13 to 15, respectively. These figures can be compared with Figures 3-30 to 3-32 for Models-3/CMAQ-APT. On July 13, there are similarities between the O_3 concentration patterns simulated by Models-3/CMAQ-PinG and Models-3/CMAQ-APT in the vicinity of point sources with explicit plume-in-grid treatment. For example, the two point sources located in Maryland show an O_3 "plume" near the source and a decrement in O_3 concentrations farther downwind. Models-3/CMAQ–APT shows O_3 increments that are more limited spatially and downwind increments that are more pronounced compared to Models-3/CMAQ-PinG, but the overall patterns are consistent.

The temporal profiles of O_3 concentrations predicted by Models-3/CMAQ-PinG have already been compared to the observed concentrations and the base simulation concentrations predicted by Models-3/CMAQ (QSSA) in Figures 4-3 and 4-4. As in the case of the Models-3/CMAQ-APT simulation, these profiles show little influence of Models-3/CMAQ-PinG at the sites considered in Figures 4-3 and 4-4.

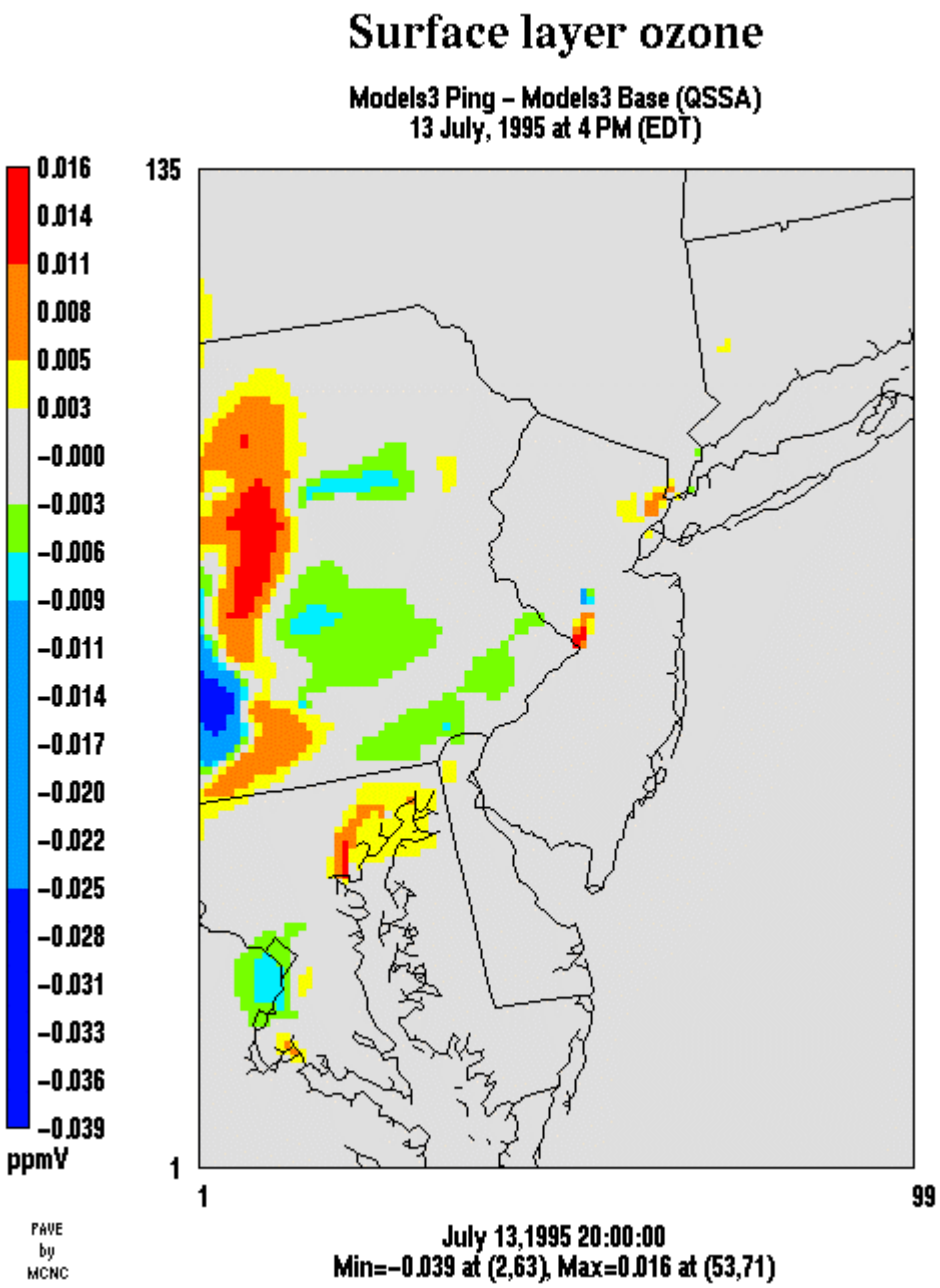

Figure 4-8
Differences (PinG – Base) in surface O_3 concentrations, 4 km resolution domain, 4 p.m. EDT, 13 July 1995.

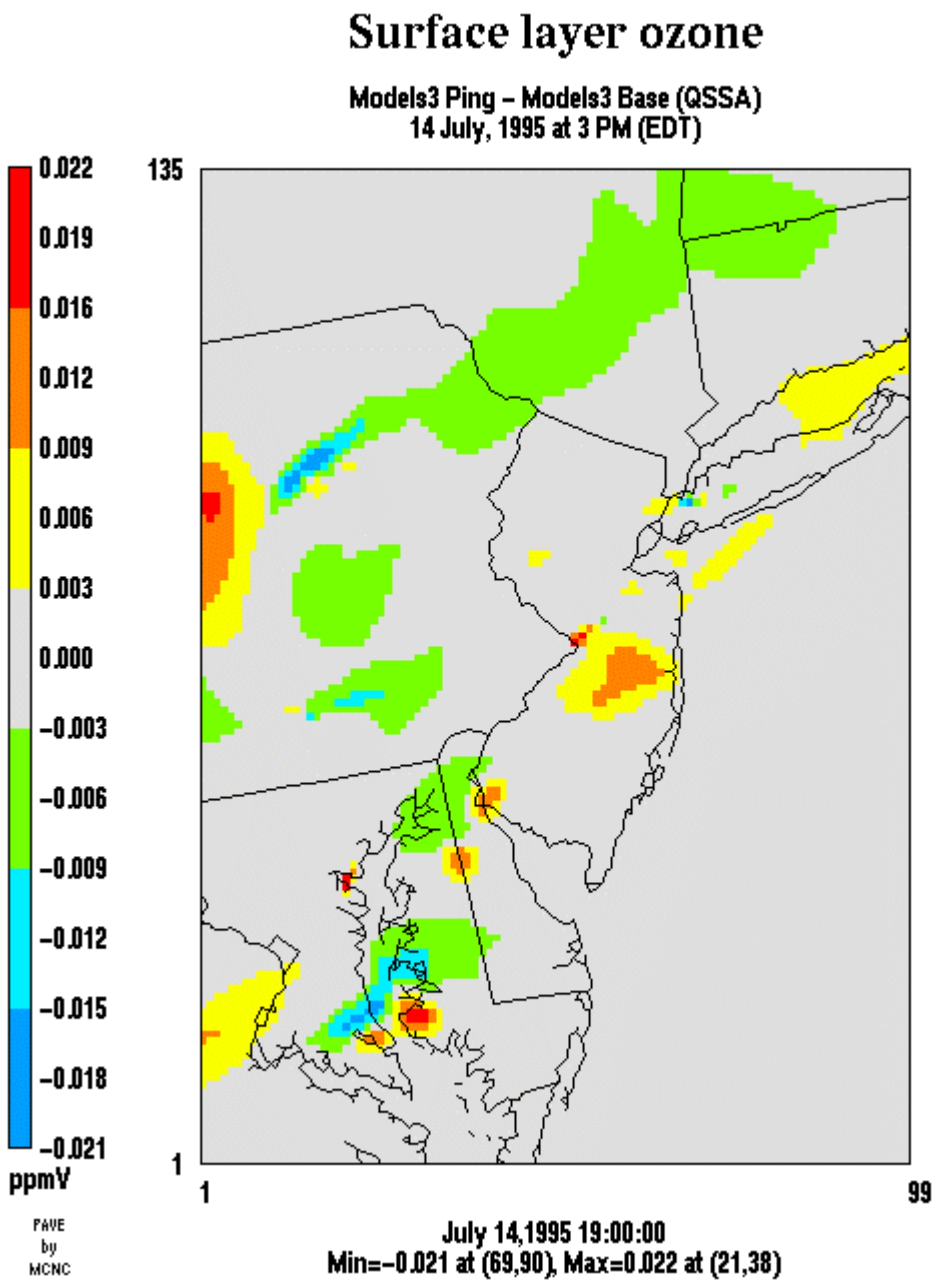

Figure 4-9
Differences (PinG – Base) in surface O_3 concentrations, 4 km resolution domain, 3 p.m. EDT, 14 July 1995.

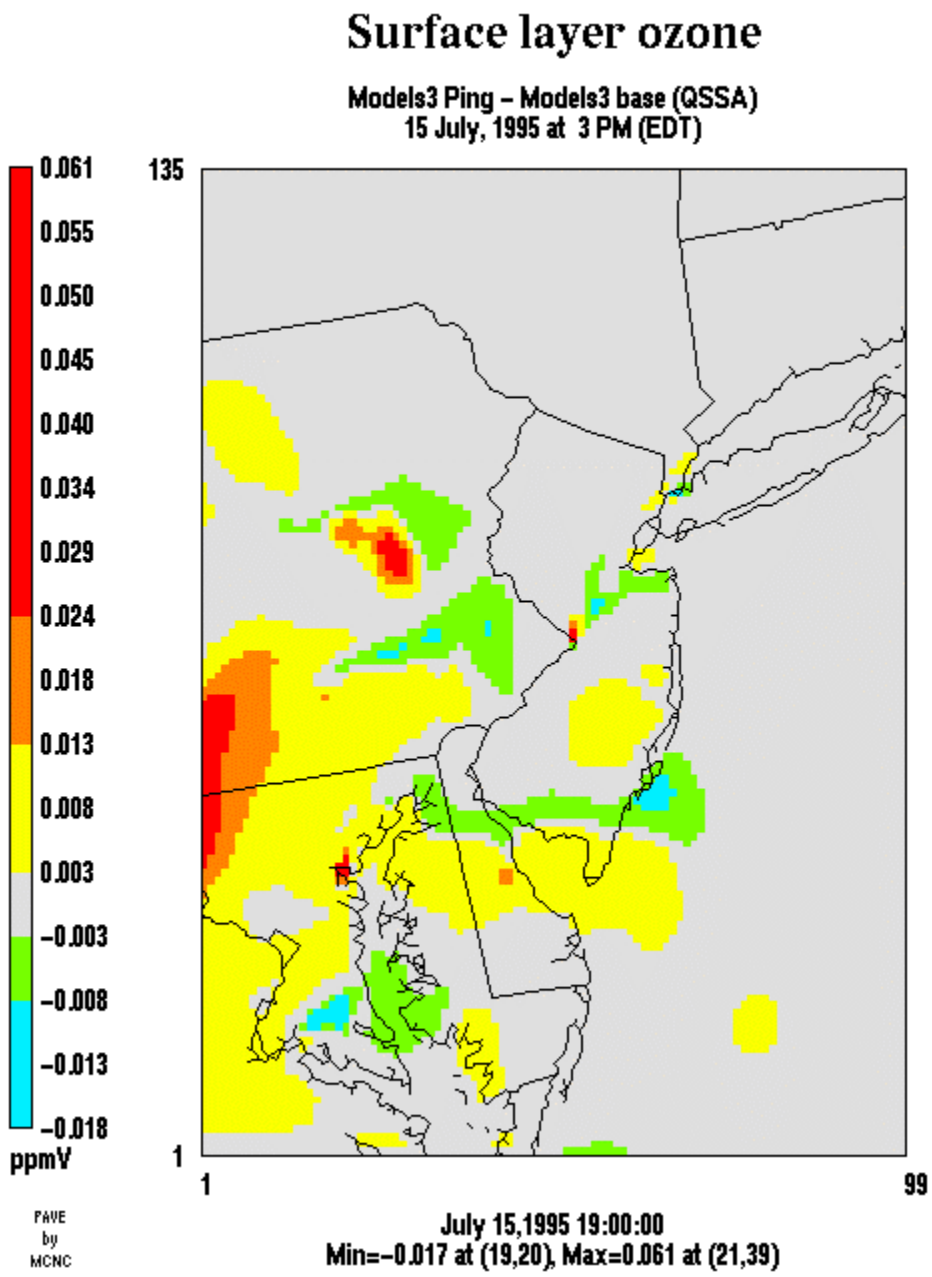

Figure 4-10
Differences (PinG – Base) in surface O_3 concentrations, 4 km resolution domain, 3 p.m. EDT, 15 July 1995.

Table 4-3
Models-3/CMAQ-PinG performance statistics for O_3 concentrations for 13-15 July 1995 in the 12 km resolution NARSTO-Northeast domain.

Performance Measure[a]	Performance statistics
1-hour average O_3 concentrations	
Paired peak error[b]	-53%
Gross error	30%
Fractional gross error	0.28
Bias	14%
Fractional bias	0.07
8-hour average O_3 concentrations	
Paired peak error[b]	-40%
Gross error	26%
Fractional gross error	0.24
Bias	13%
Fractional bias	0.08

(a) Performance measures are as defined by Seigneur et al. (2000); statistics are for observed O_3 concentrations greater than 40 ppb at 299 sites.
(b) Paired in both space and time.

Table 4-4
Models-3/CMAQ-PinG performance statistics for O_3 concentrations for 13-15 July 1995 in the 4 km resolution NARSTO-Northeast domain.

Performance Measure[a]	Performance statistics
1-hour average O_3 concentrations	
Paired peak error[b]	-20%
Gross error	31%
Fractional gross error	0.31
Bias	6%
Fractional bias	-0.03
8-hour average O_3 concentrations	
Paired peak error[b]	-9%
Gross error	26%
Fractional gross error	0.25
Bias	6%
Fractional bias	0.01

(a) Performance measures are as defined by Seigneur et al. (2000); statistics are for observed O_3 concentrations greater than 40 ppb at 64 sites.
(b) Paired in both space and time.

The performance statistics for Models-3/CMAQ-PinG are presented in Tables 4-3 and 4-4 for the 12 km and 4 km resolution domains, respectively. These statistics show little difference when compared to those of the corresponding base case (see Tables 4-1 and 4-2).

4.2.3 HNO_3 Concentrations

Figures 4-11 to 4-13 show the effect of the plume-in-grid treatment using Models-3/CMAQ-PinG on the surface HNO_3 concentrations for the 12 km resolution domain for July 13 to 15, respectively. These figures can be compared to the corresponding results from the Models-3/CMAQ-APT simulation, shown in Figures 3-33, 3-36, and 3-39.

The differences between these two sets of figures can be related to the earlier discussion on the O_3 results presented in Section 4.2.2. Overall, Models-3/CMAQ-APT predicts large areas with decrements in HNO_3 concentrations whereas Models-3/CMAQ-PinG predicts large areas with increments in HNO_3 concentrations. We note that some of the similarities that occurred for the O_3 concentrations downwind of isolated point sources also appear for the HNO_3 concentrations. For example, the North Carolina point source and the two Georgia point sources show HNO_3 decrements downwind. However, these HNO_3 decrements are smaller spatially in the Models-3/CMAQ-PinG simulation and are followed by increments farther downwind (probably due to transfer of plume material to the host model) that do not occur in the Models-3/CMAQ-APT simulation.

The most significant discrepancies occur in the Ohio River Valley and the downwind areas. The reasons that were given to explain these discrepancies in the O_3 concentrations apply also to the HNO_3 concentrations. Clearly, a release of plume material that leads to an O_3 increment in the Models-3/CMAQ-PinG simulation will enhance the oxidation rate of NO_2 to HNO_3. On the other hand, plumes being transported farther downwind without being released to the host model (e.g., Models-3/CMAQ-APT) may continue to display a lower NO_2 oxidation rate than the background.

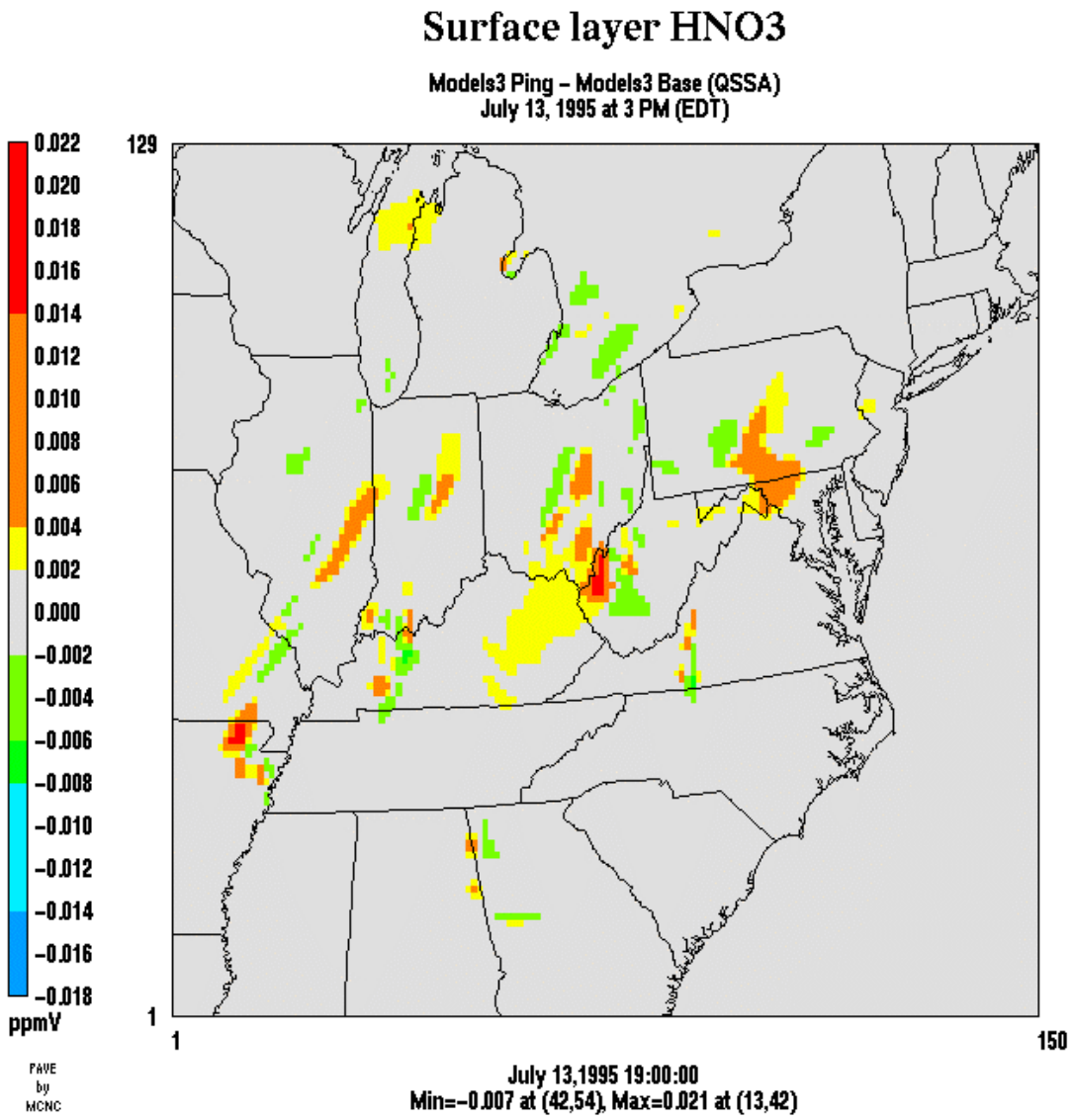

Figure 4-11
Differences (PinG – Base) in surface HNO_3 concentrations, 12 km resolution domain, 3 p.m. EDT, 13 July 1995.

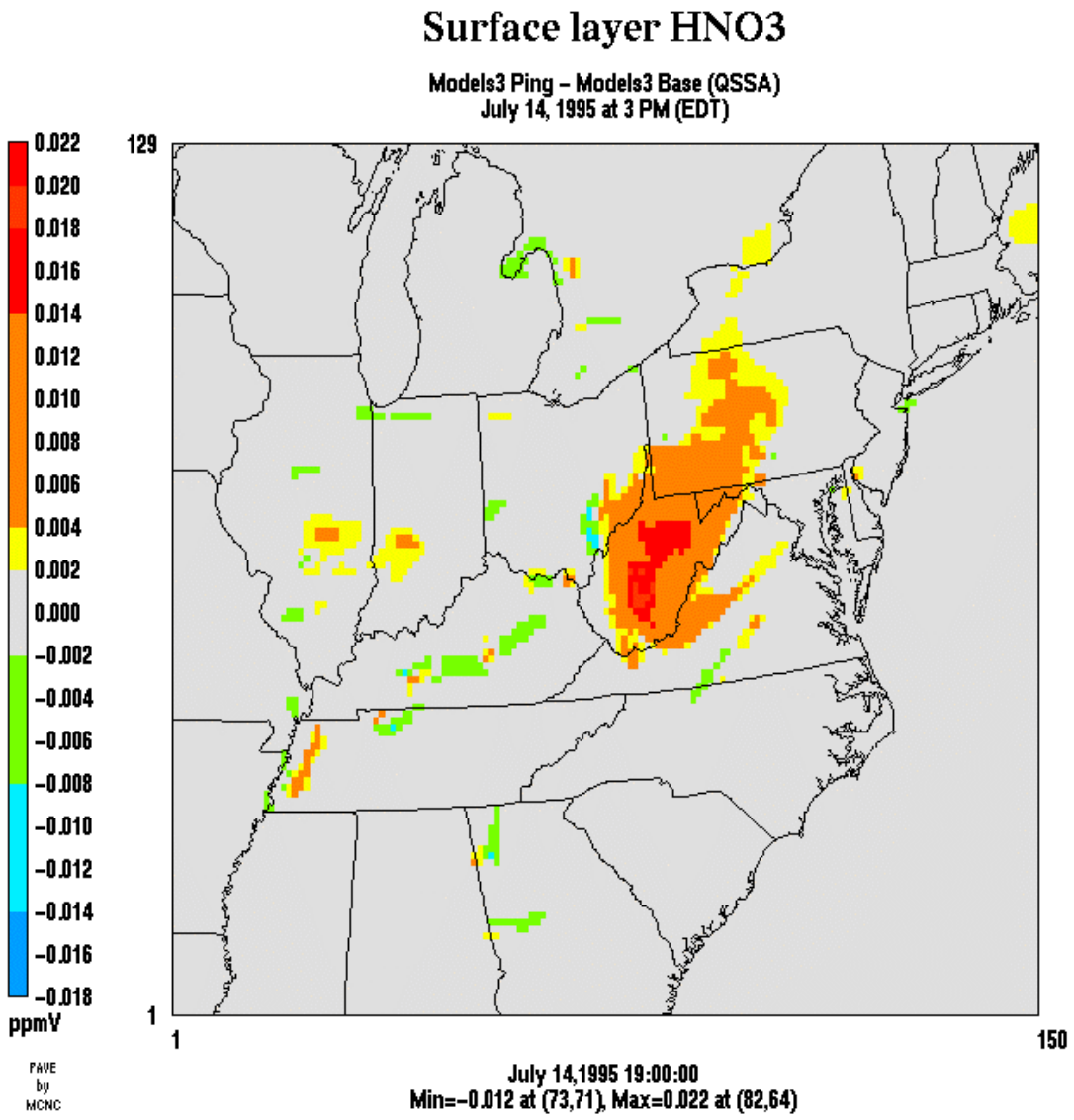

Figure 4-12
Differences (PinG – Base) in surface HNO_3 concentrations, 12 km resolution domain, 3 p.m. EDT, 14 July 1995.

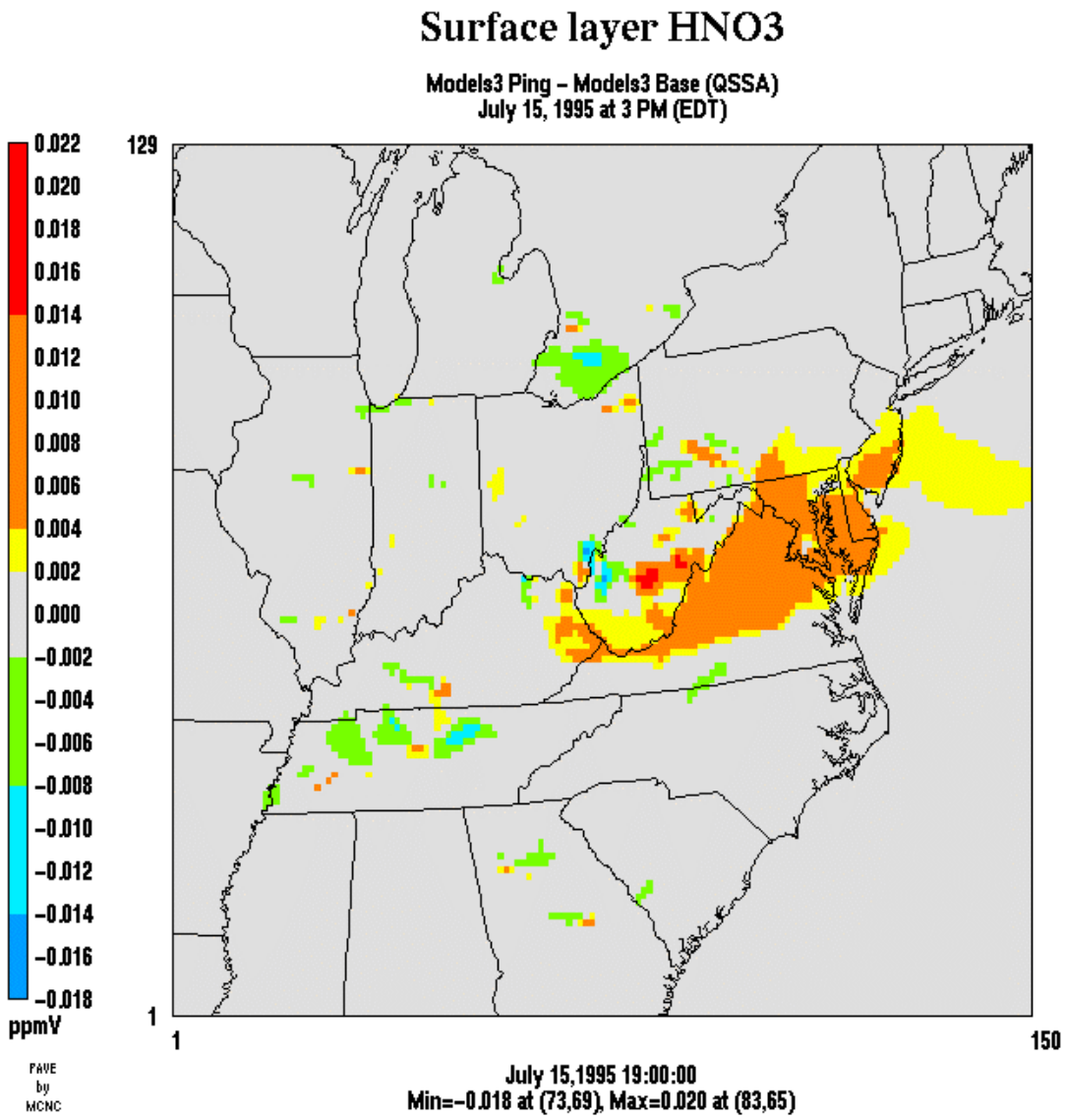

Figure 4-13
Differences (PinG – Base) in surface HNO_3 concentrations, 12 km resolution domain, 3 p.m. EDT, 15 July 1995.

Figures 4-14 to 4-16 show the effect of the plume-in-grid treatment on the surface HNO_3 concentrations for the 4 km resolution domain for July 13 to 15, respectively. These figures can be compared with Figures 3-42 to 3-44 for Models-3/CMAQ-APT. The qualitative analysis made above for the O_3 concentrations holds here as well. If we consider a single point source that is not affected by the boundary conditions, there are strong similarities between the two sets of simulations. For example, for the point source located in eastern Maryland, both the APT and PinG simulations show similar downwind decreases in HNO_3 concentrations on July 13, except on the eastern edge where Models-3/CMAQ-PinG predicts an increase in HNO_3 concentrations. However, the influence of the different boundary conditions appears clearly in central Pennsylvania. As the simulations progress from July 13 to 15, the two plume-in-grid simulations diverge. On July 15, Models-3/CMAQ-APT predicts lower HNO_3 concentrations than the base simulation over most of the domain and Models-3/CMAQ-PinG predicts greater HNO_3 concentrations than the base simulation over most of the domain. This divergence between the two plume-in-grid simulations does not seem to result from the plume-in-grid treatment of isolated point sources (as discussed above, the models predict different but qualitatively similar plumes for such sources), but rather from the treatment of several point sources located in the Ohio River Valley. For such situations, the ability of Models-3/CMAQ-APT to treat overlapping plumes explicitly may prove very valuable.

Over the five-day simulation and the entire 12 km resolution modeling domain, the Models-3/CMAQ-PinG simulation leads to 10% more HNO_3 than the Models-3/CMAQ base simulation. In the surface layer, the Models3/CMAQ-PinG simulation leads to 5% more HNO_3 than the Models-3/CMAQ base simulation.

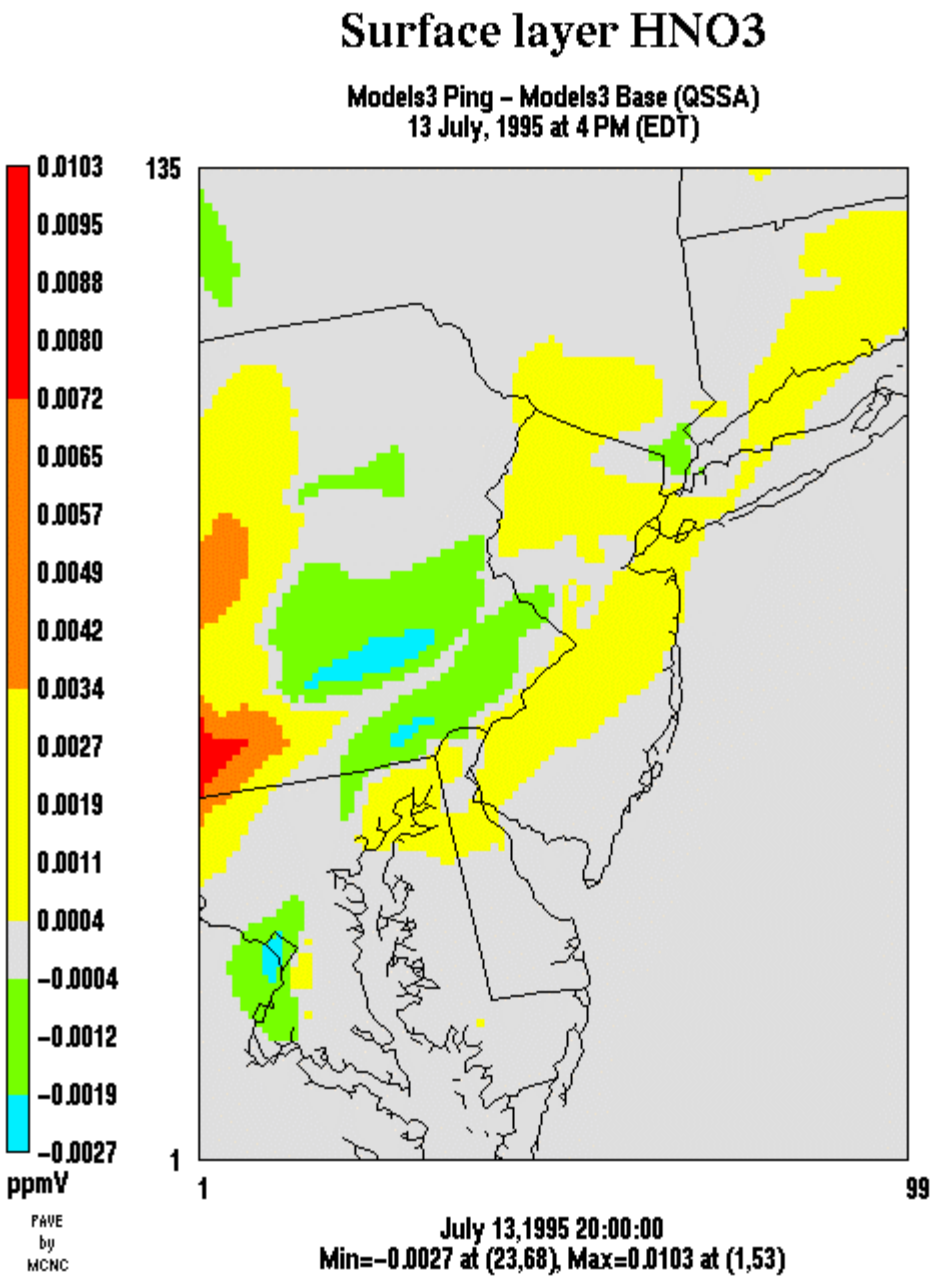

Figure 4-14
Differences (PinG – Base) in surface HNO_3 concentrations, 4 km resolution domain, 4 p.m. EDT, 13 July 1995.

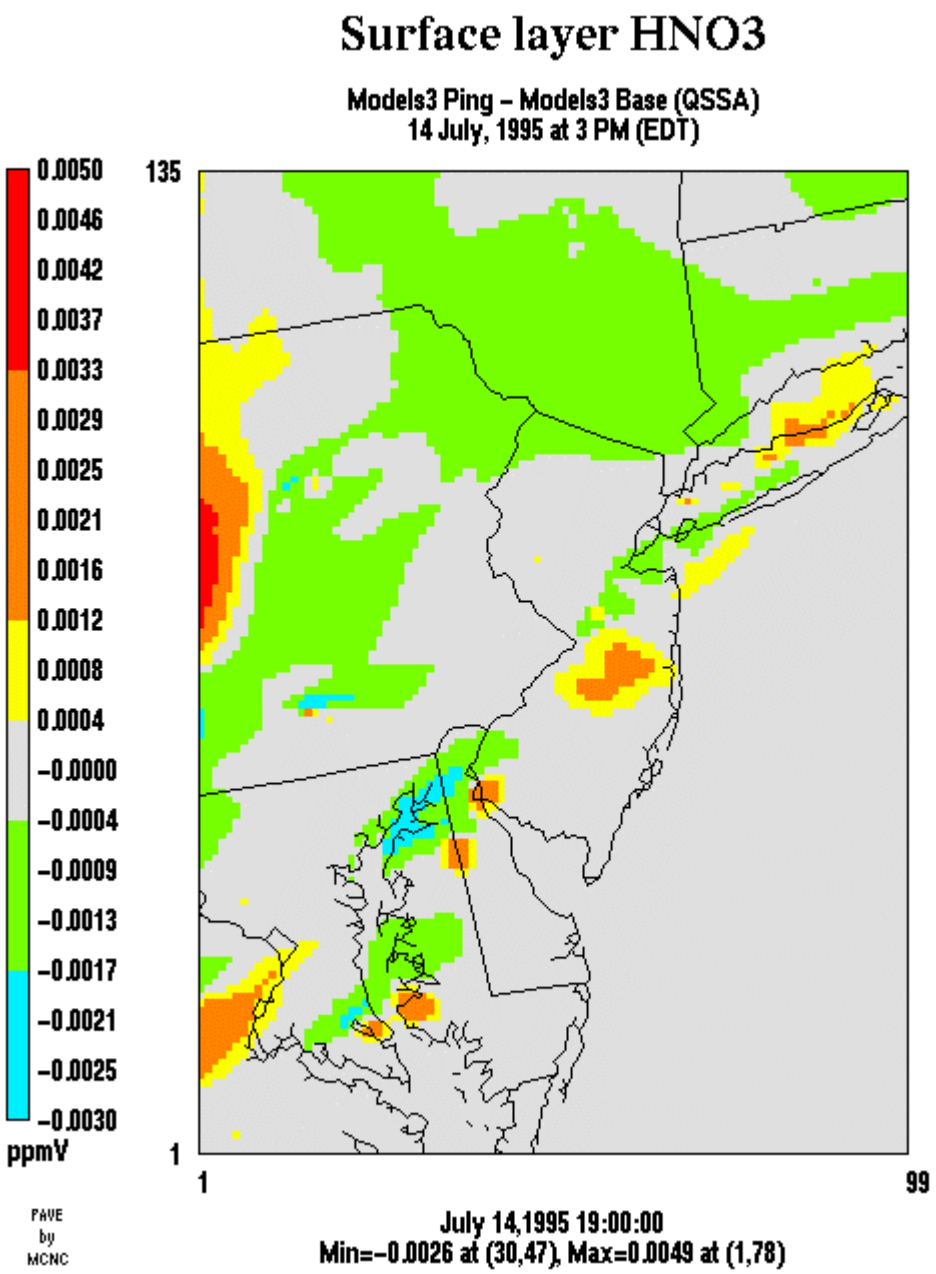

Figure 4-15
Differences (PinG – Base) in surface HNO_3 concentrations, 4 km resolution domain, 3 p.m. EDT, 14 July 1995.

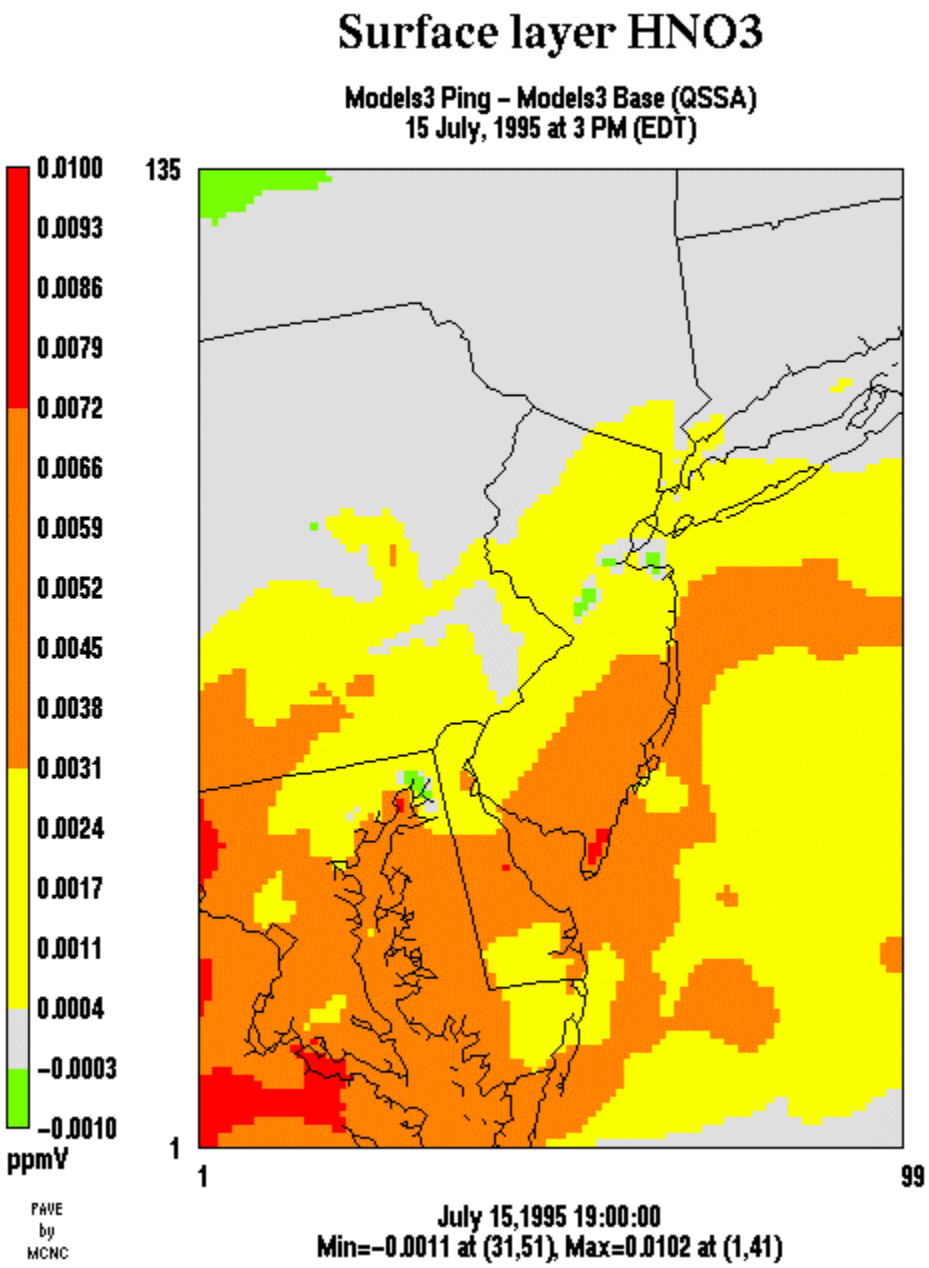

Figure 4-16
Differences (PinG – Base) in surface HNO_3 concentrations, 4 km resolution domain, 3 p.m. EDT, 15 July 1995.

5
CONCLUSION

A new state-of-the science plume-in-grid model, Models-3/CMAQ-APT, has been developed and applied to several areas. In this report, we have described recent improvements to Models-3/CMAQ-APT. Those improvements include (1) a more comprehensive set of criteria for the transfer of plume material to the host grid system that take into account both the physical dimension of the plume and its chemical maturity, (2) a more efficient numerical solver for the gas-phase chemical kinetic equations in the host model, and (3) diagnostic output that summarizes the various processes contributing to the evolution of the plume material.

Models-3/CMAQ-APT was applied to the NARSTO-Northeast area with two nested domains of 12 km and 4 km horizontal resolution, for the five-day episode of 11-15 July 1995. The thirty largest NO_x point sources in the 12 km resolution domain were explicitly simulated with plume-in-grid treatment. Six of these sources were in the 4 km resolution domain. A "background" simulation was also conducted for the 12 km resolution domain, in which the emissions from the 30 point sources were neglected. Differences in the results between the background simulation and the base and APT simulations provide a measure of the contribution of these point sources to O_3 and HNO_3 concentrations with and without PiG treatment.

The simulation results show that the use of Models-3/CMAQ-APT has a significant effect on the spatial patterns of O_3 and HNO_3 surface concentrations downwind of the sources considered for PiG treatment to distances of 100 to 200 km. O_3 concentrations from the APT simulation show both decrements and increments with respect to the base simulation. The maximum decrement is about 80 ppb, and the maximum increment is about 77 ppb. The decrements and increments compensate each other so that over the entire domain and episode, the difference in the total O_3 mass in the two simulations is negligible (0.5%).

A comparison of the base simulation and APT simulation results with those from the background simulation shows that most of the O_3 decrements are associated with lower production of O_3 immediately downwind of the point sources in the APT simulation relative to the base simulation. For a majority of the point sources considered for PiG treatment in the 12 km resolution domain, the maximum increases in O_3 concentrations in the base simulation over the background simulation values are generally 5 to 30 ppb higher than the corresponding increases in the APT simulation. Furthermore, O_3 production is generally delayed in the APT simulation as compared to the base simulation. In the base simulation, the maximum increases in O_3 concentrations over the background values generally occur within downwind distances of about 50 km, while in the APT simulation, the maximum increases typically occur further downwind, at distances of 100 to 200 km.

With one exception, the large increments in O_3 concentrations between the APT and base simulations are primarily associated with the higher titration of background O_3 in the base

simulation near and upwind of the point sources, particularly in VOC-limited environments. When the PiG treatment is used, the plume NO remains aloft and is not available for titrating surface O_3 concentrations near the source. An exception to the above generalization occurs in West Virginia, downwind of the Ohio River Valley point sources. Large increments in surface O_3 concentrations between the APT and base simulations are noted, particularly on July 14, that are primarily associated with higher O_3 production further downwind in the APT simulation than in the base simulation. In the base simulation, the NO_x in the plume undergoes rapid conversion to HNO_3 and O_3 within 25 to 50 km of the sources, leading to a depletion of NO_x, and a consequent reduction in O_3 production, at larger downwind distances. In the APT simulation, the conversion of NO_x to HNO_3 occurs at a slower rate, so that more NO_x is available for O_3 production at larger downwind distances (about 150 to 200 km from the sources in southeastern Ohio). Note that the combined NO_x emissions from the cluster of sources in southeastern Ohio and West Virginia are almost three times higher than that from the single largest source in the modeling domain (the Cumberland power plant).

The smaller increments (typically less than 10 ppb) between the APT and base simulations are associated with both higher titration of existing O_3 in the base simulation and delayed production of O_3 further downwind in the APT simulation, as the plume NO_x is transported and exposed to a NO_x-limited environment.

For HNO_3 concentrations, the differences between the APT and base simulations range from a maximum decrement of 24 ppb to a maximum increment of 9 ppb. The APT simulation generally gives lower HNO_3 concentrations than the base simulation over a large portion of the modeling domain. Thus, over the entire domain and episode, the plume-in-grid treatment leads to a decrease in HNO_3 mass of 11%.

These results suggest that it is preferable to treat major NO_x point sources with Models-3/CMAQ-APT, since both O_3 and HNO_3 production downwind of these sources are generally overpredicted if a PiG treatment is not used.

The original plume-in-grid version of Models-3/CMAQ, Models-3/CMAQ-PinG, was also applied to the same domain and episode. Comparing the results obtained with Models-3/CMAQ-APT and Models-3/CMAQ-PinG showed similarities as well as discrepancies.

- For isolated point sources located in areas that are VOC-limited, both models show similar behavior with greater O_3 and HNO_3 concentrations near the source with the plume-in-grid treatment because of lower titration of surface O_3 by plume NO.
- For isolated point sources located in areas that are primarily NO_x-limited, both models show initially similar behavior with decreases in O_3 and HNO_3 concentrations following the initial near-source increases. However, Models-3/CMAQ-PinG shows strong increases in HNO_3 concentrations farther downwind that do not generally appear in the Models-3/CMAQ-APT simulation.
- In the Ohio River Valley where several point sources are located and in the downwind areas, the two models display significantly different results. The Models-3/CMAQ-APT simulation shows results similar to those mentioned above for the areas north of the Ohio River Valley. However, in the areas south of the Ohio River Valley (e.g., West Virginia), Models-3/CMAQ-APT leads primarily to O_3 increases for the reasons discussed above (lower

conversion of NO_x to HNO_3 in the early stages of the plume as compared to the base simulation). HNO_3 concentrations show areas of increase in West Virginia but overall show decreases farther downwind. The Models-3/CMAQ-PinG simulation shows primarily increases in both O_3 and HNO_3 concentrations.

Overall, Models-3/CMAQ-PinG shows negligible changes in the O_3 budget over the entire domain and episode and a 10% increase in the HNO_3 budget.

The differences between the Models-3/CMAQ-APT and Models-3/CMAQ-PinG simulations are likely due to earlier plume-to-grid transfers in Models-3/CMAQ-PinG than in Models-3/CMAQ-APT. These results suggest that the time for plume-to-grid transfer is very influential and should be selected carefully to ensure an accurate simulation.

6
REFERENCES

Byun, D.W. and J.K.S. Ching, 1999. *Science Algorithms of the EPA Models-3 Community Multiscale Air Quality (CMAQ) Modeling System*, EPA-600/R-99/030, U. S. Environmental Protection Agency, Washington, DC.

Coats, C.J., A. Hanna, D. Hwang and D.W. Byun, 1993. Model engineering concepts for air quality models in an integrated environmental modeling system, presented at the *AWMA Specialty Conference on Regional Photochemical Measurement and Modeling Studies*, San Diego, CA.

Dabdub, D. and J.H. Seinfeld, 1995. Extrapolation techniques used in the solution of stiff ODEs associated with chemical kinetics of air quality models, *Atmos. Environ*., **29**, 403–410.

EPA, 1991. *Guideline for Regulatory Application of the Urban Airshed Model*, U. S. Environmental Protection Agency, Research Triangle Park, NC.

EPRI, 2000. *SCICHEM Version 1.2: Technical Documentation*, EPRI Technical Report 1000713, EPRI, Palo Alto, CA.

Gillani, N.V., 1986. *Ozone Formation in Pollutant Plumes: Development and Application of a Reactive Plume Model with Arbitrary Crosswind Resolution*, EPA-600/S3-86-051, U.S. Environmental Protection Agency, Research Triangle Park, NC.

Gillani, N.V. and J.E. Pleim, 1996. Subgrid scale features of anthropogenic emissions of NOx and VOC in the context of regional Eulerian models, *Atmos. Environ*., **30**, 2043–2059.

Gillani, N.V., J.F. Meagher, R.J. Valente, R.E. Imhoff, R.L. Tanner, and M. Luria, 1998. Relative production of ozone and nitrates in urban and rural power plant plumes 1. Composite results based on data from 10 field measurements days, *J. Geophys. Res.*, **103**, 22,593–22,615.

Gillani, N.V. and J.M. Godowitch, 1999. Plume-in-grid treatment of major point source emissions, Chapter 9, in Byun and Ching, 1999, *op. cit*.

Houyoux, M., 2000. Personal (e-mail) communication.

Jacob, D.J., L.W. Horowitz, J.W. Munger, B.G. Heikes, R.R. Dickerson, R.S. Artz and W.C. Keene, 1995. Seasonal transition from NO_x- to hydrocarbon-limited conditions for ozone production over the eastern United States, *J. Geophys. Res*., **100**, 9315–9324.

Karamchandani, P., A. Koo and C. Seigneur, 1998. A reduced gas-phase kinetic mechanism for atmospheric plume chemistry, *Environ. Sci. Technol.*, **32**, 1709–1720.

Karamchandani, P. and C. Seigneur, 1999. Simulation of sulfate and nitrate chemistry in power plant plumes, *J. Air Waste Manage. Assoc.*, **49**, PM-175–181.

Karamchandani, P., K. Vijayaraghavan, S.-Y. Wu, C. Seigneur, L. Santos, I. Sykes, J.-F. Louis, T. Nehrkorn and J. Henderson, 2000a. *Development and Evaluation of a State-of-the-Science Plume-in-Grid Air Quality Model*, Draft Report, EPRI, Palo Alto, CA.

Karamchandani, P., L. Santos, I. Sykes, Y. Zhang, C. Tonne and C. Seigneur, 2000b. Development and evaluation of a state-of-the-science reactive plume model, *Environ. Sci. Technol*., **34**, 870–880.

Kumar, N. and A.G. Russell, 1996. Development of a computationally efficient, reactive subgrid-scale plume model and the impact in the northeastern United States using increasing levels of chemical detail, *J. Geophys. Res.,* **101**, 16,737–16,744.

Mathur, R., J.O. Young, K.L. Schere and G.L. Gipson, 1998. A comparison of numerical techniques for solution of atmospheric kinetic equations, *Atmos. Environ*., **32**, 1535–1553.

Morris, R.E., M.A. Yocke, T.C. Myers, and R.C. Kessler, 1991. Development and testing of UAM-V: A nested-grid version of the Urban Airshed Model, *Proc. AWMA Specialty Conference: Tropospheric Ozone and the Environment II*.

Myers, T.C., P.D. Guthrie and S.-Y. Wu, 1996. *The Implementation of a Plume-in-Grid Module in the SARMAP Air Quality Model (SAQM)*, SYSAPP-96/06, Systems Applications International, Inc.

Pun., B., C. Seigneur, and W. White, 2001. *Day of the Week Behavior of Ozone and PM*, Final Report, Coordinating Research Council, Alpharetta, GA.

Rew, R.K. and G.P. Davis, 1990. NetCDF: An interface for scientific data access, *IEEE Comput. Graph. and Appl.*, **10**, 76–82.

Richards, L.W., J.A. Anderson, D.L. Blumenthal, A. Brandt, J.A. Mcdonald, N. Waters, E.S. Macias and P.S. Bhardwaja, 1981. The chemistry, aerosol physics and optical properties of a western coal-fired power plant plume, *Atmos. Environ.*, **15**, 2111–2134.

Sandu, A., J.G. Verwer, M. van Loon, G.R. Carmichael, F.A. Potra, D. Dabdub and J.H. Seinfeld, 1997. Benchmarking stiff ODE solvers for atmospheric chemistry problems – I. Implicit vs. explicit, *Atmos. Environ*., **31**, 3151–3166.

Seaman, N.L. and S.A. Michelson, 2000. Mesoscale meteorological structure of a high-ozone episode during the 1995 NARSTO-Northeast Study, *J. Appl. Met*., **39**, 384–398.

Seigneur, C., T.W. Tesche, P.M. Roth, and M.K. Liu, 1983. On the treatment of point source emissions in urban air quality modeling, *Atmos. Environ.,* **17**, 1655–1676.

Sillman, S., J.A. Logan, and S.C. Wofsy, 1990. A regional scale model for ozone in the United States with subgrid representation of urban and power plant plumes, *J. Geophys. Res.,* **95**, 5731–5748.

Sykes, R.I., W.S. Lewellen, S.F. Parker and D.S. Henn, 1988. *A Hierarchy of Dynamic Plume Models Incorporating Uncertainty, Volume 4: Second-order Closure Integrated Puff*, EPRI, EPRI EA-6095 Volume 4, Project 1616-28.

Sykes, R.I. and D.S. Henn, 1995. Representation of velocity gradient effects in a Gaussian puff model, *J. Appl. Met.*, **34**, 2715–2723.

Sykes, R.I., S.F. Parker, D.S. Henn and W.S. Lewellen, 1993. Numerical simulation of ANATEX tracer data using a turbulence closure model for long-range dispersion, *J. Appl. Met.*, **32**, 929–947.

Verwer, J.G., J.G. Blom, M. van Loon and E.J. Spee, 1996. A comparison of stiff ODE solvers for atmospheric chemistry problems, *Atmos. Environ*., **30**, 49–58.

Seigneur, C., B. Pun, P. Pai, J.-F. Louis, P. Solomon, C. Emery, R. Morris, M. Zahniser, D. Worsnop, P. Koutrakis, W. White, I. Tombach, 2000. Guidance for the performance evaluation of three-dimensional air quality modeling systems for particulate matter and visibility, *J. Air Waste Manage. Assoc*., **30**, 588–599.

Target:
Tropospheric Ozone and Precursors

About EPRI

EPRI creates science and technology solutions for the global energy and energy services industry. U.S. electric utilities established the Electric Power Research Institute in 1973 as a nonprofit research consortium for the benefit of utility members, their customers, and society. Now known simply as EPRI, the company provides a wide range of innovative products and services to more than 1000 energy-related organizations in 40 countries. EPRI's multidisciplinary team of scientists and engineers draws on a worldwide network of technical and business expertise to help solve today's toughest energy and environmental problems.

EPRI. Electrify the World

Printed on recycled paper in the United States of America

1005161

EPRI • 3412 Hillview Avenue, Palo Alto, California 94304 • PO Box 10412, Palo Alto, California 94303 • USA
800.313.3774 • 650.855.2121 • askepri@epri.com • www.epri.com